Copyright Warning & Restrictions

The copyright law of the United States (Title 17, United States Code) governs the making of photocopies or other reproductions of copyrighted material.

Under certain conditions specified in the law, libraries and archives are authorized to furnish a photocopy or other reproduction. One of these specified conditions is that the photocopy or reproduction is not to be "used for any purpose other than private study, scholarship, or research." If a, user makes a request for, or later uses, a photocopy or reproduction for purposes in excess of "fair use" that user may be liable for copyright infringement,

This institution reserves the right to refuse to accept a copying order if, in its judgment, fulfillment of the order would involve violation of copyright law.

Please Note: The author retains the copyright while the New Jersey Institute of Technology reserves the right to distribute this thesis or dissertation

Printing note: If you do not wish to print this page, then select "Pages from: first page # to: last page #" on the print dialog screen

ABSTRACT

ROLE OF ZETA POTENTIAL IN MICRO-CARRIER PROCESS

by
Pallavi Mehta

The micro-carrier process recently developed at NJIT is a new high rate settling technology for water and wastewater treatment. This process utilizes the micro-carrier as a flocculating enhancement agent to achieve rapid removal of colloidal particles. This thesis consist of two parts, namely, 1) A review of the flocculation process utilized in water and wastewater treatment, and 2) An experimental program to evaluate the role of zeta potential in the flocculation process.

The results of this study indicated that the DLVO theory (Darjaguin, Landau, Overbeek, Verwey theory) is applicable to micro-carrier process in the absence of polyelectrolytes. The best flocculation was achieved when the zeta potential approached the minimum value. It was observed that in the presence of different polyelectrolytes non-DLVO forces have a significant impact.

ROLE OF ZETA POTENTIAL IN MICRO-CARRIER PROCESS

by
Pallavi Mehta

A Thesis
Submitted to the Faculty of
New Jersey Institute of Technology
In Partial Fulfillment of the Requirements for the Degree of
Master of Science in Applied Chemistry

Department of Chemical Engineering, Chemistry and Environmental Science

January 1999

APPROVAL PAGE

ROLE OF ZETA POTENTIAL IN MICRO-CARRIER PROCESS

Pallavi Mehta

Dr. Yuan Ding, Thesis advisor — Date
Assistant Professor of Civil and Environmental Engineering, NJIT

Dr. Robert Dresnack, Committee member — Date
Professor of Civil and Environmental Engineering, NJIT

Dr. David Kristol, Committee member — Date
Professor of Chemistry, NJIT

Dr. Barbara Kebbekus, Committee member — Date
Professor of Chemistry, NJIT

BIOGRAPHICAL SKETCH

Author: Pallavi Mehta

Degree: Master of Science

Date: January 1999

Undergraduate and Graduate Education:

- Master of Science in Applied Chemistry,
  New Jersey Institute of Technology,
  Newark, NJ, 1999

- Master of Science in Physical Chemistry,
  Bombay University,
  Bombay, India, 1996

- Bachelor of Science in Chemistry,
  Bombay University,
  Bombay, India, 1994

Major: Applied Chemistry

This Thesis is dedicated to
my beloved parents

ACKNOWLEDGEMENT

I would like to express my sincere gratitude to my advisor, Dr. Yuan Ding for her guidance, inspiration and financial support throughout my study program.

I would also like to thank my thesis committee members Dr. R Dresnack, Dr. David Kristol and Dr. B. Kebbekus for their invaluable time and insightful advise.

I would also like to thank Dr. R. Raghu, Dr. S. Mukharji and Mr. C. Patel for their help and guidance.

Special thanks to Dr. R. Kane and Ms. Annette Damiano for their help.

This study was supported by USEPA (United States Environmental Protection Agency)

TABLE OF CONTENTS

TABLE OF CONTENTS
(Continued)

Chapter **Page**

TABLE OF CONTENTS
(Continued)

LIST OF TABLES

Table **Page**

LIST OF FIGURES

Figure **Page**

LIST OF FIGURES
(Continued)

Figure **Page**

CHAPTER 1

INTRODUCTION

1.1 Background

During recent years, the words 'Pollution', 'Environment' and 'Ecology' have come into increasingly frequent usage. The cleanliness of the world we live in has become a concern for people. Eighty percent of water pollution is due to activities on land. Water and wastewater originating from land erosion, decay of vegetation, dissolution of minerals, domestic and industrial waste discharges, contains significant amount of toxic pollutants. The detrimental effects of non-point source pollution, particularly urban runoff, have received considerable attention.

Urban wet weather flow (WWF) is comprised of three basic sub areas.

1) Combined sewer overflow (CSO)
2) Sanitary sewer overflow
3) Storm water discharge

Storm water runoff mobilizes large quantity of contaminants from the urban environment. Inputs of heavy metals on urban surfaces originate from vehicle exhausts, tire wear, corrosion of building materials and atmospheric deposition **[1]**.

Studies have shown that toxic pollutants present in wastewater include

1) Organic chemicals such as benzene, xylene, toluene, polyaromatic hydrocarbons (PAH), polychlorinated biphenyl, pesticides, herbicides.
2) Heavy metals such as arsenic, antimony, cadmium, chromium, lead and mercury.
3) Microorganisms, bacteria, viruses etc.

In a study of sediment samples of four combined sewer overflow (CSO) outfalls, along the lower Passaic River in New Jersey, the results indicated that sediments proximate to the CSO outfalls were contaminated with a range of chemicals. These chemicals included toxic metals, polycyclic aromatic hydrocarbons (PAHs), polychlorinated biphenyls (PCBs), pesticides and other chemicals. The spatial distribution of these contaminants strongly suggested that the CSO was the primary source of contamination in sediments near these outfalls **[2]**.

Urban WWF contains a great variety of pollutants. Colloidal particles play an important role in carrying these pollutants. In a study of the distribution of metals in microcolloidal (0.45 to 20 micrometers) and dissolved size fractions, it was found that 44 to 83% of the total zinc existed in forms smaller than 0.45 micrometer and 6 to 43% of iron existed in the same range **[3]**. The colloidal particle plays a significant role in carrying the heavy metals. Table 1.1 **[4,5]** shows the concentration distribution of different metals with respect to size. It is seen that the majority of heavy metals are associated with particles less than 10 micrometers, which fall in the colloidal range.

Table 1.1 Metal Distribution versus Particle Size

Suspended solid size micrometers	Metal distribution %							
	Cd	Co	Cr	Cu	Mn	Ni	Pb	Zn
> 100	18	9	5	7	8	8	4	5
10-100	36	31	24	30	21	29	23	35
<10	46	60	71	63	71	63	73	60

In addition it is known that as the number of colloidal particles increases in the water body, the amount of dissolved oxygen in it decreases. All these contaminants have

detrimental effects on human health. Storm water runoff from urban roadways often contains significant quantities of metal elements and solids. Characklis and Wiesener (1997) investigated water quality, metals concentrations and particle size distribution in urban runoff. Samples taken under both storm and background conditions indicated that concentrations of particle number, organic carbon, suspended solids, iron and zinc increased during storms **[6]**.

All the above reports suggest the importance of colloidal particles in carrying environmental contaminants such as heavy metals, organic compounds etc. and thus has detrimental effects on the receiving water bodies.

1.2 What are Colloidal Particles?

Particles suspended in water, whether generated precipitatively as part of a treatment process or present as a natural constituent of a waste stream, can vary in size over many orders of magnitude. Any particle that has dimensions between $1x10^{-6}$ to $1x10^{-9}$meter is defined as a colloidal particle. Colloidal solutions are classified as lyophilic and lyophobic. Lyophilic colloids are those that have strong attraction for a solvent medium, whereas lyophobic colloids are those that have little attraction for a solvent medium or are dispersions of essentially insoluble solid phase in a solvent medium **[7]**. Further, particles are said to be stable if they are resistant to aggregation and unstable if aggregation occurs.

Colloidal particles play an important role in the transport of pollutants. Due to their large specific area, colloidal particles facilitate adsorption of heavy metals, organic ions and water borne microorganisms. Therefore, removal of colloidal particles is of paramount importance in wastewater treatment.

Particles of colloidal dimensions form very stable dispersions which do not settle and which are not amenable to the conventional filtration process **[8]**. Individual colloidal particles are too small to be seen by the naked eye. Generally, a high concentration of colloids will impart a cloudiness or haziness to the water. Since a properly sized depth filter will only remove particles greater than 10 microns, colloidal particles will tend to pass straight through. Making the filter media finer is generally not a practical option, since this would lead to very high-pressure loss through the filter, and rapid plugging of the filter bed.

It is apparent that considering hydrodynamic effects alone, time scales of up to several years may be required for the settlement of such particles to a considerable extent. Hence it is feasible that colloidal particles may be removed from dispersions by methods other than the above mentioned methods.

1.3 Removal of Colloidal Particles

Sedimentation with coagulation is generally considered a cost-effective method in removing large quantities of fine-grained suspended solids (SS) from water and wastewater. Removal of colloidal particles by sedimentation requires an effective control of the coagulation-flocculation process. Coagulation is a chemical technique directed towards destabilization of particle suspension. The most commonly used coagulant is aluminum sulfate (alum). Coagulation is usually followed by flocculation, which is a slow mixing technique promoting the aggregation of destabilized (coagulated) particles. Coagulation followed by flocculation as an aid to sedimentation and filtration has been practiced for years.

Various kinds of flocculating agents including indifferent electrolytes, metal salts such as aluminum sulfate, aluminum chloride, ferric chloride, ferric sulfate and various polymeric flocculent have been widely used for carrying out flocculation process. Different kinds of interactions can be operative between colloidal particles. An understanding of the role of chemistry in particle-particle interactions may serve in the better selection of the type and concentrations of the chemicals to cause effective coagulation and removal of suspended solids.

1.4 Micro-carrier as Weighted Clarifier

In potable water treatment, the addition of micro-carrier during flocculation gives floc with high–performance characteristics. In recent years, micro-sand as weighted carrier of colloidal particles, in flocculation process, a new high rate chemical clarification process, was developed and applied to drinking water supply **[9]**. This technology may be applicable for treating combined wet and dry weather flow. This high rate process consists of the addition of micro-carrier and coagulant into the influent in a mixing chamber followed by flocculation and sedimentation. The initiation of the coagulation-flocculation process is improved by the presence of electrolyte and polyelectrolyte, which increases the bonding of the flocs to the micro-carrier, resulting in higher settling velocity.

The micro-carrier enhanced weighted flocculation, consists of incorporating a high-density substance in the floc, thus increasing its natural sedimentation capabilities. Some of these technologies are for instance, The Microsep® (International Water Solutions Corporation) the Actiflo®(Omnium de Traitement et de Valorisation [OTV]) and DensaDeg® (Infilco Degremont, Inc.)

A number of micro-carrier pilot units have been evaluated for treating wastewater in the U.S. and this process is being installed at an increasing number of wastewater treatment plants. However, a review of the current literature indicated that the basic operation parameters are not available to the technical community. For engineers to develop the micro-carrier high rate settling process design and equipment specification, and to control the flocculation process it is necessary to understand the basic principle of the high rate sedimentation.

1.5 Objective of the Thesis

The principal objectives of this thesis were 1) To review the process of flocculation in terms of various colloidal interactions and the kinetics of flocculation process and 2) To study the behavior of the high rate settling process enhanced by micro-carrier on a synthetic surface runoff sample. From the review of the current literature it was found that micro-carrier enhances the removal of colloidal particles by the formation of heavy flocs. Therefore, it is necessary to compare this technique to the conventional technique by considering the fundamental parameters controlling the phenomenon.

The experimental study includes the study of the flocculation process in the presence of micro-carrier, effect of micro-carrier on zeta potential and hence the colloidal stability of solutions. Emphasis has also been given to the study of various parameters controlling aggregation and removal of colloidal particles by the micro-carrier-weighted flocculation.

In this study experiments were carried out using electrolyte, polyelectrolyte and micro-carrier. Charge neutralization and bridging mechanisms of electrolyte and polyelectrolyte results in the colloidal destabilization and hence causes the flocculation of colloidal particles.

In the various phases of the study the controlling parameters of the process such as various types of coagulants and their doses were studied. In addition to these the effectiveness of various types of polyelectrolytes required to achieve maximum flocculation was also one of the important aspect of this study.

CHAPTER 2

FLOCCULATION PROCESS: A REVIEW

Flocculation is an important step in water and wastewater treatment as well as in many solid-liquid separation processes. Particles in water vary widely in origin, concentration and size. Flocculation is a process of combining small particles into larger aggregates. This aggregation process is variously known as agglomeration, coagulation, or flocculation. These terms are used in different ways depending upon the area of application and on the mechanism of aggregation. However, there is a lack of agreement on the distinction between the terms coagulation and flocculation. Thus, the term "flocculation" is used here.

Flocculation is a complex process; many physical and chemical processes are involved and hence it is a physiochemical process. Many of the important properties of colloidal systems are determined directly or indirectly by the interaction forces between particles. Flocculation occurs only if particles collide with each other and can adhere when bought together by collision. To a large extent these two processes, which could be termed "colloidal interaction" and "flocculation kinetics" are discussed in the following paragraphs.

2.1 Colloidal Interactions

When two particles approach each other, several types of interactions can come into play that may have major effects on flocculation process. The two most studied colloidal interactions are van der Waals interactions and electrical repulsion. These forces form the

basis of the well-known DLVO theory. In addition to these DLVO forces, various other types of interaction such as hydrophobic interactions, hydration effects, steric interactions, polymer bridging etc. play a considerable role in the flocculation of colloidal particles.

2.1.1 van der Waals Interaction

The universal attractive forces between atoms and molecules, known as van der Waals forces, play a very important role in the interaction of colloidal particles. van der Waals force is caused by the interactions of induced and permanent dipole moments in the constituent molecules of the two interacting colloidal particles. The interaction energy may be calculated in two ways.

In the classical approach (Hamaker approach) the interaction between two macroscopic bodies is obtained by the pairwise additivity of all the interactions between molecules. In the macroscopic approach, the interaction is considered as arising from electric and magnetic polarization, giving a fluctuating electromagnetic field within the media and in the gap between them. Lifshitz in 1956 derived an expression for the force between two semi-infinite media separated by a plane-parallel gap. However, proper application of this approach requires detailed information and the dielectric responses of the interacting media and hence Hamaker approach is still widely used **[10]**.

In the Hamaker approach, for two spheres of radii a_1 and a_2 separated by a distance d, the interaction energy is given by,

$$V_A = -\frac{A}{6d}\left(\frac{a_1 a_2}{a_1 + a_2}\right) \qquad (2.1)$$

where V_A is the interaction energy between the two spheres and A is the Hamaker constant. For equal spheres of radius a_1 the interaction energy equation is,

$$V_A = -\frac{Aa}{12d} \tag{2.2}$$

Equation 2.2 is applied to the interaction of media across a vacuum. With a modified Hamaker constant, the same equation can also be used for interaction through a liquid **[11]**.

2.1.2 Electrical Interaction

Most particles in aqueous media are charged due to various reasons such as ionization of surface groups, isomorphous substitution, and specific ion adsorption etc.**[12]**. The influence of electrical charge on colloidal surface is very important to their physical chemistry. The charged surface of particles and oppositely charged layer of counter-ions adjacent to it constitute an electrical double layer. A widely accepted model for the double layer is that due to Stern, later modified by Graham in which part of the counter-ion charge is located close to the particle surface (the so called "Stern layer") and the remainder is distributed more broadly in the diffuse layer **[13]**.

The extent of the diffuse layer depends on ionic strength and for fairly low potentials, the Poisson and Boltzmann expression is applicable and leads to the following expression.

$$\varphi = \varphi_\delta \exp(-\kappa x) \tag{2.3}$$

where φ is the potential at a distance x from the Stern plane and κ is the Debye-Huckel parameter **[14]**. For aqueous solutions at 25° C, κ is given by,

$$\kappa = 2.3 \times 10^{9} \left(\sum c_i z_i^{2}\right)^{1/2} \qquad (2.4)$$

Figure 2.1 shows the effect of electrolyte concentration on the distribution of potential in the double layer, for the case of an indifferent electrolyte concentrations and a salt with a specifically adsorbing counter ion giving charge reversal **[15]**.

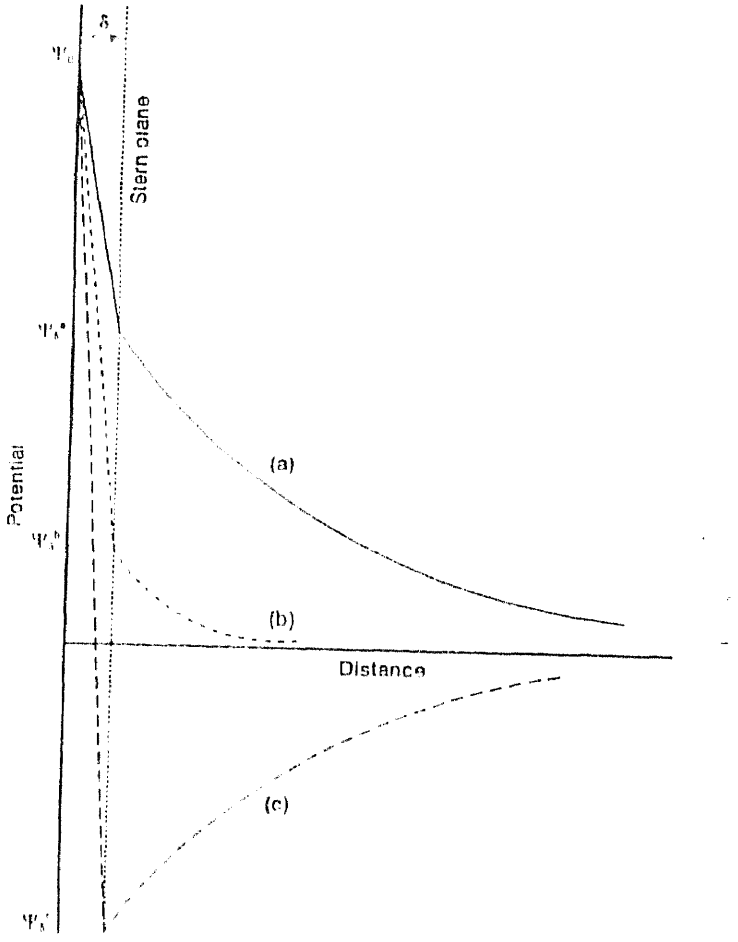

Figure 2.1 Variation of Potential Close to a Charged Interface.

In the case of indifferent electrolytes, the diffuse layer charge is equal and opposite to the surface charge. It is seen in Figure 2.1 that in case of indifferent electrolytes, at low concentration, (a) surface potential drops to zero in the bulk solution and this drop is divided between the Stern and the diffuse layer. In the case of high salt concentration, (b) potential will fall sharply through the Stern layer to the value φ_δ. In the case of a salt with a specifically adsorbing ion, (c) the adsorption of counterions can continue until the Stern layer charge more than compensates the surface charge and reversal of charge occurs. This is the reason why charge reversal is observed when some hydrolyzing metal ions are used as flocuulants and is of great practical importance in particle aggregation.

The interaction between charged particles is governed predominantly by the overlap of diffuse layer. So the potential most relevant to the interaction is that at the boundary between the Stern and diffuse layer (the Stern potential φ_δ) rather than the potential at the particle surface. There is no direct method to experimentally determine the Stern potential but the zeta potential or electrokinetic potential is considered to be an adequate substitute **[16]**.

When two charged particles approach each other in an electrolyte solution, their diffuse layers overlap and in case of similarly charged particles a repulsion is observed between them. This repulsive interaction energy can be calculated in two ways. One is to solve the Poisson-Boltzmann equation directly but this is usually unable to give an analytical solution. The other method is to construct the formula from known expressions for each of the surfaces involved. The most fundamental solutions are those of the sphere-sphere interactions and plate-plate interactions. For sphere-sphere interaction application of linear superposition approximation yields the following equation **[17]**.

$$V_E = 32\pi\varepsilon a(kT/ze)^2\gamma^2\exp(-\kappa d) \quad (2.5)$$

where ε is the permittivity of the charge, e is the elementary charge, z is the valence of the ions, and γ is the dimensionless function of the surface function (taken as zeta potential here)

$$\gamma = \tanh(\frac{ze\varphi_0}{4kT}) \quad (2.6)$$

2.1.3 The DLVO Theory and Its Application

To explain the stability of a hydrophobic colloidal suspension Derjaguin and Landau in USSR and Verwey and Overbeek in Netherlands independently developed a quantitative theory of stability of lyophobic colloids. This theory is commonly referred to as the DLVO theory, which has been accepted and used for colloidal systems. In the formulation of the theory van der Waals attraction and electrostatic repulsion energy are taken into consideration. **[18]**.

In essence, the DLVO theory states that the total pair interaction between colloidal particles consists of van der Waals attractive energy and electrostatic repulsive energy and these two interaction energies can be combined to yield an overall energy of interaction between colloidal particles.

Combining equation (2.2) and (2.5) the total interaction energy between two equal particles can be obtained as **[19]**,

$$V_T = 32\pi\varepsilon a(kT/ze)^2 r^2\exp(-\kappa d) - \frac{A}{12\pi d^2} \quad (2.7)$$

The potential energy diagram for the interaction of colloidal particles is shown in Figure 2.2

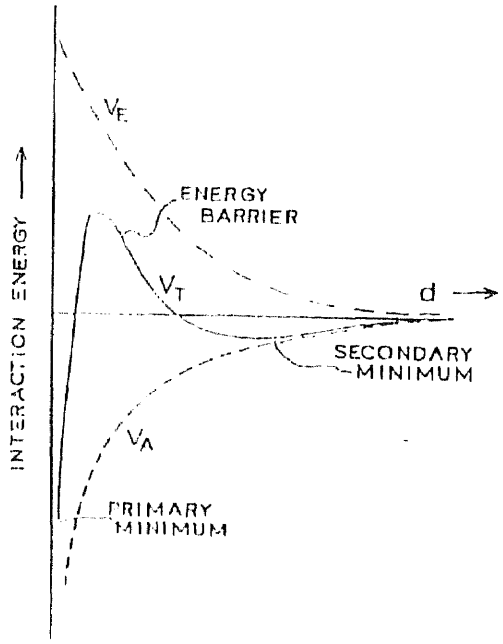

Figure 2.2 Schematic Representation of Total Energy of Interaction versus Surface to Surface Separation Distance **[20]**.

In Figure 2.2 the terms V_A, V_E, and V_T, represents attraction energy, electrical energy, and Total energy respectively. As ionic strength increases zeta potential reduces and the energy barrier becomes lower and particle aggregation occurs. Once the barrier is overcome, then the particles are held by van der Waals force of attraction, in a deep primary minimum, where in principal attraction is infinitely strong, but due to hydration effects, the primary minimum is at finite depth. Also as at larger distances van der Waals interaction is always greater than electrical energies and hence a secondary minimum in the potential energy curve is observed which can be responsible for the formation of fairly week aggregates **[20]**.

Addition of salt or indifferent electrolyte reduces the potential energy barrier and critical coagulation concentration corresponds to a zero interaction energy and force, thus,

$V_T = 0$

Under this condition, equation 2.6 leads to the following expression for the critical flocculation concentration (C_f) for a symmetrical electrolyte

$$C_f = k(\frac{\gamma^4}{A^2 z^6}) \tag{2.8}$$

where k is a constant which depends upon the properties of the dispersion medium, A is the appropriate Hamaker constant It is noted that when zeta potential is very high, the term γ approaches unity, C_f becomes inversely proportional to the sixth power of the valence z. This dependence of C_f on z is known as the Schulze-Hardy rule **[21]**.

There are very few cases where the inverse sixth power law is followed. One such example is the flocculation of synthetic latex by various salts where the critical values for Na^+, Ba^{+2} and La^{+3} were found to be in the ratio 1: 0.014: 0.0014. The theoretical ($1/z^6$) ratios [1:0.016:0.0016] are quite close **[22]**.

In most of the flocculation processes, flocculants used are not simple different electrolyte and they undergo many more important reactions in addition to electrostatic ones.

2.1.4 Specifically Adsorbed Ion

Any ion whose adsorption at the surface is influenced by forces other than simply by electric potential can be regarded as being specifically adsorbed. The additional forces

may be chemical in nature (involving some degree of covalent bonding with surface atoms) or physical. For chemical forces to be involved, it is clear that adsorption must occur into the inner or compact part of the double layer **[23]**. Specifically adsorbed ions can be recognized by their ability to reverse the sign of the zeta potential and a useful distinction can be made between specifically adsorbed ions and those, which are chemically adsorbed. A physically adsorbed ion does not affect the point of zero charge, but can reverse the sign of the zeta potential. Chemically adsorbed ion on the other hand shifts the point of zero charge and can remain adsorbed even when the underlying surface has the same sign as itself.

2.2 Non-DLVO Forces

The DLVO theory is the most widely applicable quantitative theory of colloidal stability However, there are many cases where the combination of the two principal interaction forces alone dose not give satisfactory agreement with experimental results. In such cases, in addition to DLVO forces various other forces, generally termed "structural forces," may have to be considered. These structural or non-DLVO forces include hydration interactions, hydrophobic interactions, steric interactions and polymer bridging. which are discussed in this section.

2.2.1 Hydration Effects

Since most particles carry a negative surface charge and hence ionic surface groups, some hydration of these groups is observed, and this bound water layer plays an important role in the interaction of such particles. Hydration at a particle surface results in an increased

repulsion between approaching particles. The most direct evidence for hydration effects is seen from measurements of the force between mica sheets separated by different salt solutions at low ionic strength **[24]**. When the ionic strength is low, the repulsion follows the expected exponential form for double layer interaction, and double layer repulsion is completely overcome by van der Waals forces. However, at higher concentration about 1 mM, an extra short-range repulsive force is observed owing to adsorbed hydrated cation. This force increases as the degree of hydration increases and is exponential in nature over the range 1.5 to 4 nm. Divalent cations gave rise to strong short-range repulsive force, which prevent coagulation.

2.2.2 Hydrophobic Interaction

The nature of water in contact with a hydrophobic surface will be different from that of ordinary bulk water which is significantly structured because of hydrogen bonding between the molecules. The presence of hydrophobic surface could restrict the natural structuring tendency of water, simply by imposing a barrier, which prevents the growth of clusters in a given direction. This could result in an increased free energy of the water confined in a gap between two such surface and results in an increased free energy of the water in relation to bulk water. This leads to an attraction between the hydrophobic surfaces, and results in the formation of agglomerates. Attraction between hydrophobic surfaces can be at surprisingly long range up-to about 80nm. **[25]**. The process known as oil agglomeration, where quite large particles such as coal are bound together by adhering to oil films is very dependent on the hydrophobicity of the particles.

2.2.3 Steric Interaction

Adsorbed layers of polymer play an important role in aggregation. In case of colloidal particles, dispersions with larger adsorbed amounts of polymers can give greatly enhanced stability by an effect known as steric effect. This is observed in case of terminally adsorbed block co-polymers. The most important factor determining the degree of steric stabilization is the thickness of the adsorbed double layer relative to the particle size. One of the reasons for the steric stability in an aquatic environment could be the presence of adsorbed layers of natural organic material such as humic substances. Humic substances are known to enhance the stability of inorganic colloid and can greatly increase the dosage of flocculent required in water treatment **[26]**.

2.2.4 Polymer Bridging

Long chain polymers generally adsorb on particles at various points along the chain and it is possible that a single polymer molecule can become attached to two or more particles. This mechanism is known as polymer bridging, which was postulated first by Ruehrwein and Ward **[27]**. For polymer bridging to occur there should be sufficient unoccupied particle surfaces for attachment of polymer segments from chains attached to other particles. Also these polymer bridges should be of such an extent that they span the distance over which inter particle repulsion operates. It is observed that generally high molecular weight polymers give more effective bridging flocculation. Also at lower polymer dosage there are insufficient polymers to form adequate bridging links and at higher polymer concentration there is insufficient free particle surface for bridging and steric repulsion due to adsorbed layer prevents bridging. Thus there is an optimum dosage

of polymer, which gives good bridging flocculation, and it usually depends on particle concentration **[28]**.

An alternative mechanism for the flocculation by polymers is electrostatic patch effect. In this case the adsorption of polyelectrolytes on an oppositely charged particles occur in such a way that there are patches of excess charge due to local charge reversal and areas of unoccupied surface still bearing the original particle charge. Interaction occurs in such a way that the positive and negative areas of different particles are adjacent and give a strong electrical interaction **[29]**.

Many theories have been proposed on the relation between the collision efficiency and the fractional coverage of the solid surface by adsorbed polymer. When the zeta potential of the particles and the ionic strength are such that repulsion outweighs the attraction, then there is a potential energy barrier. In the presence of an energy barrier, only a certain fraction of collisions are effective and this fraction is known as collision efficiency α. The reciprocal is known as the stability ratio W. A detailed analysis of the stability ratio is given in Russel et. al. **[30]**

La Mer et al.**[31]** proposed that the rate of flocculation should be equal to the product of the particle collision frequency and collision efficiency factor, which describes the fraction of collisions actually leading to bridging The treatment of collision efficiency was reevaluated by Hogg **[32]**.

In addition to La Mer's assumptions, he assumed that the particles in suspension are in random orientation and are free to rotate in response to hydrodynamic forces or interaction with other particles. His model for the flocculation efficiency as a function of the extent of polymer adsorption predicts that for particles, which are large relative to the

adsorbed polymer molecules, collision efficiencies are very high (close to 100%) over a broad range of surface coverage ($0.1< \theta < 0.9$). The collision efficiency increases with increase in the particle size and decreases with increasing polymer molecular weight. The La Mer et al. model probably underestimates collision efficiencies by allowing for no reorientation of particles as they approach each other. Whereas Hogg's model which allows the particles to have complete freedom of reorientation during the collision process may overestimate the collision efficiency.

Moudgil, in 1987 **[33]**, proposed a model to calculate the probability of flocculation by polymers. The model is based upon the assumptions included in earlier models but a basic difference is made in classifying surface sites on solids as either active or non-active sites. Thus, it is proposed that fraction of active sites ϕ plays a dominant role in the flocculation of solids by polymer bridging. The collision efficiency factors calculated on the basis of this model agree with the experimental flocculation results. The value of ϕ is a main factor in determining the efficiency as well as the relative rates of adsorption and flocculation processes.

According to Gregory, 1993 **[34]**, various interaction forces determine the overall stability of colloids. Colloidal stability can be explained in terms of total interaction energy. These inter-particle forces or colloidal interactions are linearly dependent on particle size and become stronger relative to external forces. These colloidal forces have little influence on the transport of particles but can have a major effect on collision efficiencies and on adhesion between particles.

2.3 Flocculation Kinetics

Two colliding particles adhere to each other and form an aggregate. Aggregation is primarily a kinetic phenomenon and the rate of aggregation of a suspension can be written as **[35]**,

$$\frac{dn}{dt} = - K_a n^2 \tag{2.9}$$

where n is the number concentration of particles in suspension at time t and K_a is a second order rate constant. For aggregation,

$$K_a = \alpha_a \beta \tag{2.10}$$

where β is mass transport coefficient and α_a is collision efficiency.

Particle aggregation rate can be described by the rate at which a certain size aggregate is being formed by smaller aggregates minus the rate at which the aggregate combines to form a larger aggregate (neglecting aggregate break up). This is given by Smoluchowski equation.

$$\frac{dn_k}{dt} = \frac{1}{2} \sum_{i+j=k} \alpha_a \beta(i, j) n_i n_j - n_k \sum_{all\ i} \alpha_a \beta(i, k) ni \tag{2.11}$$

where i, j and k refer to particle size, n_i and n_j is the number density of the particle. First summation is over sets of sizes that when added produce a size k and the second summation reflects the loss of size k aggregates as they combine with all other aggregate sizes to form larger particles.

2.3.1 Collision Frequency Factor

It is generally accepted that there are three mechanisms, which cause particle collision. They are Brownian motion, fluid shear and differential settling. Mass transport coefficients (β) for the three transport processes are as follows **[36]**.

For Brownian diffusion,

$$\beta_{bd}(i, j) = \frac{2kT(di + dj)^2}{3\mu \quad didj} \tag{2.12}$$

where di and dj are the radius of the two combining particles, μ is the fluid viscosity, T is the absolute temperature, and k is the Boltzmann constant.

For velocity gradient,

$$\beta_{vg}(i, j) = \frac{1}{6}(di + dj)^3 G \tag{2.13}$$

where G is velocity gradient.

For differential settling,

$$\beta_{ds}(i, j) = \frac{\pi g}{72\mu}(\rho_p - \rho)(di + dj)(di - dj) \tag{2.14}$$

where ρ_p and ρ are densities of the particles and the fluid, respectively, and g is gravity of acceleration.

In the Smoluchowski's approach (rectilinear approach), it is considered that all particles move in straight line until contact occurs between them and particle volume is conserved (coalesced sphere assumption) during aggregation process. The assumption of rectilinear model neglects hydrodynamic interactions and short range forces between

approaching particles. This hydrodynamic interaction reduces the frequency of inter-particle contacts from the rates predicted with Smoluchowski approach.

The curvilinear model considers these hydrodynamic effects and thus the actual collision rate is less than rectilinear rates. The effects of hydrodynamic interaction on particle transport by Brownian diffusion are described in Figure 2.3 **[37]**. In these calculations, van der Waals interactions are included as the separating distance between particle decreases. It is observed that reduction in the transport rate, relative to rectilinear approach are more for monodisperse systems (d_i/d_j =1) than for heterodisperse systems.

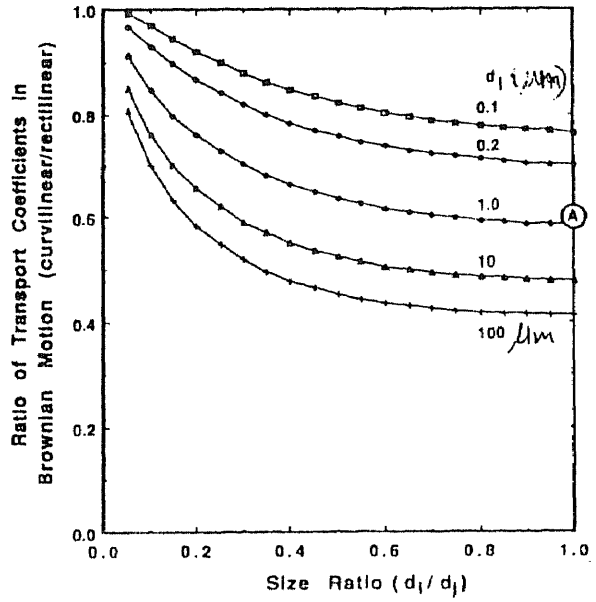

Figure 2.3 Effects of Particle Size on Mass Transport Coefficients in Brownian Motion **[37]**

In case of fluid shear it was observed that hydrodynamic interactions in aggregation by fluid shear were relatively small for monodisperse suspensions and become increasingly important as the system becomes more heterodisperse. This is shown in Figure 2.4. Also the hydrodynamic interaction become more important as H_A becomes

smaller, which is a dimensionless quantity defined as

$$H_A = \frac{A}{18\pi\mu d_j^3 G} \tag{2.15}$$

where A is Hamaker constant, d_j is the diameter of the larger of the two interacting particles. Thus, the rectilinear approach becomes inappropriate in case of heterodisperse system.

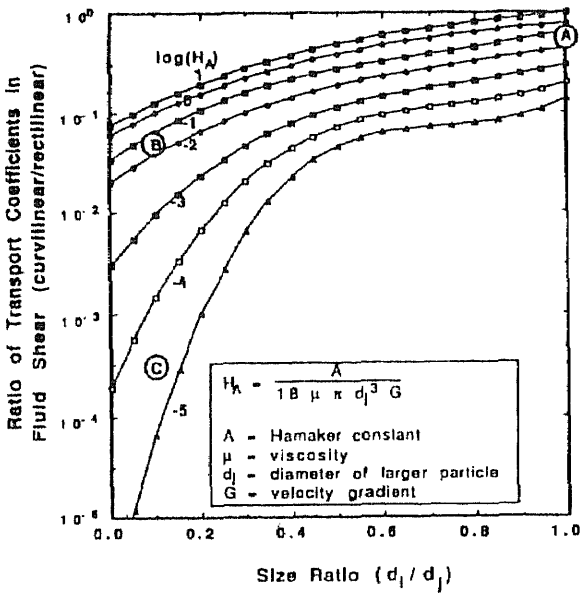

Figure 2.4 Effects of Particle Size on Mass Transport Coefficient in Fluid Shear [37]

2.3.2 Collision Efficiency

The colloidal stability of particles can be described by sticking or stability factor, α, as

$$\alpha = \frac{\text{rate at which particles attach}}{\text{rate at which particles collide}}$$

Various approaches can be used to determine values of α experimentally. In one approach, chemical conditions are used in which repulsive particle interactions are expected to be negligible and the aggregation rate observed under these conditions is assumed to be the collision rate in the denominator of above equation. Values of α are than calculated for any experimental aggregation rate by dividing it by the fastest rate observed. In another approach particle collision rate are calculated from mass transport theories.

In 1984, Valioulis and List **[38]** generated numerical computations of collision efficiency of particles in Brownian diffusion including the effects of double layer forces at constant surface charge, hydrodynamic forces and van der Waals forces. From this, collision efficiency can be determined for varying values of the Hamaker constant A in van der Waals attraction, the ionic strength I, and different ratios of radii of particles (R_i/R_j).

Collision rate can be increased by stirring the suspension so that collisions between particles can be dominated by fluid motion. van de Ven and Meson studied the effects of interaction forces between pairs of equal sized spheres in shear flow and calculated a semi-empirical formula for the collision efficiency **[39]**. This was extended by Alder **[40]** to the collisions between unequal sized spheres and his results indicated that in shear flow homocoagulation is favored over heterocoagulation however the reverse can be true in some carefully chosen conditions.

When fluid shear dominates particle transport, combining equations 2.9, 2.10 and 2.13 leads to the following equation **[41]**.

$$\ln \frac{n_t}{n_0} = \frac{4\phi\alpha_a G t}{\pi} \qquad (2.16)$$

where n_t and n_0 are number concentrations of particles at time t and at the beginning of the experiment, respectively, and ϕ is the volume fraction of solid material in the suspension.

On rearranging equation 2.16 leads to,

$$\alpha_a = \frac{\pi}{4\phi Gt} \ln \frac{n_0}{n_t} \tag{2.17}$$

All terms on the right hand side of the equation (2.17) are constants or experimentally accessible. Experimental values of the stability ratio as a function of concentrations of polyelectrolytes are illustrated in Figure 2.5 **[42].**

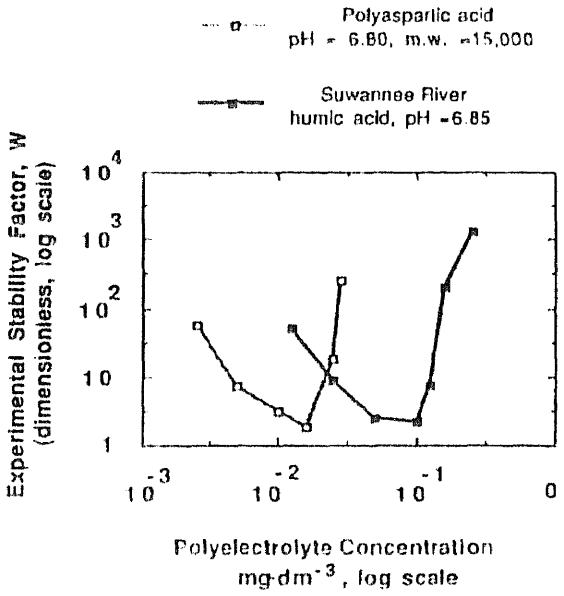

Figure 2.5 Experimental Values of the Stability Ratio (W) as a Function of Polyelectrolyte Concentration **[42]**

A trajectory model, which incorporates inter-particle forces, such as hydrodynamic resistance, van der Waals, and electrostatic forces as well as fluid flow velocity was developed to investigate particle flocculation in turbulent flow. Brownian diffusion,

gravity, and inertial forces were neglected in the trajectory model. This model calculation showed that the collision efficiency could be enhanced by decreasing the agitation speed and particle size ratio and by increasing the Hamaker constant. The effects of agitation speed on collision efficiency and frequency are opposite. The effect of particle size ratio on the collision efficiency and frequency are similar to those of the agitation speed **[43].**

2.4 Flocculating Agents

2.4 1 Electrolytes in Colloidal Particle Removal

Various electrolytes, such as ferric chloride, ferrous sulfate, aluminum sulfate, aluminum chloride, are used in removal of colloidal particles. The primary coagulants used in wastewater treatment, hydrolyze in water and evolve as aluminum or ferric hydroxide flocs. Trivalent aluminum and iron cations have some common characteristics when these salts are dissolved in water. The metal (M) ion hydrates and is hydrolyzed to form monomeric and polymeric species MOH^{+2}, $M(OH)_2^{+}$, $M_2OH_2^{+4}$, $M(OH)_3$ (S), and $M(OH)_4^{-1}$**[44].**

Francois in 1988 described the application of mathematical expression of kinetics of flocculation **[45]**, to hydrolysis of metal salt when used as a coagulant. He demonstrated that using higher mixing intensities, a longer rapid mixing period, a higher concentration of suspended solids or a higher coagulant dose, could raise the rate constant of particle removal. Under very acidic conditions, both Fe^{+3} and Al^{+3} remain in solution. As pH is increased or as coagulant concentration is raised hydrolysis occurs to form metal hydroxides $M(OH)_3$(S)

Hydrolysis speed and efficiency depends on pH, alkalinity and water temperature. Efficiency increases as insoluble hydroxide form for entrapment and as hydrolysis products are formed with higher charge, which enhances neutralization. Alum gives best removal of turbidity between pH 6.0 and 7.5. Between pH 8.5 and 10.0, alum is an inefficient coagulant because hydrolysis continues in this pH range until soluble aluminates predominate and little flocs form **[46]**.

2.4.2 Role of Polymers in Enhancing Flocculation

In addition to various electrolytes such as ferric chloride or aluminum sulfate, polymeric flocculants are also widely employed to promote toxic pollutant adsorption during floc formation before sedimentation. These polymeric flocculants can be based on natural products, such as starches or alginates, or extracts from various types of seeds. **[47]**. The flocculation of colloidal particles by introduction of polymer into the liquid suspension is an important solid-liquid separation process in various municipal wastewater treatments.

In case of polymers, carrying an opposite charge to the particles, the electrical repulsion is reduced and the particles can be de-stabilized. When the adsorbing material has the same sign of charge as the particles, repulsion is increased and particles restabilized. In case of non-ionic polymers, electrical interaction can still be affected, though in a less drastic manner. Adsorption of polyelectrolytes at the particle/liquid interface plays an important role in the flocculation and stabilization behavior of colloidal suspensions. These polymeric materials are often highly effective at low doses. It has been well demonstrated in the literature that polyelectrolytes can affect particle flocculation by two mechanisms: Polymer bridging and electrostatic patch attraction

The bridging of colloidal particles by polymer chain results in larger structural units that are readily separated from aqueous dispersing medium. Cationic polymers are widely used for flocculation of negatively charged wastewater. It was believed that low molecular weight polycations cause flocculation because they neutralize the particle charge, and the high molecular weight polycations work via a combined electrostatic and bridging mechanism. It has been noted that optimum flocculation proceeds when the particle charge has been reduced to around zero **[48]**.

Many others note that the molecular mass of cationic flocculent should not be an important factor, and flocculent efficiency should depend upon the charge density of the polyelectrolyte. Trivanti et. al. has explained that increasing the charge density **[49]** of polymers will increase their electrostatic attraction to particles of opposite charge and more extended adsorbed polymer configurations will favor flocculation.

On the other hand, Smith Palmer et al. **[50]** studied the flocculation of kaolin suspensions using cationic polyacrylamides of similar high molar mass but of different charge densities and they found that the settling rates decreased as the charge densities increased.

Lindquist and Straton studied the flocculation power of cationic polyethylenimines on negatively charged silica sol particles as a model system. They proposed both polymer bridging and charge neutralization may function simultaneously and the relative importance between them is pH dependent. At high pH (>9), polymer bridging should dominate flocculation due to the low cationic charge of basic polymers and at low pH (<9), strong electrostatic attraction between polycations and negative particles is the dominant mechanism **[51]**.

Polymer adsorption may also increase colloidal stability by increasing the coulombic repulsion between the particles. J. Gregory in 1972 observed that in contrast to simple electrolytes, polymers often show an optimum range of flocculation concentration above which the sol particles restabilized. In this study suspension of polystyrene particles was flocculated by a series of cationic polymers of varying molecular weights. The rates of flocculation were compared with those obtained by addition of sodium nitrate **(52)**. It is also been observed that at a concentration above an optimum concentration, flocculation rate decreases. The rate of polymer flocculation was found to increase with decreasing ionic strength and the maximum rate observed was approximately about twice the rate with high electrolyte concentration.

It follows from the discussion above that either destabilization or restabilization can occur on introduction of polyelectrolyte into a colloidal system. Critical in deciding the efficiency of treatment is concentration of the polyelectrolyte added in relation to colloidal concentration.

CHAPTER 3

LABORATORY PROCEDURE AND EXPERIMENTAL SET-UP

3.1 Sample Preparation

Sampling of natural surface run-off is weather dependent and depends on the events such as total rainfall, rainfall intensity together with background characteristics, which greatly affect the experimental variables. Synthetic samples were prepared for the experimental program.

The dry residual materials collected from the parking facility (NJIT Parking lot # 6) were found to contain the basic characteristics of the parking-lot surface run-off samples and hence such residues were collected and used to prepare the synthetic sample. In analyzing the dry residual materials for the organic content it was found that there are two types of materials, the low organic content material and the high organic content material.

1) The low organic content material (sandy like) was found in the areas along the walls of the parking lot. The total volatile solid content of this type of material was found to be less than 1% by weight. The size of this material was less than 450 micrometers. This sandy like material was sieved and divided into seven particle size ranges as shown in Table 3-1

Table 3-1 Dry Sample Size Characteristics

Particle size range (micrometers)	Control sieve No. (ASTM)
less than 53	270
53 --- 75	270 – 200
75 --- 106	200 – 140

Table 3-1 Dry Sample Size Characteristics (Continued)

106 --- 150	140 – 100
150 --- 250	100 – 60
250 --- 425	60 – 40
Larger than 425	40

After performing a series of sample preparation tests, the quantity of each range for preparing the sample was determined. It was found that the material with grain size larger than 106 micrometers would settle too fast to make a uniform sample while the material with grain size smaller than that would remain suspended, hence it was concluded that particles smaller than the 106 micrometers were more suitable for suspension.

2) The high organic content material was found attached to the ground surface under parked car. The total volatile solid content of this type of material was found to be approximately 18% by weight. In performing sample preparation tests, it was found that this material either settles at the bottom of the jar or floats on the surface. In order to obtain suspended volatile solids this material was first ground with different compositions of clay content and then used to prepare the sample. After grinding with clay, it was found that this type of material remained in suspended state.

Thus after performing a series of tests, the above two types of materials were used to prepare the synthetic sample in such a manner as to give enough colloidal suspended particles and natural sample characteristics. This synthetic sample was used throughout the different experimental phases in order to understand the zeta potential behavior and role of microcarrier in micro-carrier enhanced flocculation.

3.2 Types of Coagulants

Three types of coagulants were used through out the experimental phases. These three coagulants are aluminum sulfate (electrolyte), different types of polyelectrolytes, and micro-carrier.

3.2.1 Electrolyte

Various coagulants such as ferric chloride, ferrous sulfate, aluminum sulfate (alum), aluminum chloride have been used in the removal of colloidal particles. Compared with alum, ferric chloride coagulates over a broader pH range and forms a heavier floc, however liquid ferric chloride is acidic and corrosive and causes staining and requires special materials of construction.

Aluminum salts work efficiently but their continued use is questioned due to chemical cost, the impact of residual aluminum upon receiving waters and a possible link between aluminum and Alzheimer's disease. A disadvantage of adding alum is the high concentrations of sulfate ions, which remains in solution posing downstream treatment difficulties and leading to increase total dissolved solids levels. In its favor however, is the avoidance of handling, corrosion and staining difficulties when compared with the use of iron salts.

Alum [$Al_2(SO_4)_3.14H_20$] was used as an electrolyte for this study. Alum solutions were prepared using deionized water. The zeta potential distribution of alum solutions of different concentration is presented in the Figure 3.1. It can be seen that the zeta potential increases with an increase in electrolyte concentrations within the range of 10 to 100 mg/L. Alum salts when hydrolyzed in water forms charged hydrolysis products which

increases the overall charge of the solution and the observed zeta potential value increases. Figure 3.2 illustrates the distribution of pH values of different concentration of electrolytes. The pH value was found to decrease from 5.2 to 3.5 gradually when the alum concentration increases from 10 to 100 mg/L. This is as expected since alum salt on hydrolysis, forms various hydrated products and protons concentration increases in the solution and thus the pH of the solution decreases.

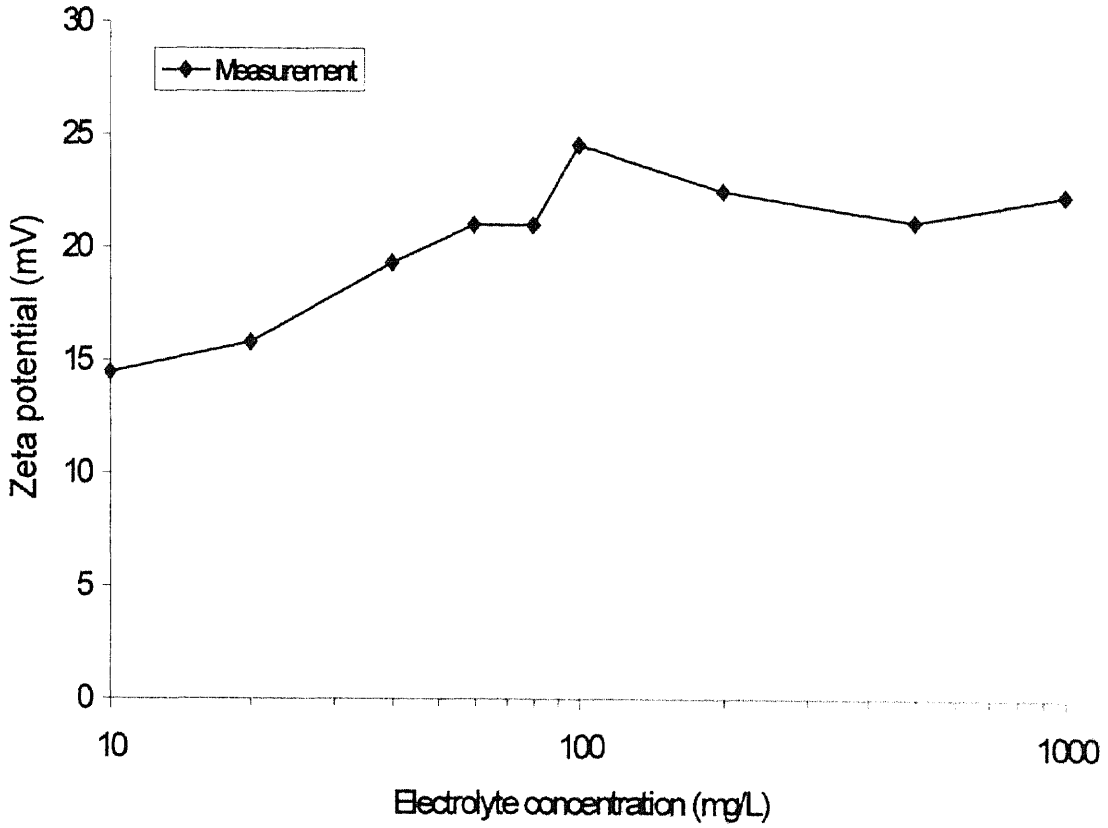

Figure 3-1 Zeta Potential versus Electrolyte Concentration.

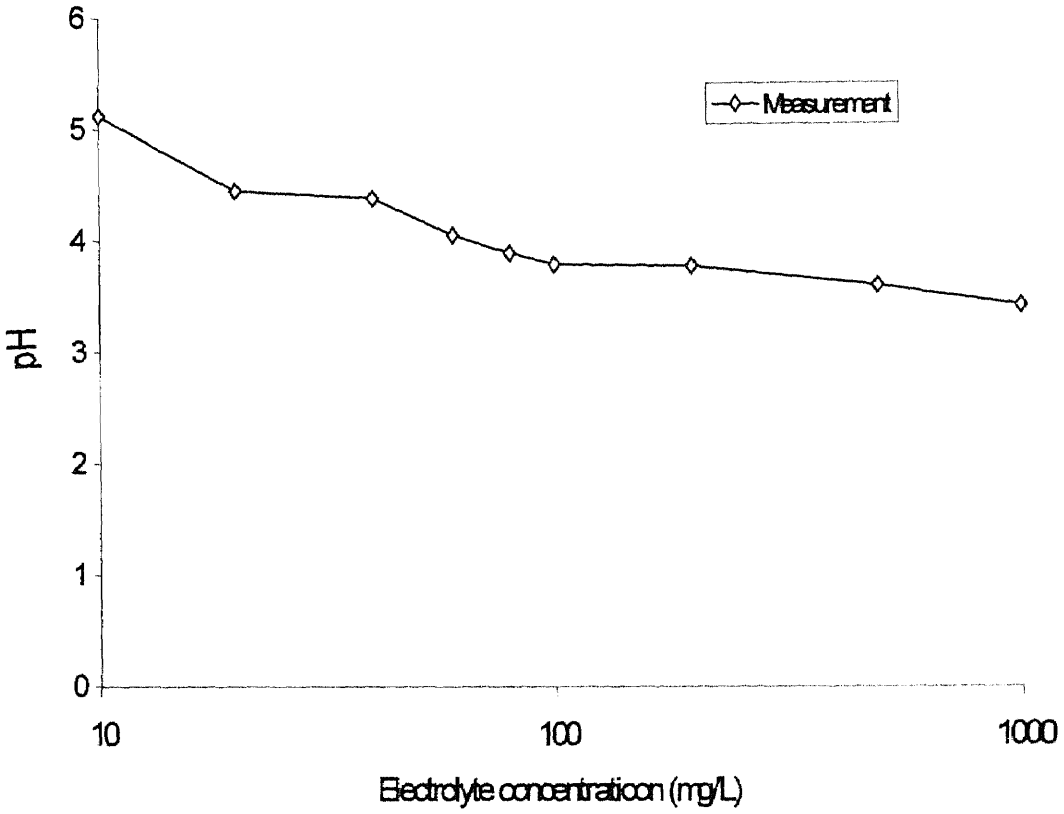

Figure 3-2 pH versus Electrolyte Concentration

3.2.2 Polyelectrolyte

In this study, four different polyelectrolytes obtained from Calgon Corporation, Pittsburgh, Pennsylvania, were used. All the four polyelectrolytes are emulsion polymers. Table 3-2 presents basic characteristics of these four polyelectrolytes and charge associated with it.

Table 3-2 Polyelectrolytes and their Properties

Polyelectrolyte type	Polyelectrolyte charge	Relative charge	Relative molecular wt.	% by weight
POL-EZ 2696	Non-ionic	High	10^{15}	38 %
POL-EZ 2466	Cationic	High	10^{15}	38 %
POL-EZ 3466	Cationic	High	10^{15} - 10^{20}	25-27 %
POL-EZ 7736	Anionic	High	10^{15} - 10^{20}	26 %

Zeta potential distribution versus polyelectrolyte concentration for each type of polyelectrolyte are illustrated in Figure 3.3

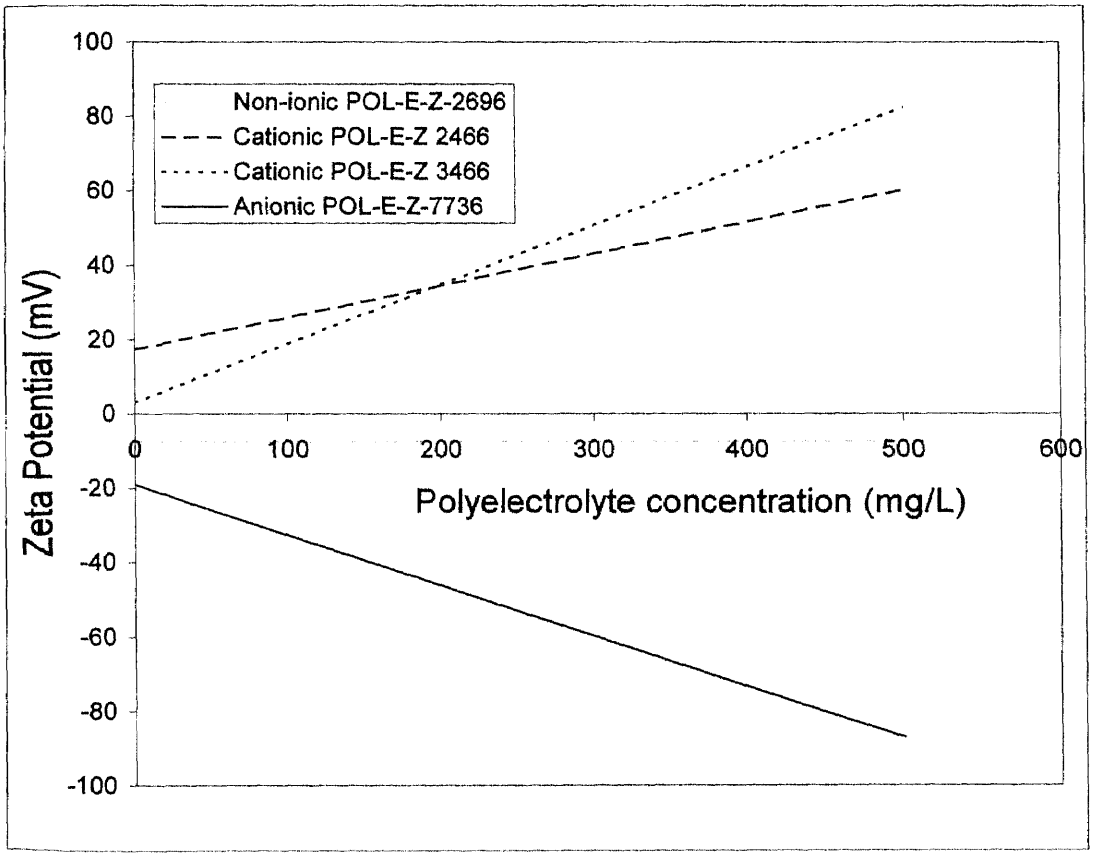

Figure 3-3 Zeta Potential versus Polyelectrolyte Concentration

3.2.3 Micro-carrier

An Ottawa sand was used as a microcarrier in weighted flocculation. Ottawa sand was chosen as it is commercially available and has been used in the study of soil analysis. The size range of Ottawa sand used was below 150 micrometer and ottawa sand of this size range was obtained by sieve analysis. This was decided on the basis of a review in which it was found that in the case of grain size below 160 micrometer, there is a fairly uniform settling velocity distribution **[9].** All containers and micro-carrier were first washed thoroughly with a detergent and hot water and then rinsed with hot water to remove all traces of residual washing compound. These were finally rinsed with particle free water to ensure that no other particles were attached to the sand and involved in the process.

3.3 Instruments and Procedure

3.3.1 Jar Test Apparatus

Jar test procedures are widely used to evaluate the efficiency and the effectiveness of the coagulant in the wastewater treatment. This procedure provides with a vigorous distribution of the polymers, during the rapid mix cycle and ensures that adsorption step will uniformly cover the necessary surface of each particle. Slow mixing provides for growth and testing a series of doses gives the range of optimum coagulants needed to achieve the best removal of colloidal particles. In a conventional jar test a series of six cylindrical beakers are stirred simultaneously by paddle stirring after the addition of flocculent doses. Micro-carrier enhanced jar test due to its different physical conditions is a new technology. A new jar test procedure was developed by Dr. Yuan Ding, for the micro-carrier weighted jar test which has been adopted in this study. For a detailed description of the jar test the reader is referred to Dr. Yuan Ding, Dept. of Civil and

Environmental Engineering, NJIT. In essence, the jar test apparatus consists of six 2000-mL square beakers mounted on a multiple stirring machine equipped with a variable speed drive. The jar test apparatus used in experimental program is shown in Figure 3-4.

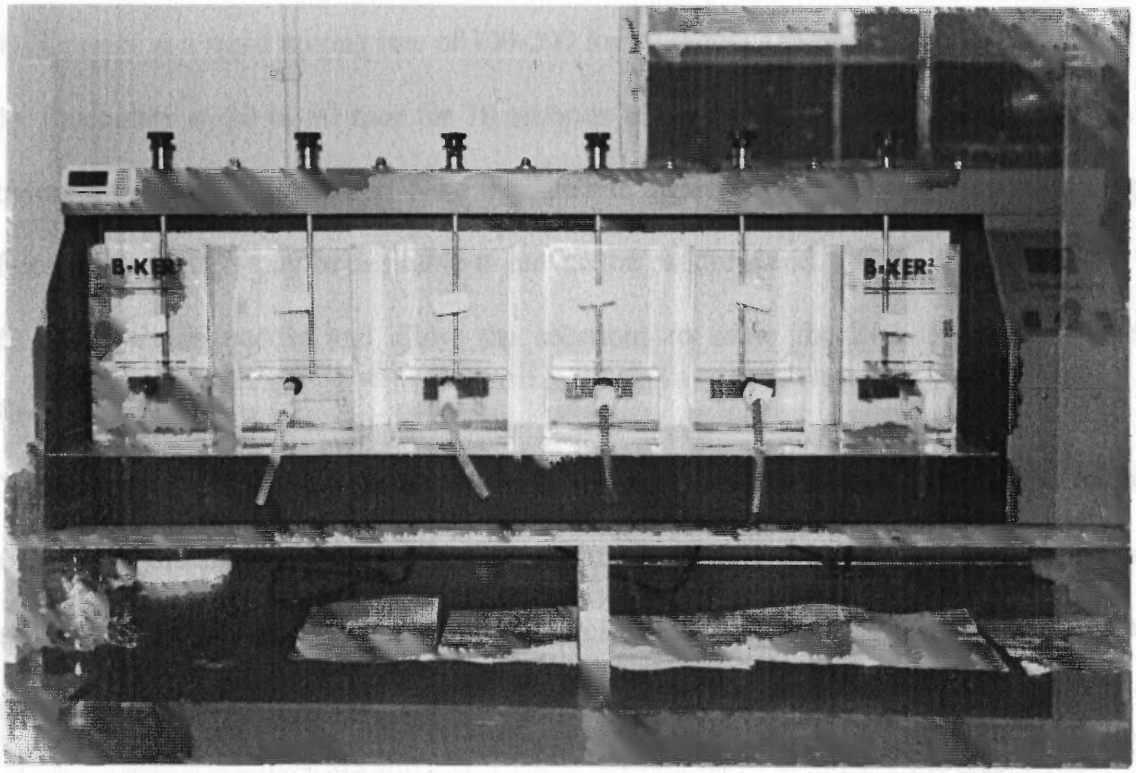

Figure 3-4 Jar Test Apparatus

The detailed procedure of the jar test is enumerated as follows. The jar test procedure includes the following steps:

1) Prepare a synthetic sample and analyze its background parameters such as pH, turbidity and zeta potential.

2) Place 1000 mL of the sample into a 2000-mL jar on the six-jar laboratory stirrer and check stirrer operation. A light table facilitates viewing of the contents of the beakers.

3) Add a predetermined amount of micro-carriers and electrolyte solutions with polyelectrolyte to each of the designated jars.

4) Operate at a rapid mixing rate of 100-200 for 10 seconds to one minute

5) Flocculate at 30 to 60 rpm for 10 seconds to 20 minutes. Record the elapsed time before a visible floc is formed. Note the size and appearance of the floc formed. If large flocs are formed, it may be desirable to reduce the paddle speed.

6) Remove the paddle and allow the solutions to settle for 2 to 30 minutes after flocculation.

7) Take the supernatant solution one inch below the surface of water in each jar taking care not to disturb the sediment in the sampling procedure. Measure the turbidity of the supernatant in each jar. Select the optimum dosage on the basis of supernatant clarity and settling of flocs.

3.3.2 Zeta Potential Analyzer

There are several ways of measuring zeta potential including electro-osmosis, streaming potential and micro electrophoresis. Micro electrophoresis is the most widely used method to measure zeta potential. The zeta potential analyzer used in this study, was manufactured by Brookhaven Instruments Corporation. (see Figure 3-5) and is based on

microelectrophoresis. A detailed outline of the theory behind the zeta potential measurement is given in appendix A.

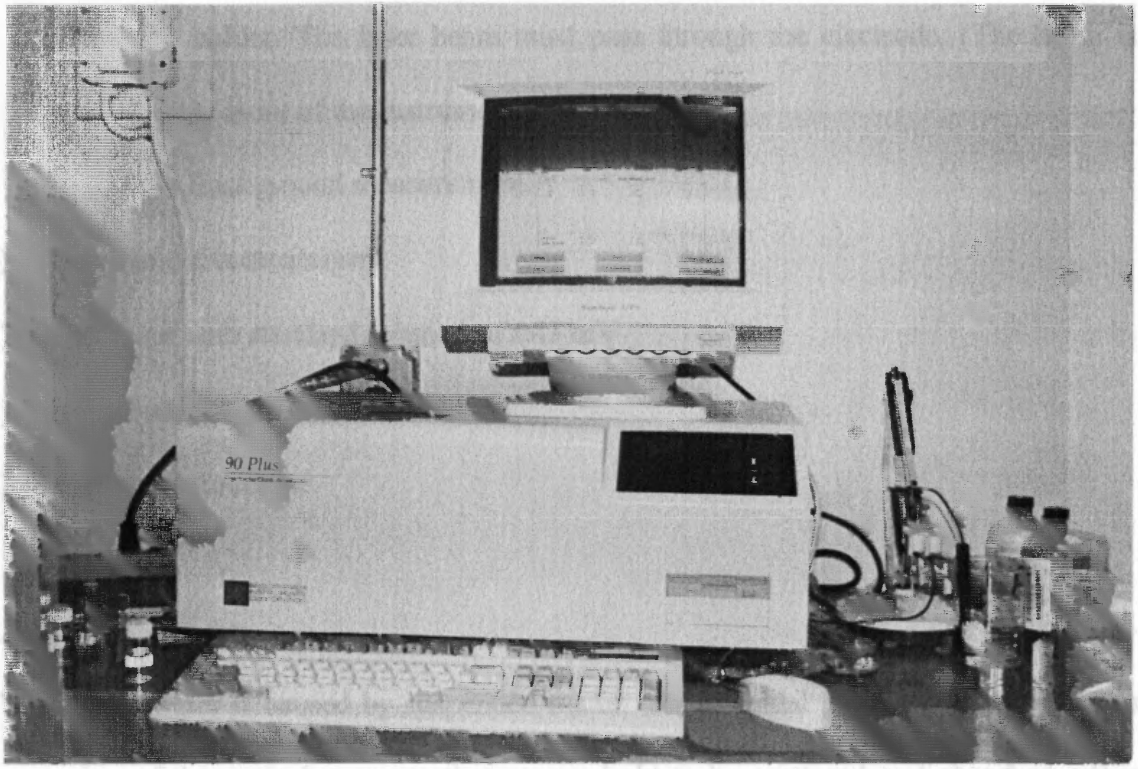

Figure 3.5 Zeta Potential Analyzer

The principal steps involved in the Zeta potential measurement are as follows.

1) For blank, standard and sample measurement the following procedure is followed.

   a) Pour or pipette about 1 mL of solution of interest into a four-sided clear square glass cell. (The cell should be rinsed once or twice with the solution)

   b) Clean the electrode by rinsing with filtered water. Sonicate for a few seconds in clear water. Then rinse with the solution of interest.

c) Insert the electrode assembly into the cell slowly and making sure that the solution in the cell is not displaced sufficiently to overflow.

d) Insert the cell into the cell compartment such that the electrodes are parallel to the front of the zeta potential analyzer with the connector positioned to the right side of the cell holder. The laser beam must pass through the electrode. (The beam is parallel to the front of the instrument).

e) Make Background measurement

3) Blank sample measurement

4) Calibration with standard solution of ±43 mV

5) Sample preparation

6) Sample measurement

3.3. 3 Turbidimeter

Turbidity in water is caused by suspended matter and colloidal particles. Turbidity is an expression of the optical property that causes light to be scattered and absorbed rather than transmitted in straight lines through the sample. Nephalometric methods are used for the measurement of the turbidity in terms of Nephalometric units. This method is based on the comparison of the intensity of light scattered by a standard reference suspension under the same conditions. For this study HF Scientific DRT-15CE turbidimeter is used.

Turbidimeter consisting of a nephelometer with a light source for illuminating the sample and one or more photoelectric detectors with a readout device to indicate intensity of light scattered at 90° to the path of incident light. The principal steps involved in the measurement of turbidity are as follows.

1) Turbidimeter calibration: HF turbidimeters are calibrated using HF scientific factory certified secondary standards or formazin. The available secondary standards are 10,100 and 1000 NTU (nephalometric turbidity unit). The 0.02 NTU standard is a reference standard, which is contained in the pre-selected cuvettes with light shield caps. The instrument should be calibrated using all the above secondary standard solutions.

2) For measurement of turbidities less than 40 NTU: Thoroughly shake the sample. Wait until air bubbles disappear and pour samples in turbidimeter tube. Read turbidity directly from the instrument scale.

3) For measurement of turbidities above 40 NTU: Dilute sample with one or more volumes of turbidity free water until turbidity falls between 30-40 NTU. Compute turbidity of original sample from the turbidity of the diluted sample and dilution factor.

3.3.4 pH Meter

The pH meter used in this study is combined with the zeta potential analyzer. The standard method **[53]** for the measurement of pH is used to measure the pH of the various samples. The principal steps involved in pH measurement are as follows

1) Calibrate the pH meter. It must be calibrated at a minimum of two points that bracket the expected pH of the sample and are calibrated at pH 7.0 and pH 4.0/10.0.

2) Place the sample or buffer solution in a clean glass beaker using a sufficient volume to cover the sensing elements of the electrodes and to give adequate clearance for the magnetic stirring bar.

3) After rinsing and gently wiping the electrodes immerse them into the sample beaker and stir at a constant rate to provide homogeneity and suspension of the solids. Rate of stirring should minimize the air transfer rate at the air water interface of the solution.

4) Note and record sample pH.

5) Repeat measurement on the successive volumes of the sample until values differ by less than 0.1 pH units.

3.4 Experiments

A synthetic sample was first prepared and characterized, for various parameters such as turbidity, zeta potential and pH. Experimental variables to be included are: electrolyte concentration, polyelectrolyte type and concentration, rapid mixing time and rotation rate, flocculation time and rotation rate, supernatant zeta potential, supernatant turbidity and supernatant pH. A number of different jar tests were then performed on the synthetic sample in order to study the flocculation behavior of the micro-carrier process and the effect of zeta potential on the efficiency of the process. The basic operating conditions for a jar test such as rapid mixing rate and rotation time, flocculation mixing rate and rotation time, size and type of micro-carrier etc. are adopted from a process developed by Dr. Yuan Ding. This process is summarized as follows.

Table 3-3 Summary of the Operating Parameters

PARAMETER	VALUE
Rapid mixing rate -- stage 1	150 rpm
Rapid mixing duration -- stage 1	10 seconds
Rapid mixing duration -- stage 2	10 seconds
Rapid mixing rate – stage 2	100 rpm
Flocculation mixing rate	60 rpm
Flocculation mixing duration	10 seconds
Micro-carrier concentration – 1	3 g/L
Micro-carrier size --- 1	0-150 micrometers

Table 3-3 Summary of the Operating Parameters (Continued)

Settling time	3 min
Settling time	8 min
Electrolyte concentration	10 --- 80 mg/L
Polyelectrolyte concentration	0.3 --- 1.5 mg/L

3.5 Experimental Design

The principal aim of this study was to understand the role of microcarrier in enhancing flocculation and to study the various parameters such as colloidal interactions, collision efficiency etc. which influences the removal of colloidal particles. The experimental design of this study consisted of the following phases

I. Effectiveness of the micro-carrier process.

II. Tests to determine the optimum concentration of electrolyte in presence of polyelectrolytes

III. Tests to determine the effect of different concentrations of polyelectrolytes.

3.5.1 Phase I

The purpose of phase I testing was to determine the coagulation behavior in absence and in presence of micro-carrier. Also, best electrolyte concentration in absence of polyelectrolyte was determined in this phase. Electrolyte concentration was varied from 0 to 80 mg/L. In Phase I-A varying concentration of aluminum sulfate was used as a coagulant while in phase I-B varying concentration of aluminum sulfate and a fixed concentration of micro-carrier was used. The comparison of both these sub-phases provided the information on the effectiveness of the micro-carrier process and also helped

in evaluating the zeta potential behavior of the micro-carrier process and other parameters governing the process. The parameters for Phase I-A and I-B are shown in Table 3-4.

Table 3-4 Parameter for Phase I

Test Phase	Additives	Jar 1	Jar 2	Jar 3	Jar 4	Jar 5	Jar 6
Phase I-A	Electrolyte (mg/L)	0	10	20	40	60	80
Phase I-B	Micro-carrier	Size 0-150 micrometer , 3 gm/L					
	Electrolyte (mg/L)	0	10	20	40	60	80

3.5.2 Phase II

The purpose of phase II was to study the role of different charged type polyelectrolyte in facilitating the microcarrier enhanced removal of colloidal particles. In this phase, four different types of polyelectrolytes were used and then effect of polyelectrolyte on optimizing the dose of electrolyte was determined in this phase. Three different charged polyelectrolytes: anionic, cationic and non-ionic polyelectrolytes were used. The micro-carrier, electrolyte and polyelectrolyte type or concentrations used in this phase are presented in Table 3-5.

Table 3-5 Parameter for Phase II

Test phase	Additive	Jar 1	Jar 2	Jar 3	Jar 4	Jar 5	Jar 6
Phase II-A	Micro-carrier	Size 0-150 micrometer , 3 gm/L					
	Electrolyte (mg/L)	0	10	20	40	60	80
	Polyelectrolyte I (mg/L)	1	1	1	1	1	1
Phase II-B	Micro-carrier	Size 0-150 micrometer , 3 gm/L					

Table 3-5 Parameter for Phase II (Contniued)

	Electrolyte (mg/L)	0	10	20	40	60	80
	Polyelectrolyte II (mg/L)	1	1	1	1	1	1
Phase II-C	Micro-carrier	Size 0-150 micrometer , 3 gm/L					
	Electrolyte (mg/L)	0	10	20	40	60	80
	Polyelectrolyte III (mg/L)	1	1	1	1	1	1
Phase II-D	Micro-carrier	Size 0-150 micrometer , 3 gm/L					
	Electrolyte (mg/L)	0	10	20	40	60	80
	Polyelectrolyte IV (mg/L)	1	1	1	1	1	1

3.5.3 Phase III

The purpose of this phase was to determine the influence of polyelectrolyte concentration on the removal of colloidal particles. The best electrolyte concentration based on phase II was used for each jar in this phase. The polyelectrolyte concentration setup ranging from 0.3 to 1.5 mg/L is illustrated in Table 3-6.

Table 3-6 Parameter for Phase III

Test phase	Additive	Jar 1	Jar 2	Jar 3	Jar 4	Jar 5	Jar 6
Phase III-A	Micro-carrier	Size below 150 micrometer , 3 gm/L					
	Electrolyte (mg/L)	40	40	40	40	40	40
	Polyelectrolyte I (mg/L)	0.3	0.5	0.7	1.0	1.2	1.5
Phase III-B	Micro-carrier	Size below 150 micrometer , 3 gm/L					
	Electrolyte (mg/L)	40	40	40	40	40	40
	Polyelectrolyte II (mg/L)	0.3	0.5	0.7	1.0	1.2	1.5
Phase III-C	Micro-carrier	Size below 150 micrometer , 3 gm/L					
	Electrolyte (mg/L)	40	40	40	40	40	40

Table 3-6 Parameter for Phase III (Continued)

	Polyelectrolyte III (mg/L)	0.3	0.5	0.7	1.0	1.2	1.5
Phase III-D	Micro-carrier	Size below 150 micrometer , 3 gm/L					
	Electrolyte (mg/L)	40	40	40	40	40	40
	Polyelectrolyte IV (mg/L)	0.3	0.5	0.7	1.0	1.2	1.5

CHAPTER 4

RESULTS AND DISCUSSIONS

4.1 Phase I

This chapter discusses the observation results and the possible mechanism of micro-carrier weighted flocculation. In Phase I-A, varying concentrations of electrolyte were used and in Phase I-B, in addition to electrolyte, a known quantity of micro-carrier was used to carry out the flocculation. After conducting a jar test with the above mentioned coagulants on a synthetic sample and allowing the solution to settle, the supernatant solutions were sampled after 3 minute and 8 minute settling time. These samples were than analyzed for zeta potential, residual turbidity and pH. Table 4-1 and 4-2 shows the measurement of various parameters, including the experimental conditions, for Phase I-A and Phase I-B respectively.

Table 4-1 Observation for Phase I-A

PARAMETER	Jar 1	Jar 2	Jar 3	Jar 4	Jar 5	Jar 6
Alum concentration (mg/L)	0	10	20	40	60	80
Turbidity (3 min. settling time)	104.3	103.9	87.6	47.4	44.4	43.5
% removal in turbidity	25.5	25.8	37.43	66.15	68.29	68.93
Turbidity (8 min. settling time)	98.3	91.3	66.2	23.9	24.2	25.8
% removal in turbidity	29.79	34.79	52.72	82.93	82.72	81.58
pH (3 min. settling time)	6.69	6.79	6.73	6.52	6.18	5.74
pH (8 min. settling time)	6.88	6.97	6.86	6.53	6.29	5.66
Zeta potential (3 min. settling time)	-16.58	-16.78	-16.98	-13.47	1.14	1.55
Zeta potential (8 min. settling time)	-14.64	-13.02	-15.89	-13.23	0.00	6.0

Table 4-2 Observation for Phase I-B

PARAMETER	Jar 1	Jar 2	Jar 3	Jar 4	Jar 5	Jar 6
Micro-carrier Type	Ottawa Sand					
Micro-carrier size	0-150 micrometer					
Micro-carrier concentration	3 gm.					
Alum Concentration (mg/L)	0	10	20	40	60	80
Turbidity (3 min settling time)	47.3	42.1	28.1	8.5	3.1	5.2
% removal in turbidity	40.12	46.70	64.43	89.24	96.07	93.41
Turbidity (8 min settling time)	53.6	29.0	10.3	3.7	1.5	2.5
% removal in turbidity	32.16	63.3	86.97	95.32	98.11	96.84
pH (3 min. settling time)	7.2	7.1	7.2	6.7	6.4	5.7
pH (8 min. settling time)	7.3	7.2	7.1	7.0	6.8	6.2
Zeta potential (3 min. settling time)	-25.0	-24.7	-19.9	-18.7	4.7	13.7
Zeta potential (8 min. settling time)	-17.0	-15.4	-19.7	-17.0	-18.8	-9.7

Colloidal particles in wastewater are negatively charged. When counter-ions are adsrobed, on colloidal particles the particle charge is reduced and flocculation occurs. Specific adsroption is regarded as arising from interactions of non-electrostatic interactions which is evident from the charge reversal of particles when treated with an excess of counter-ions. With the charge reversal the surface potential becomes sufficiently high and causes restabilization of the particles **[15]**.

Figures 4-1 and 4-2 show variation in zeta potential as a function of electrolyte concentration for Phase I-A and Phase I-B at 3 minute and 8 minute settling time respectively. In Phase I-A, as expected, zeta potential value decreases as electrolyte concentration increases and at a concentration of 60 mg/L approximately a neutral zeta potential value is observed. As the concentration increases from 60 mg/L to 80 mg/L, a

charge reversal in zeta potential is observed, due to the specific, non-coulombic, chemical binding and restabilization occurs. This is as expected from the above mentioned theory. Hence, in this case electrolyte concentration of 60 mg/L can be considered as an optimum coagulation concentration.

In case of Phase I-B the zeta potential variation with electrolyte concentration shows a decrease in zeta potential value as the electrolyte concentration increases. In case of 8 min settling time zeta potential values are slightly negative. However, the overall pattern follows the trend as observed in case of Phase I-A. Since the use of micro-carrier shows the same kind of zeta potential behavior we can conclude that micro-carrier has no effect on the reduction of charge on the particle or on destabilization of colloidal particles.

On conducting a jar test using micro-carrier alone, it was found that turbidity of original sample increased appreciably. It was also observed that when only micro-carrier is used in the process no flocculation was observed and the residual turbidity increased significantly. Thus micro-carrier process also require addition of electrolyte to initiate the charge neutralization process.

Figures 4-3 and 4-4 shows relationship between removal in turbidity (percentage) and electrolyte concentration. Maximum removal in turbidity, which is an indicator of maximum destabilization of colloidal particles, occurs at neutral value of zeta potential (at electrolyte concentration of 60 mg/L). This is true for both Phase I-A and Phase I-B. These results are clearer from Figures 4-5 and 4-6 which show the variation in residual turbidity as a function of zeta potential where it is observed that as the zeta potential value decreases the residual turbidity decreases and turbidity is minimum at the neutral zeta potential value.

However, in case of Phase I-B at neutral zeta potential value, turbidity can be removed up to 98%, where as in case, of Phase I-A only 82% removal in turbidity can be obtained at similar operating conditions

Flocculation is often followed by aggregation of particles and this process is governed by several factors such as collision frequency, collision efficiency and stability ratio. These factors can also affect the separation, aggregation and transport of destabilized colloidal particles. Physical factors such as diffusion, temperature, fluid mixing, particle size have direct influence on particle collision and attachment.

The role of micro-carrier in enhancing turbidity removal can be explained to a certain extent in terms of collision efficiency. Collision efficiency, which is a measure of the effective collision leading to adherence of colliding particles, can also be presented in a reciprocal form, stability ratio (W), which is an indication of the stability of the colloidal particles. Collision efficiency or stability ratio are calculated for Phase I –A and Phase I-B (considering collision frequency factor β as a constant) using the equation 2.17 which is given as

$$\alpha_a = \frac{\pi}{4\phi G t} \ln \frac{n_0}{n_t}$$

where α_a is collision efficiency of aggregation; ϕ is volume fraction of solid material in suspension; G is velocity gradient; t is flocculation time and n_0/n_t is determined from turbidity measurement, which represents the rate of disappearance of primary particles.

Figure 4-7 shows the variation of experimental stability ratio as a function of electrolyte concentration. It was observed that experimentally calculated stability ratio, is high in case of Phase I-A, while it was low in case of Phase I-B. As collision efficiency increases the effective collisions between particles leading to attachment of particles

increase. This result suggests that collision efficiency is greater when micro-carrier is employed in the coagulation process, which indicates that higher number of collisions are effective in Phase I-B compared to Phase I-A. This results in adhesion of higher number of particles and greater removal in turbidity is observed.

A comparison is also made for the variation of pH as a function of electrolyte concentration, which is shown in Figure 4-8 and 4-9. This shows a decrease in pH as electrolyte concentration increases.

This decrease in pH values is the result of the hydrolysis of alum salts, which increase the H ion concentration and increase acidity in the solution **[44]**. pH values were observed in range of 5.5 to 7.5, for both set of jar tests, which is the best range of pH (as mentioned in section 2.4.1) for which aluminum salts give good flocculation and the best removal in turbidity.

4.2 Phase II

Results of Phase I indicated that micro-carrier enhances flocculation of colloidal particles in presence of electrolyte by increasing the collision efficiency of the process. The study was further extended to Phase II. In Phase-II, in addition to electrolyte and micro-carrier, four different polyelectrolytes were also used and the effects of these polyelectrolytes on the process were studied. In this phase, all the three different types of polyelectrolyte i.e. cationic, anionic and non-ionic polyelectrolytes were used at concentration of 1 mg/L and electrolyte concentration was varied from 0 to 80 mg/L. Four sets of jar tests were conducted using four different polyelectrolytes and supernatant solutions after a settling time of 3 minute and 8 minute were collected and analyzed for zeta potential, residual turbidity and pH. Table 4-3 shows the measurement of various parameters when, non-

ionic polyelectrolyte POL-E-Z 2696 is used as a coagulant aid (Phase II-A). Similarly, Table 4-4, 4-5 and 4-6 shows the measurement of various parameters, for cationic POL-E-Z 2466 (Phase II-B), cationic POL-E-Z 3466 (Phase II-C) and anionic POL-E-Z 7736 (Phase II-D) respectively.

Table 4-3 Observations for Phase II-A

PARAMETER	Jar 1	Jar 2	Jar 3	Jar 4	Jar 5	Jar 6
Micro-carrier type	Ottawa Sand					
Micro-carrier size	0-150 micrometer					
Micro-carrier concentration	3 gm.					
Alum concentration (mg/L)	0	10	20	40	60	80
Polyelectrolyte type	POL-E-Z 2696 (Non-ionic Polyelectrolyte)					
Polyelectrolyte conc. (Mg/L)	1	1	1	1	1	1
Turbidity (3 min. settling time)	3.2	2.3	1.2	0.5	0.8	2.6
% removal in turbidity	96.24	97.3	98.59	99.42	99.06	96.95
Turbidity (8 min settling time)	2.5	1.9	1.15	0.5	0.4	1.2
% removal in turbidity	97.06	97.77	98.71	99.42	99.53	98.59
pH (after 3 min settling time)	7.0	7.5	7.3	7.0	6.5	5.5
pH (after 8 min settling time)	7.4	7.4	7.4	7.0	6.6	5.8
Zeta potential (after 3 min settling time)	-21.9	-12.4	-18.4	-18.6	-11.4	6.8
Zeta potential (after 8 min settling time)	-21.0	-12.6	-17.8	-14.5	-12.1	2.3

Table 4-4 Observations for Phase II-B

PARAMETER	Jar 1	Jar 2	Jar 3	Jar 4	Jar 5	Jar 6
Micro-carrier Type	Ottawa Sand					

Table 4-4 Observations for Phase II-B (Continued)

Micro-carrier size	0-150 micrometer					
Micro-carrier concentration	3 gm.					
Alum concentration (mg/L)	0	10	20	40	60	80
Polyelectrolyte type	POL-E-Z 2466 (Cationic Polyelectrolyte)					
Polyelectrolyte conc. (mg/L)	1	1	1	1	1	1
Turbidity (3 min. settling time)	17.6	5.4	2.4	0.9	0.9	0.6
% removal in turbidity	81.48	94.31	97.47	99.05	99.05	99.36
Turbidity (8 min. settling time)	17.4	5.3	1.1	0.3	0.5	0.4
% removal in turbidity	81.68	94.42	98.84	99.68	99.47	99.57
pH (3 min. settling time)	7.2	7.0	7.1	6.5	7.0	5.7
pH (8 min. settling time)	7.3	7.1	6.9	6.6	6.0	5.8
Zeta Potential (3 min. settling time)	-19.7	-22.3	-16.5	-15.8	-9.4	0.3
Zeta Potential (8 min. settling time)	-23.3	-23.3	-10.6	1.8	7.5	14.5

Table 4-5 Observations for Phase II- C

PARAMETER	Jar 1	Jar 2	Jar 3	Jar 4	Jar 5	Jar 6
Micro-carrier Type	Ottawa Sand					
Micro-carrier size	0-150 micrometer					
Micro-carrier concentration	3 gm.					
Alum concentration (mg/L)	0	10	20	40	60	80
Polyelectrolyte type	POL-E-Z 3466 (Cationic Polyelectrolyte)					
Polyelectrolyte conc. (mg/L)	1	1	1	1	1	1
Turbidity (3 min. settling time)	14.5	8.6	6.3	5.1	11.2	13.4
% removal in turbidity (3 min)	89.42	93.72	95.40	96.27	91.82	90.21
Turbidity (8 min. settling time)	11.2	6.1	4.7	4.3	7.8	9.6
% removal in turbidity (8 min)	91.82	95.54	96.56	96.86	94.30	93.0
pH (3 min. settling time)	6.9	7.0	6.8	6.3	5.8	5.0

Table 4-5 Observations for Phase II- C (Continued)

pH (8 min. settling time)	7.2	7.0	6.8	6.5	5.9	5.0
Zeta potential (3 min. settling time)	-13.9	-0.8	6.5	14.0	17.1	21.4
Zeta potential (8 min. settling time)	-10.4	3.3	5.2	17.9	19.5	22.4

Table 4-6 Observations for Phase II-D

PARAMETER	Jar 1	Jar 2	Jar 3	Jar 4	Jar 5	Jar 6
Micro-carrier Type	Ottawa Sand					
Micro-carrier size	0-150 micrometer					
Micro-carrier concentration	3 gm.					
Alum concentration (mg/L)	0	10	20	40	60	80
Polyelectrolyte type	POL-E-Z 7736 (Anionic Polyelectrolyte)					
Polyelectrolyte conc. (mg/L)	1	1	1	1	1	1
Turbidity (3 min. settling time)	35.7	6.6	3.9	1.4	3.2	8.2
% removal in turbidity	51.75	91.08	94.72	98.10	95.67	88.91
Turbidity (8 min. settling time)	32.6	3.5	2.8	1.2	2.0	4.1
% removal in turbidity	55.94	95.27	96.21	98.37	97.29	94.45
pH (3 min. settling time)	6.8	6.8	6.7	6.4	5.9	5.1
pH (8 min. settling time)	7.3	7.1	6.8	6.4	6.0	5.3
Zeta potential (3 min. settling time)	-31.5	-26.7	-28.3	-19.8	-18.9	5.5
Zeta potential (8 min. settling time)	-35.2	-24.4	-29.2	-23.2	-20.1	8.5

Figures 4-10 and 4-11 show the variation of zeta potential as a function of electrolyte concentration, for all the four polyelectrolytes at settling times of 3 min and 8 min respectively. The variations in the zeta potential values observed were as follows. For all

four polyelectrolytes the zeta potential decreased initially and then charge reversal was observed, which is negligible in case of non-ionic and anionic polyelectrolytes, but was significant in case of both the cationic polyelectrolytes.

Figures 4-12 and 4-13 show the relation between removal in turbidity and electrolyte concentration. For all four sets of jar test, best removal in turbidity was observed at electrolyte concentration of 40 mg/L. These results were compared to the results obtained in Phase I, where electrolyte concentration of 60 mg/L gave best removal in turbidity. This led to the conclusion that when polyelectrolytes were used in a small quantity a reduction of 33.3 % in the dose of electrolyte concentration is found effective. Thus polyelectrolytes work as additives which at very low concentration and at reduced salt concentration give a good removal in turbidity.

In case of flocculation by polyelectrolytes, charge neutralization and polymer bridging play a significant role in the destabilization of colloidal particles. In case of high molecular weight polymers, polymer bridging plays a dominant role in removal of colloidal particles. **[48].** Considering polymer bridging as the dominant mechanism with these polyelectrolytes, (high molecular weight) a good turbidity removal is observed at positive zeta potential values in case of cationic polyelectrolytes.

Figures 4-14 and 4-17 show the relationship between residual turbidity and corresponding zeta potential values for four different polyelectrolytes. It was observed that POL-E- Z 2696 gave a turbidity of less then 3 NTU in a broad range of zeta potential values (approximately –23 mV to +3 mV). Similarly for other three polyelectrolytes it is observed that quite a good flocculation is observed over a comparatively large range of zeta potential. Considering the operating parameters, the flocculation is observed in a very short time.

On the basis of DLVO theory, charge neutralization should result in low values of zeta potential to eliminate the overall repulsive forces and flocculation should occur. In this case, appearance of good floc and high removal in turbidity was observed even at highly negative or positive values and over a broad range of zeta potential values. Thus there are various forces other than DLVO, influencing the overall process of colloidal particle removal.

As mentioned earlier aggregation can also depend upon other factors such as collision factor, collision efficiency, settling kinetics etc. Collision efficiency and stability ratios were calculated for all four different polyelectrolytes using equation 2-17 and were plotted as a function of electrolyte concentration in Figure 4-18. It is seen from the graph that the stability ratios were least at 40 mg/L electrolyte concentration and then increases as electrolyte concentration was increased. It was also observed that the stability ratio falls in a very narrow range for all the four polyelectrolytes. Experimentally calculated stability ratios were very low for all the four different polyelectrolytes, which indicates that, in-spite of presence of some repulsive forces, high collision efficiency enhances the removal of colloidal particles. This high collision efficiency indicates a higher number of collisions are effective and leads to high rate of adherence of particles to each other which eventually leads to observed removal in turbidity. In terms of removal efficiency of different polyelectrolytes, it is observed that all the four polyelectrolytes works almost equally well in removing colloidal particles

Variation in pH values as a function of electrolyte concentration, were shown in Figure 4-19 and 4-20. It was seen that pH decreases as the electrolyte concentration increases. The pH values were almost equal to those obtained in Phase II-A. For all the

three different types of electrolytes, pH values lie in the same range. There is no significance change in pH, in this phase.

In this phase the results showed that all the four polyelectrolytes work quite well in presence of micro-carrier. In addition, the phenomena can be explained to a certain extent by measuring the collision efficiencies in each case.

4.3 Phase III

In Phase III, varying amounts of all the four polyelectrolytes were used. Polyelectrolytes concentrations were varied from 0.3 mg/L to 1.5 mg/L. Electrolyte concentration of 40 mg/L was used in this phase on the basis of the results of Phase II. Jar tests were conducted using constant concentration of electrolyte and micro-carrier and varying concentration of four different polyelectrolytes and the same process of sample collection and parameter measurement was followed. Table 4-7 to 4-10 shows the measurement parameters for four sets of jar tests in this phase.

In Phase III-A, different concentrations of polyelectrolyte POL-E-Z 2696 were used. Table 4-7 shows the conditions used and observations for Phase III-A experiment.

Table 4-7 Observations for the Phase III-A

PARAMETER	Jar 1	Jar 2	Jar 3	Jar 4	Jar 5	Jar 6
Micro-carrier type	Ottawa Sand					
Micro-carrier size	0-150 micrometer					
Micro-carrier concentration	3 gm.					
Alum concentration (mg/L)	40					
Polyelectrolyte type	POL-E-Z 2696 (Non-ionic Polyelectrolyte)					
Polyelectrolyte conc. (mg/L)	0.3	0.5	0.7	1.0	1.2	1.5

Table 4-7 Observations for the Phase III-A (Continued)

Turbidity (3 min. settling time)	7.5	5.4	5.3	4.4	7.1	3.2
% removal in turbidity	50.86	64.48	65.15	71.06	53.29	
Turbidity (8 min. settling time)	5.6	4.7	4.9	3.5	7.0	2.7
% removal in turbidity	63.16	69.08	67.77	76.98	53.95	82.24
pH (3 min. settling time)	6.9	7.1	7.0	6.9	7.1	7.0
pH (8 min. settling time)	7.0	7.1	7.1	6.9	7.0	7.1
Zeta Potential (3 min. settling time)	-23.6	-23.7	-22.4	-12.1	-20.8	-10.8
Zeta Potential (8 min. settling time)	-22.0	-23.5	-22.3	-21.6	-24.1	-8.4

In Phase III-B different concentrations of polyelectrolyte POL-E-Z 2466 were used. Table 4-8 shows the conditions used and observations for Phase III-B experiment.

Table 4-8 Observations for the Phase III-B

PARAMETER	Jar 1	Jar 2	Jar 3	Jar 4	Jar 5	Jar 6
Micro-carrier type	Ottawa Sand					
Micro-carrier size	0-150 micrometer					
Micro-carrier concentration	3 gm.					
Alum concentration (mg/L)	40					
Polyelectrolyte type	POL-E-Z 2466 (Cationic Polyelectrolyte)					
Polyelectrolyte conc. (mg/L)	0.3	0.5	0.7	1.0	1.2	1.5
Turbidity (3 min. settling time)	26.2	21.9	12.4	12.7	8.9	16.2
% removal in turbidity (3 min)	83.42	86.14	92.16	91.97	94.37	
Turbidity (8 min. settling time)	19.9	16.3	10.8	11.9	9.7	13.5
% removal in turbidity (8 min)	87.41	89.69	93.17	92.47	93.87	91.46

Table 4-8 Observations for the Phase III-B (continued)

pH (3 min. settling time)	6.4	6.4	6.5	6.4	6.3	6.4
pH (8 min. settling time)	6.5	6.5	6.5	6.4	6.4	6.4
Zeta Potential (3 min. settling time)	-20.4	-19.2	-21.0	-17.0	-4.4	-17.8
Zeta Potential (8 min. settling time)	-19.5	-17.7	-15.5	-16.8	-3.6	-11.0

In Phase III-C different concentrations of polyelectrolyte POL-E-Z 3466 were used. Table 4-9 shows the conditions used and observations for Phase III-C experiment.

Table 4-9 Observations for the Phase III-C

PARAMETER	Jar 1	Jar 2	Jar 3	Jar 4	Jar 5	Jar 6
Micro-carrier type	Ottawa Sand					
Micro-carrier size	0-150 micrometer					
Micro-carrier concentration	3 gm.					
Alum concentration (mg/L)	40					
Polyelectrolyte type	POL-E-Z 3466 (Cationic Polyelectrolyte)					
Polyelectrolyte conc. (mg/L)	0.3	0.5	0.7	1.0	1.2	1.5
Turbidity (3 min. settling time)	13.6	5.9	7.8	6.4	5.6	4.3
% removal in turbidity	92.61	96.8	95.77	96.53	96.96	
Turbidity (8 min. settling time)	9.7	4.8	6.2	4.3	4.3	3.5
% removal in turbidity	94.73	97.40	96.64	97.67	97.67	98.1
pH (3 min. settling time)	6.6	6.6	6.8	6.7	6.7	6.7
pH (8 min. settling time)	6.9	6.9	6.8	6.9	6.9	6.9
Zeta potential (3 min. settling time)	-16.4	-11.9	-14.0	8.3	14.2	32.7
Zeta potential (8 min. settling time)	-13.3	-13.2	-9.5	11.5	16.5	29.9

In Phase III-D different concentrations of polyelectrolyte POL-E-Z 7366 were used. Table 4-10 shows the conditions used and observations for Phase III-D experiment.

4-10 Observations for the Phase III-D

PARAMETER	Jar 1	Jar 2	Jar 3	Jar 4	Jar 5	Jar 6
Micro-carrier type	Ottawa Sand					
Micro-carrier size	0-150 micrometer					
Micro-carrier concentration	3 gm.					
Alum concentration (mg/L)	40					
Polyelectrolyte type	POL-E-Z 7736 (Anionic Polyelectrolyte)					
Polyelectrolyte conc. (mg/L)	0.3	0.5	0.7	1.0	1.2	1.5
Turbidity (3 min. settling time)	8.9	8.6	7.6	7.3	2.0	2.3
% removal in turbidity	88.14	88.54	89.87	90.30	97.34	
Turbidity (8 min. settling time)	4.6	5.4	4.7	5.0	1.7	2.0
% removal in turbidity	93.87	92.80	93.74	93.34	97.74	97.34
PH (3 min. settling time)	6.4	6.4	6.5	6.2	6.4	6.5
PH (8 min. settling time)	6.6	6.6	6.6	6.6	6.6	6.6
Zeta Potential (3 min. settling time)	-18.0	-17.6	-17. 3	–13.0	–23.4	-17.2
Zeta Potential (8 min. settling time)	-17.5	-21.4	-18.8	-12.8	-23.4	-19.8

Figure 4-21 and 4-22 shows the zeta potential variation of different polyelectrolytes as a function of polyelectrolyte concentration. This figure shows that zeta potential value decrease initially as polyelectrolyte concentration increases and crosses neutral value in case of POL-E-Z 3466 and increases up to 30 ± 5 mV. In case of non-ionic and anionic

polyelectrolytes, the zeta potential value lies in the negative region. This kind of behavior is almost the same as observed in case of Phase II. Only in case of POL-E-Z 2466 when polyelectrolyte concentration was varied zeta potential value decreases with increase in polyelectrolyte concentration, but reaches only up-to -4 ± -1 mV and then slightly decreases again.

Figure 4-23 and 4-24 shows the variation in removal in turbidity as a function of polyelectrolyte concentration. It was observed that in case of cationic polyelectrolytes and anionic polyelectrolytes, removal in turbidity increases as polyelectrolyte concentration increases up-to 1.2 mg/L and a slight decrease in turbidity removal was observed beyond that concentration. Thus a polyelectrolyte concentration of 1.2 mg/L can be considered as the most effective polyelectrolyte concentration in these three cases. Whereas, in case of non-ionic polyelectrolyte, removal in turbidity increases up-to 1 mg/L polyelectrolyte concentration and beyond that there was no particular trend observed and hence in that case 1 mg/L can be considered as the most effective polyelectrolyte concentration.

Figure 4-25 to 4-28 shows the variation in residual turbidity as a function of zeta potential value of the resulting solution. It was observed here that for all the four polyelectrolytes a good removal in turbidity was observed at a broad range of zeta potential values. Also in case of POL-E-Z 3466 good removal in turbidity was obtained when zeta potential value was highly positive, where as in case of other three polyelectrolytes negative values of zeta potential showed a good removal in turbidity. This phenomena indicates that non-DLVO forces also play an important role in the presence of polyelectrolytes.

As applied in the previous two phases, removal in turbidity is evaluated experimentally in terms of collision efficiencies and stability ratios. In phase III, stability ratios were calculated from equation 2-17 for all the four sets of observations. Figure 4-29 shows the variation in stability factor as a function of polyelectrolyte concentration for four different polyelectrolytes. It was observed that the range of stability ratio for different polyelectrolytes was very narrow between 2.9 and 4.9 and these results can be compared with the Figure 2-5 (Chapter 2)

In Figure 2-5, a positively charged hematite solution was coagulated by negatively charged polyaspartic acid at neutral pH in presence of 1 mM NaCl solution. In this case it was observed that at low concentration of added polyelectrolyte, hematite is kinetically stable as a positively charged colloid. Polyaspartic acid provides essentially complete destabilization (W=1) at 0.2 mg/L. But stability ratio increases sharply as the polyelectrolyte concentration is increased further and shows restabilization of colloidal particles. The results obtained in figure 4-30 indicates that in micro-carrier process the value of stability ratio lie in a very narrow range, and hence the particles are destabilised over a broad range of concentration and hence gives high removal in turbidity over experimental range of concentration.

4.4 Comparison between Phase I-A, Phase I-B and Phase II-C

In Figure 4-30 a comparison of experimental stability ratio versus electrolyte concentration, is presented for three different sets of jar test from Phase I and Phase II namely Phase I-A, Phase I-B and Phase II-C. This figure summarizes the behavior of the three different coagulants in terms of stability ratios.

In case of Phase I-A, stability ratio was comparatively high and the lowest stability ratio was observed at 60 mg/L concentration. In Phase I-B the stability ratio reduces 2 to 3 times and this supports the high removal of colloidal particles in the presence of micro-carrier. It is noteworthy here that the best removal in turbidity was obtained at 60 mg/L electrolyte concentration in both the first and second set. Finally when polyelectrolyte was also used, stability ratio further reduces but the reduction from Phase I-B was comparatively low than the reduction from Phase I-A to Phase I-B. The reduction in stability ratio was approximately 0.5 to 1.5 times.

However, in the case of polyelectrolyte, least stability ratio was observed at electrolyte concentration of 40 mg/L and it again increased when the electrolyte concentration was increased and at 60 mg/L concentration it was higher than the stability ratio of the flocculation without polyelectrolyte. Thus in case of polyelectrolyte stability ratio decreases as ionic strength increases.

Thus in micro-carrier enhanced process, when polyelectrolyte is used, a lower concentration of electrolyte (40 mg/L) at this operating conditions can produce the most effective removal in turbidity in a very short time at a high shear rate.

CHAPTER 5

CONCLUSIONS AND RECOMMENDATIONS

Colloidal stability is a very complex matter. On the basis of the results of this study it can be concluded that various parameters affect the removal of colloidal particles. Destabilization of colloidal particles by charge neutralization plays a significant role in the removal of colloidal particles. A series of experiments were conducted to study the effect of micro-carrier on flocculation of colloidal particles

It was observed that in the presence of electrolyte alone, the trend in zeta potential agrees well with the DLVO theory and the lowest turbidity is observed at the neutral zeta potential value. The same kind of behavior is observed in presence of alum and micro-carrier. But the higher removal in turbidity in presence of micro-carrier can be attributed to higher collision efficiency of the process.

In the case of polyelectrolytes, it is observed that all three different kinds of polyelectrolytes are almost equally efficient in the removal of colloidal particles. The highest removal of turbidity at the zeta potential values of about –20 mV in case of anionic and non-ionic polyelectrolytes and about +20 mV in case of cationic polyelectrolyte suggests that charge neutralization and polymer bridging both play an important role in the removal of colloidal particles. Using all three different charged polyelectrolytes removal in turbidity obtained is about 98%.

From this study it can be concluded that micro-carrier does play a significant role in the removal of colloidal particle, though it does not play a significant role in the reduction of zeta potential. Micro-carrier enhances the collision efficiency of the process and this

leads to a high rate of adhesion of destabilized particles to each other and eventually to the formation of large and heavy flocs, which settles fast. Also the flocculation process was conducted for a very short time which reduces the possibilities of breaking up of the flocs and thus indirectly enhances the formation of heavy flocs and increases the sedimentation rate. The addition of electrolyte and polyelectrolyte is required in order to initiate the charge neutralization and polymer bridging process.

Further study in this area is needed in order to optimize and control various parameters to achieve better removal of colloidal particles at reduced electrolyte and polyelectrolyte dose. This in turn can reduce the dose of residual chemicals in the treated samples.

APPENDIX -A

ZETA POTNETIAL MEASUREMENT

Zeta potential analyzer works on the following principal. Due to surface charge, particles will move when placed in an electric field. Due to the motion of the charged particles, a frequency shift called the Doppler shift, ω_S, occurs in the light scattered by particles. This light is a focused laser beam of wavelength, $\lambda_o = 670nm$.

The shift in frequency, ω_S, of the scattered light from a charged particle moving with velocity V_S in an electric field, E, is given by the dot product of vectors.

$$\varpi_s = q.Vs = q.Vs\cos\phi \qquad (A\text{-}1)$$

Where ϕ is the angle between the vectors. When the electrical field is perpendicular to the incident laser beam direction, then it can be shown that ϕ is related to the scattering angle θ by

$$\phi = \theta/2 \qquad (A\text{-}2)$$

The magnitude q, of the scattering wave vector is given by

$$q = \frac{4\pi n}{\lambda_0}\sin\frac{\theta}{2} \qquad (A\text{-}3)$$

Where n is the refractive index of the liquid and λ_0 is the wavelength of the laser in vacuum

Since $V_s = \mu_e E$ where μ_e is the electrophoretic mobility and the equations can be combined to give

$$Vs = \omega s/2\pi = 0.5132\ \mu_e E \qquad \text{(A-4)}$$

where E is the magnitude of the electric field vector in units of V/cm and μ_e is in (μ /s)(V/cm). The electric field is commonly given in units of volts/cm and its range is from near 0 to a few tens of V/Cm. The electrophoretic velocities that develop, are in the range of 0 to a few hundred microns/second. Mobility is in the range of 0 to +/-10.

APPENDIX-B

FIGURES FOR CHAPTER 4

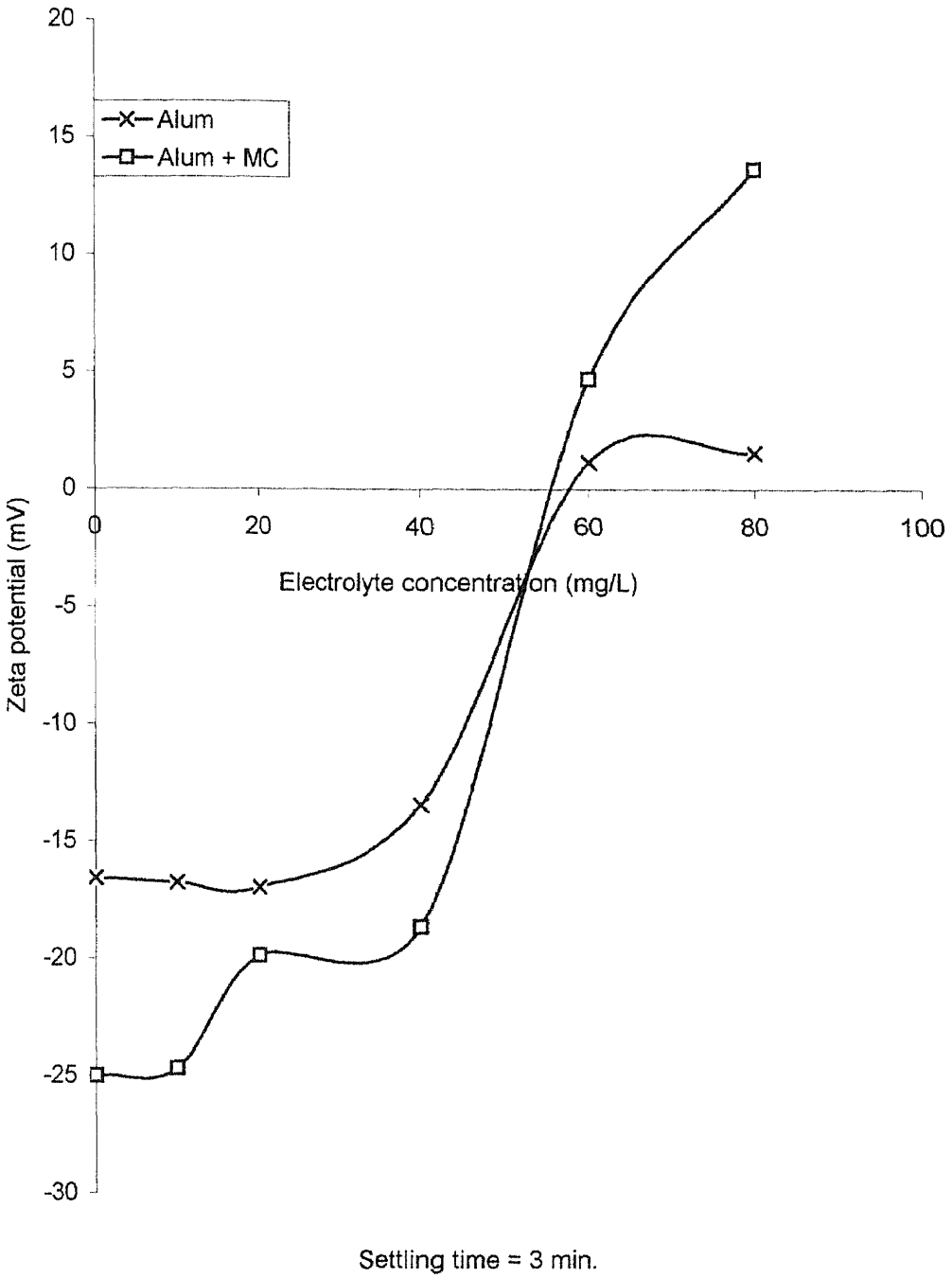

Figure 4-1 Zeta Potential versus Electrolyte Concentration

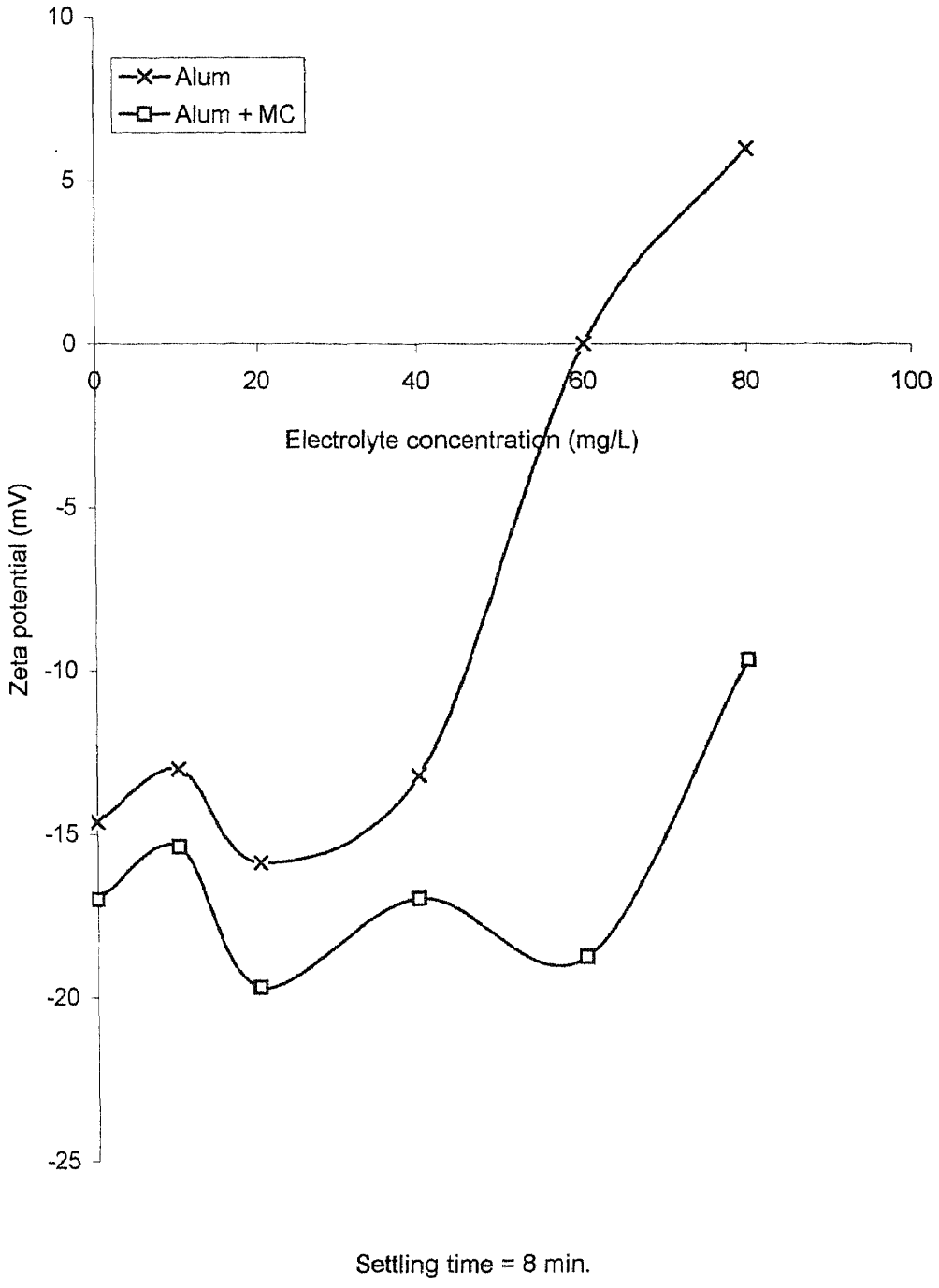

Figure 4-2 Zeta Potential versus Electrolyte Concentration

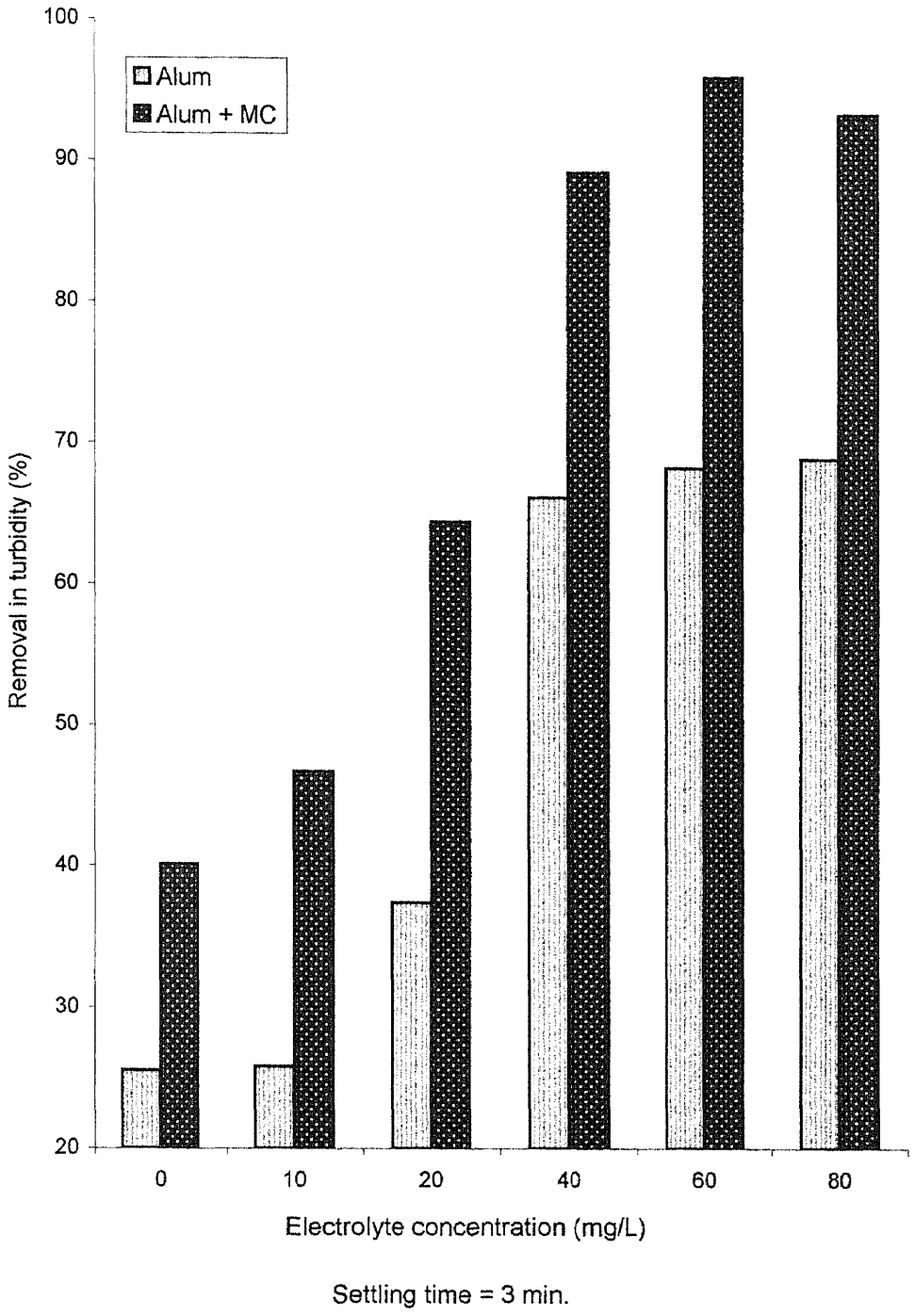

Figure 4-3 Removal in Turbidity versus Electrolyte Concentration

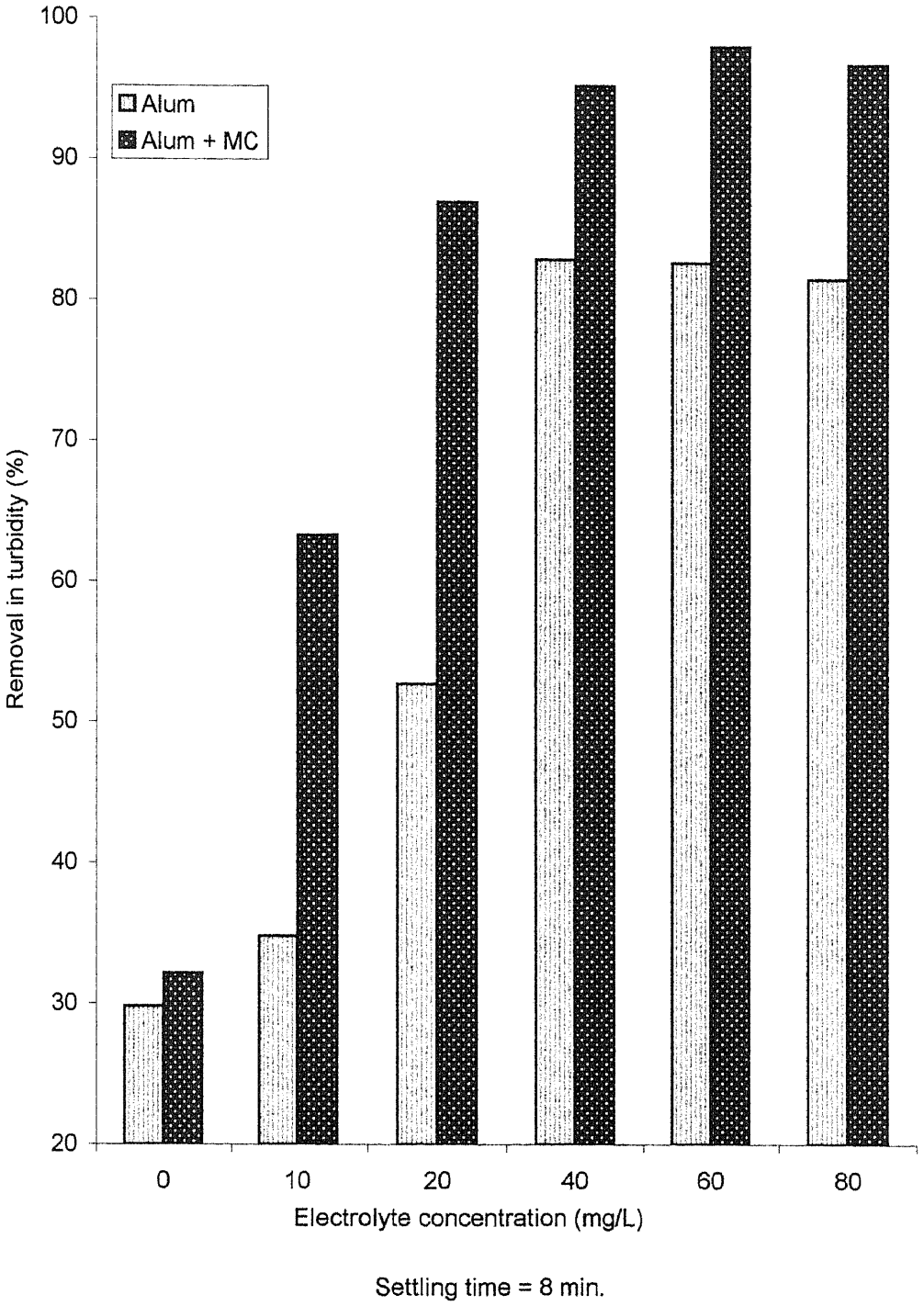

Figure 4-4 Removal in Turbidity versus Electrolyte Concentration

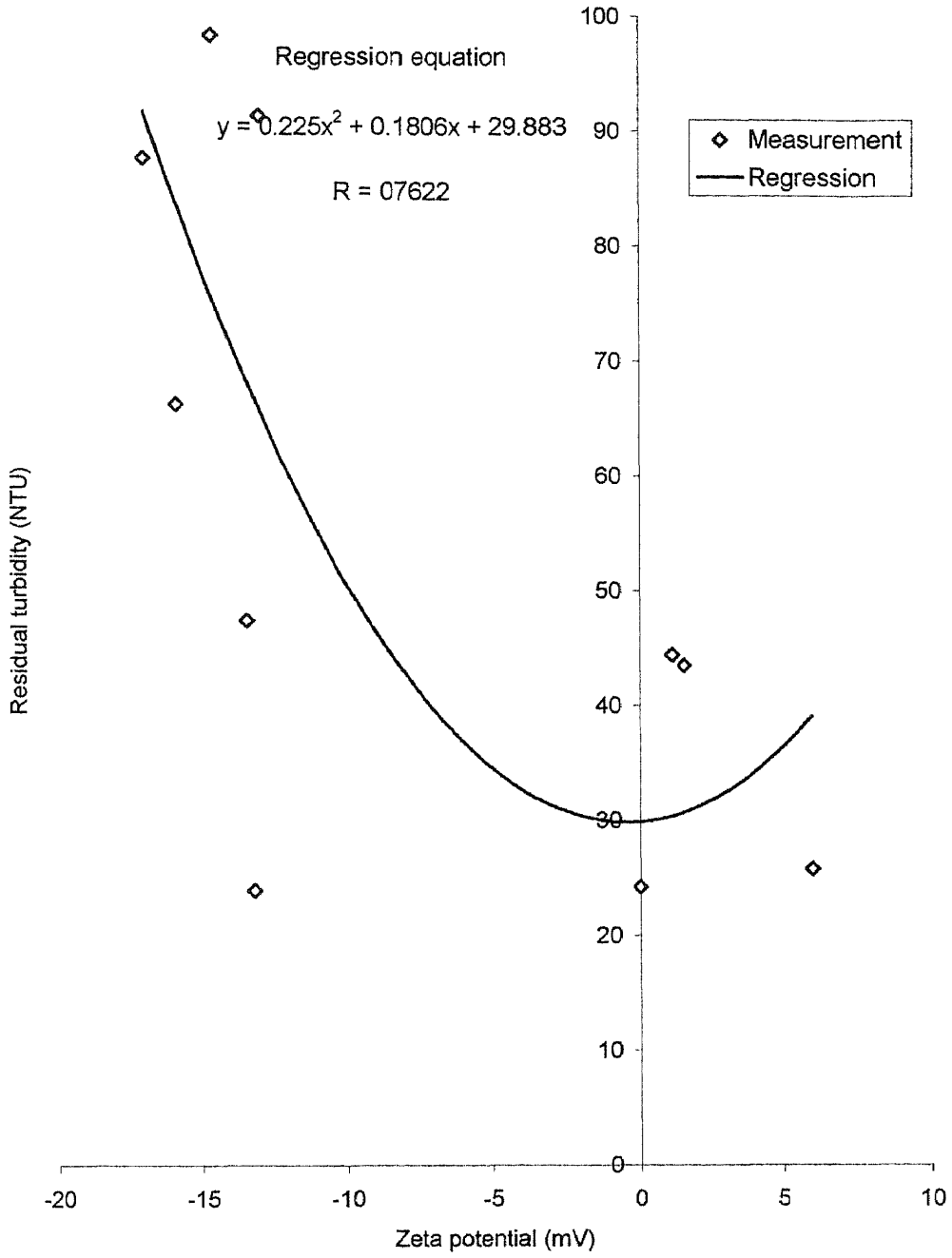

Figure 4-5 Residual Turbidity versus Zeta Potential (Phase I-A)

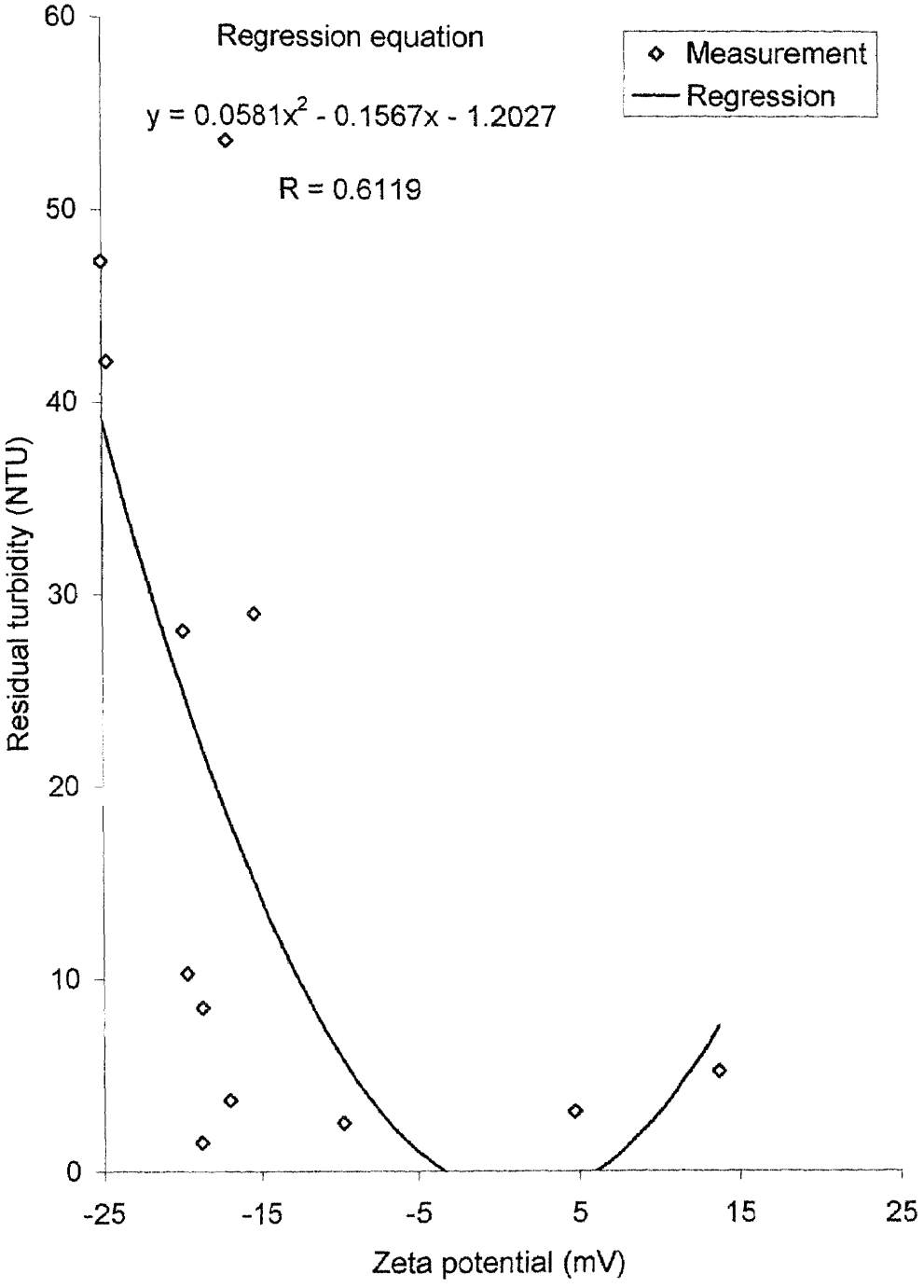

Figure 4-6 Residual Turbidity versus Zeta Potential (Phase I-B)

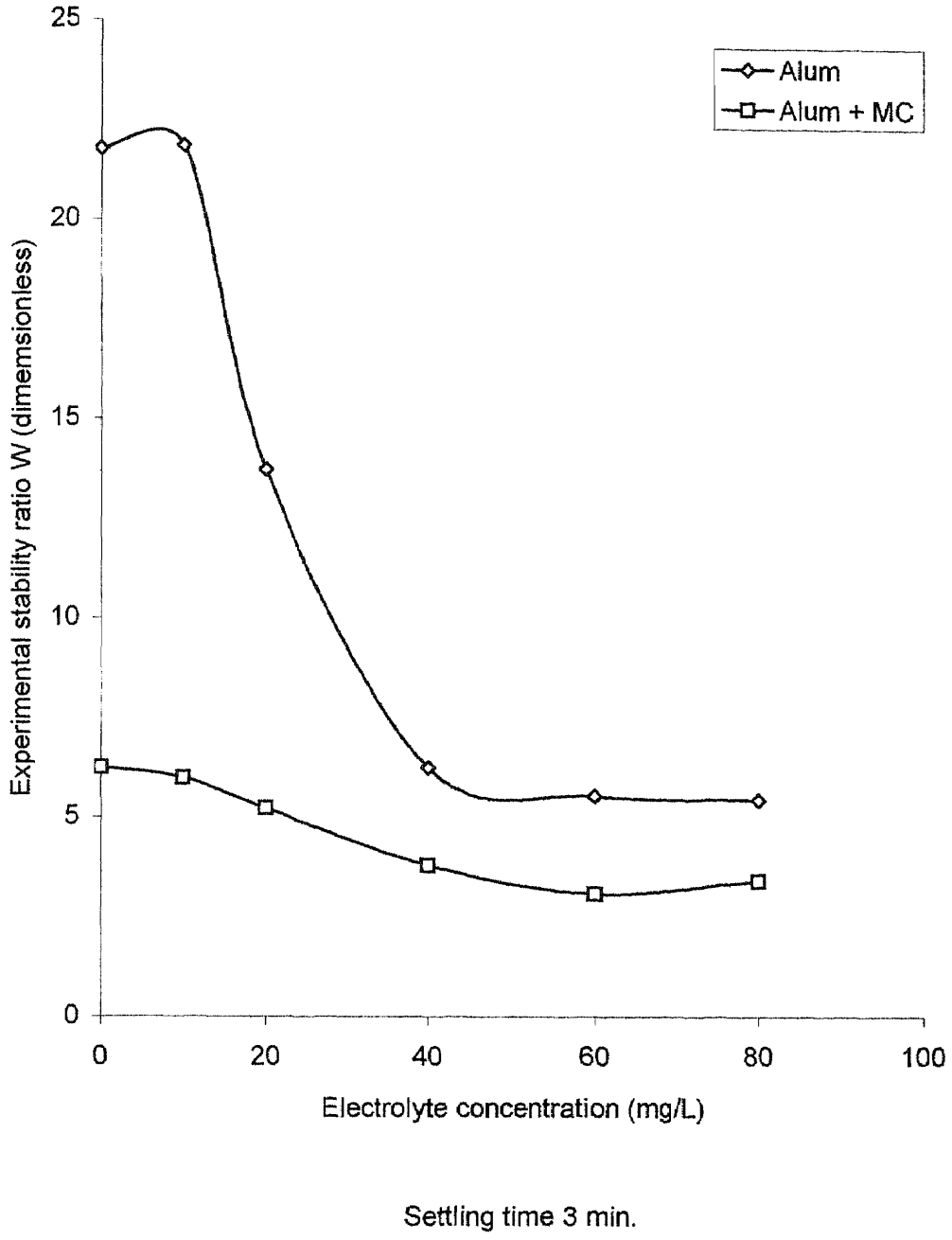

Figure 4-7 Experimental Stability Ratio versus Electrolyte Concentration

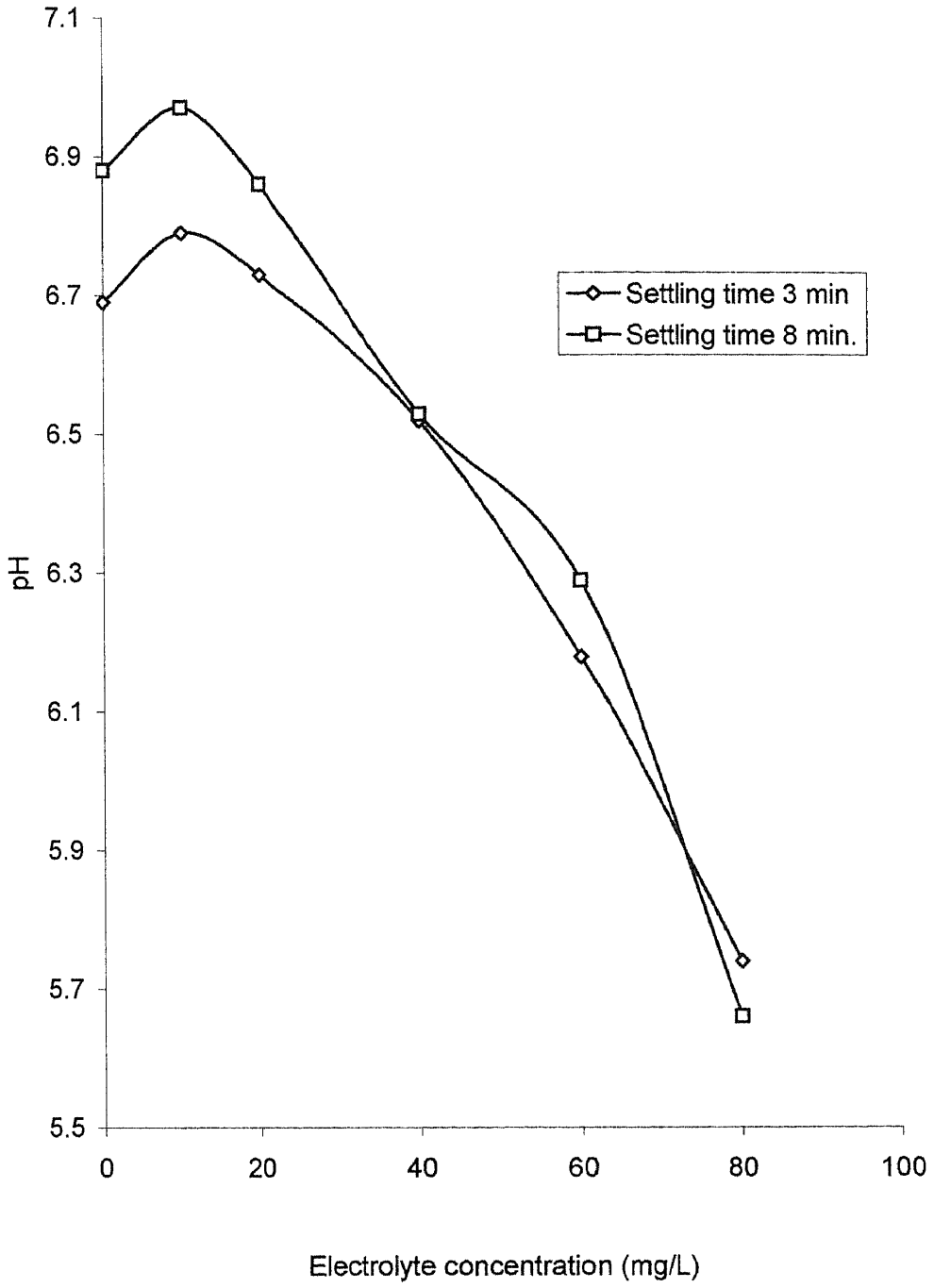

Figure 4-8 pH versus Electrolyte Concentration (Phase I-A)

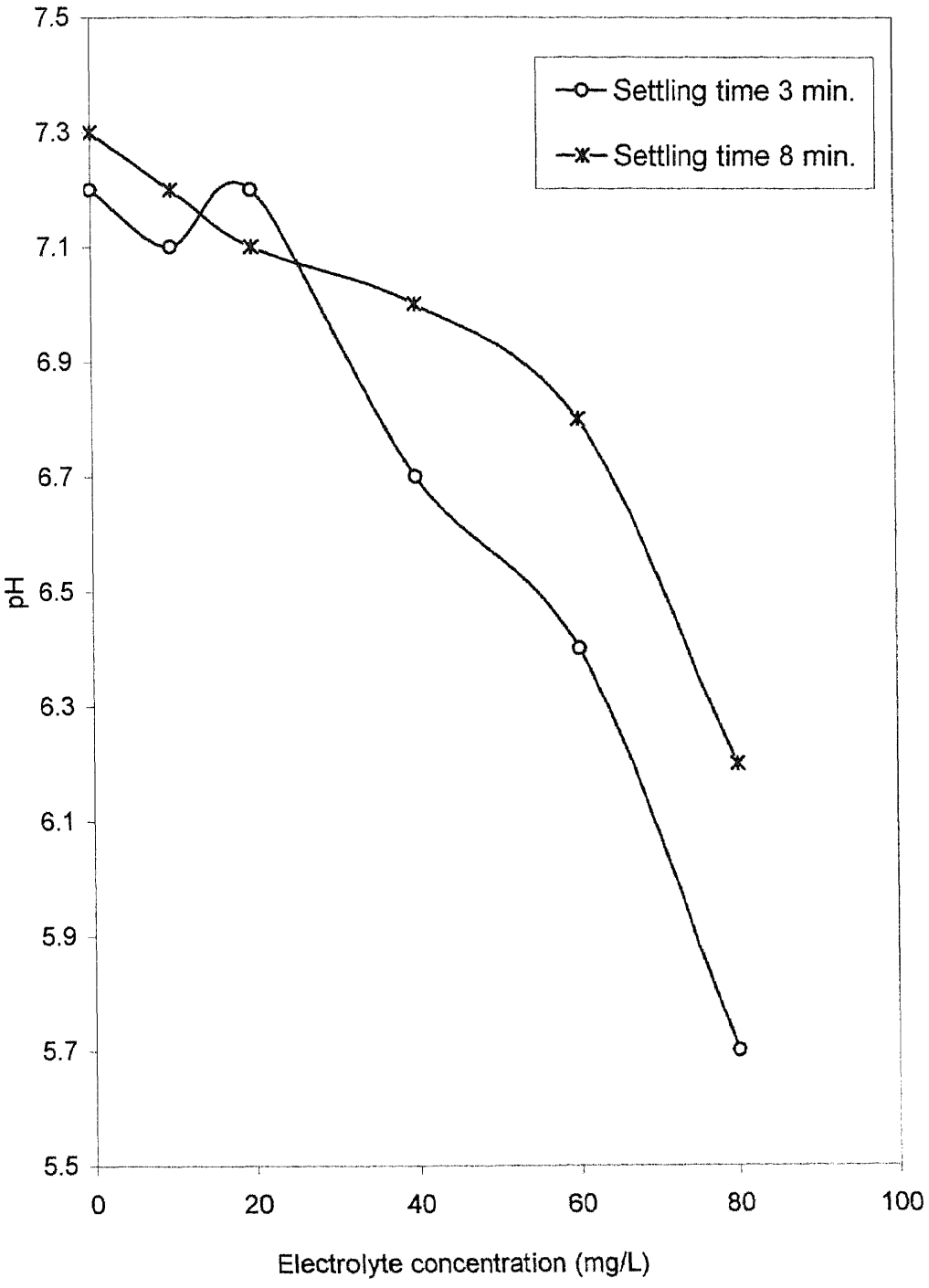

Figure 4-9 pH versus Electrolyte Concentration (Phase I-B)

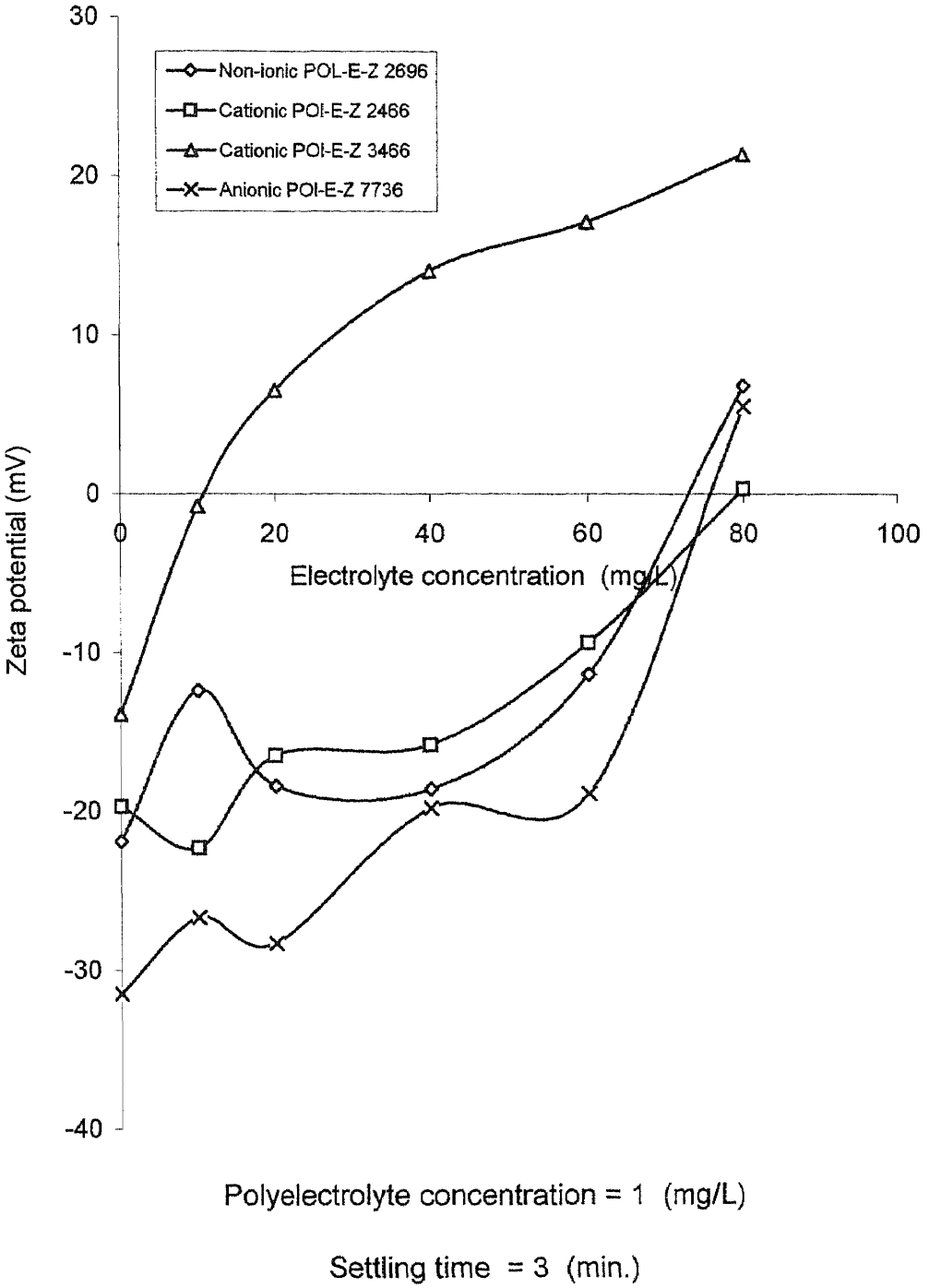

Figure 4-10 Zeta Potential versus Electrolyte Concentration

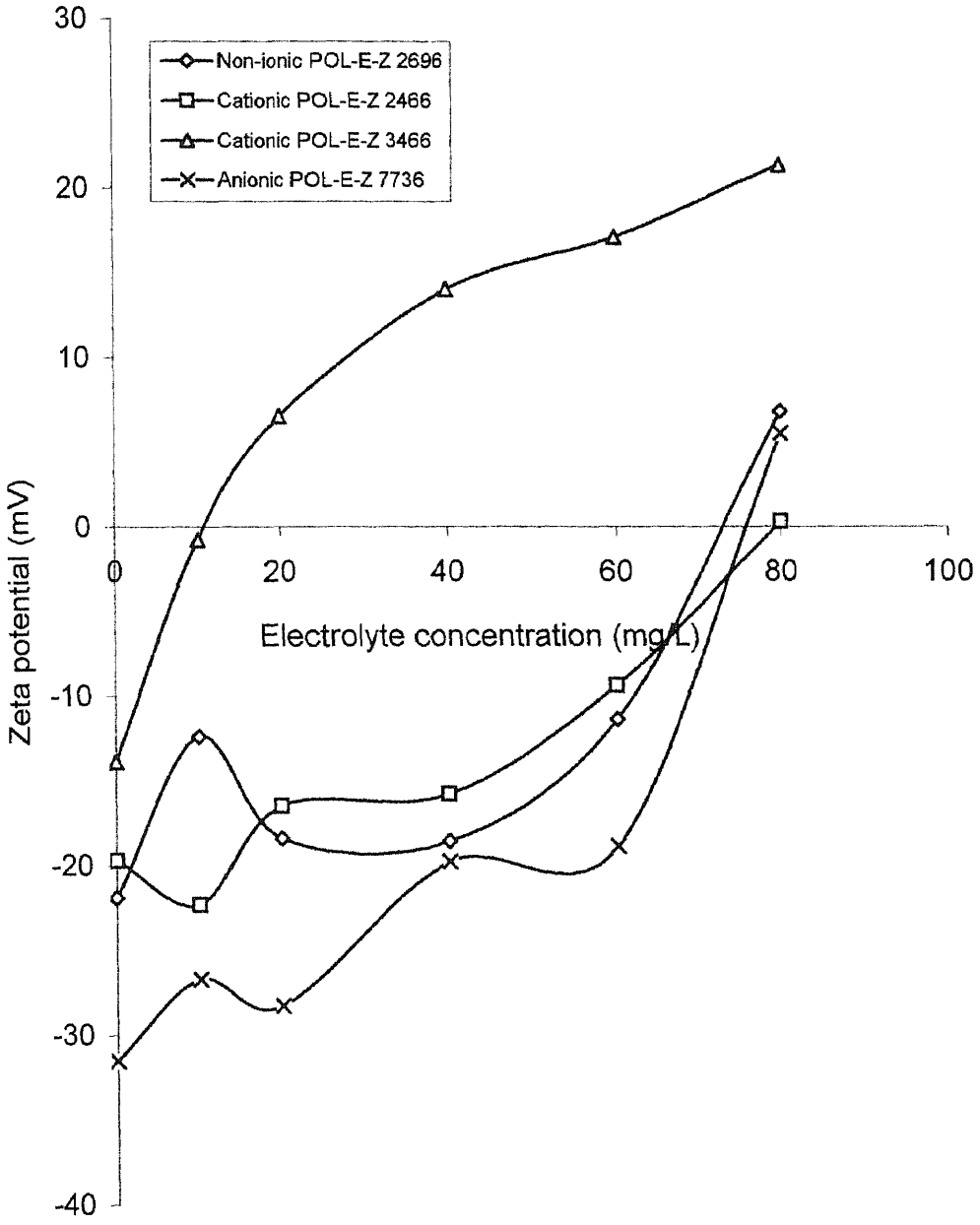

Polyelectrolyte concentration = 1 (mg/L)

Settling time = 8 (min.)

Figure 4-11 Zeta Potential versus Electrolyte Concentration

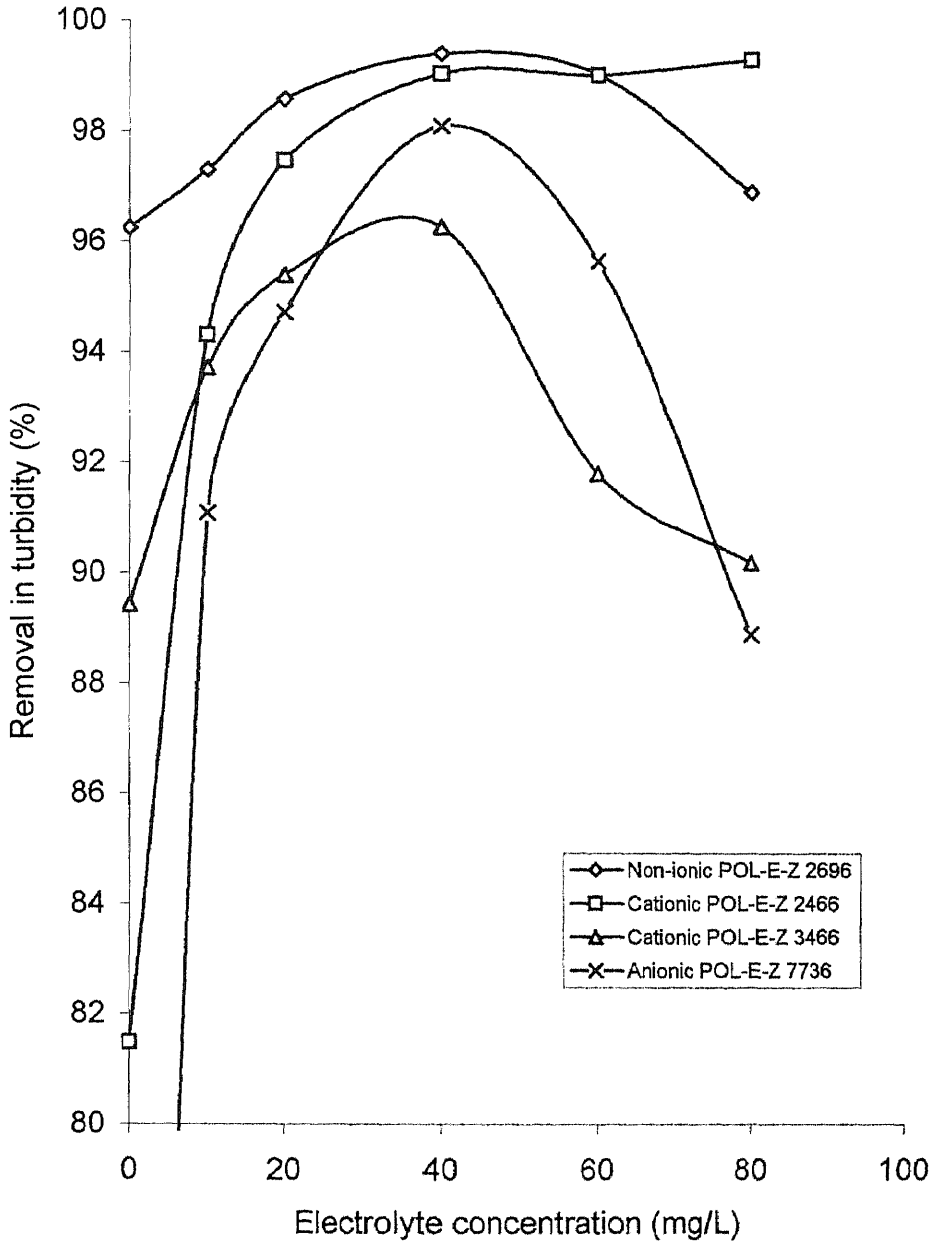

Figure 4-12 Removal in Turbidity versus Electrolyte Concentration

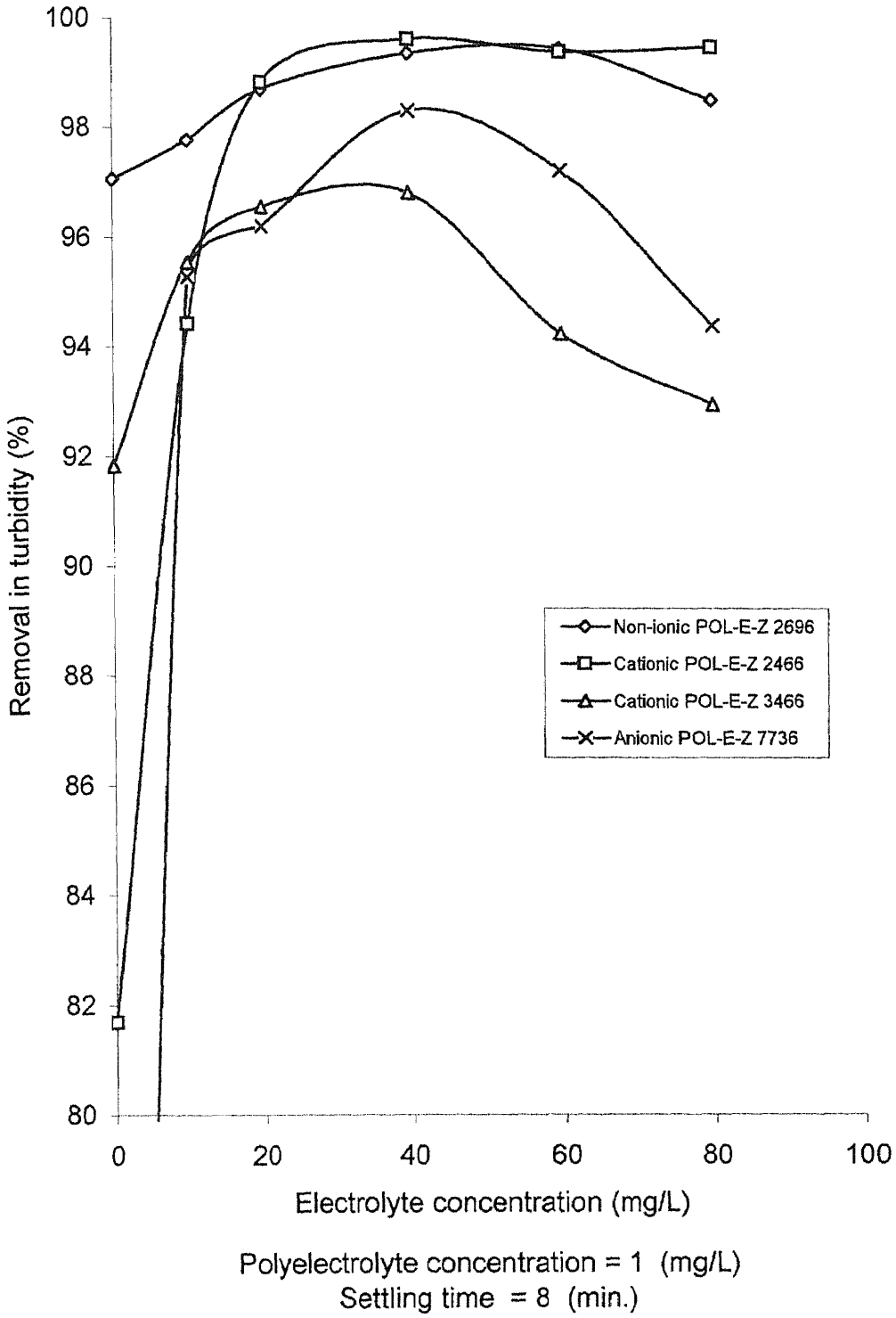

Figure 4-13 Removal in Turbidity versus Electrolyte Concentration

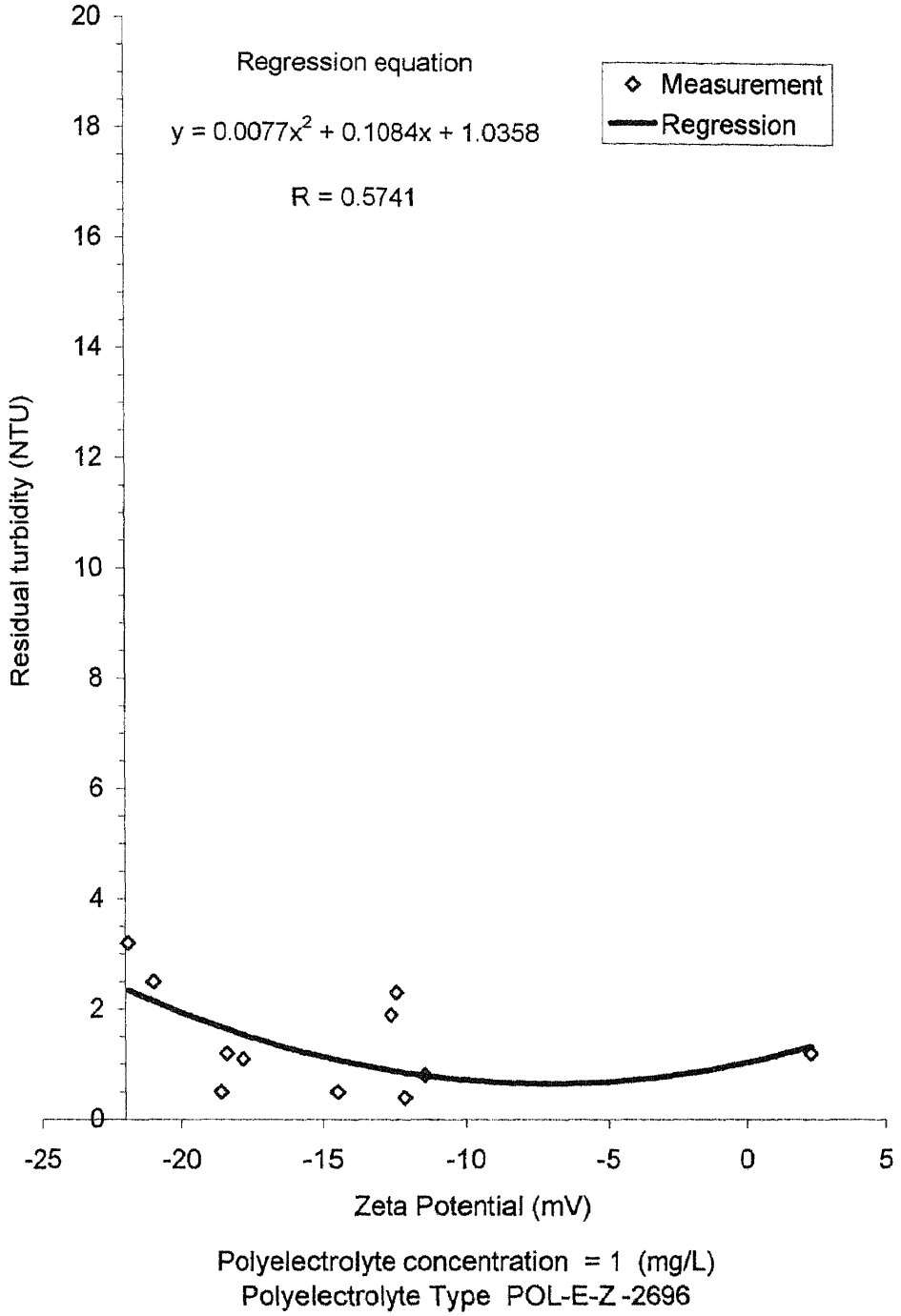

Figure 4-14 Residual Turbidity versus Zeta Potential (Phase II-A)

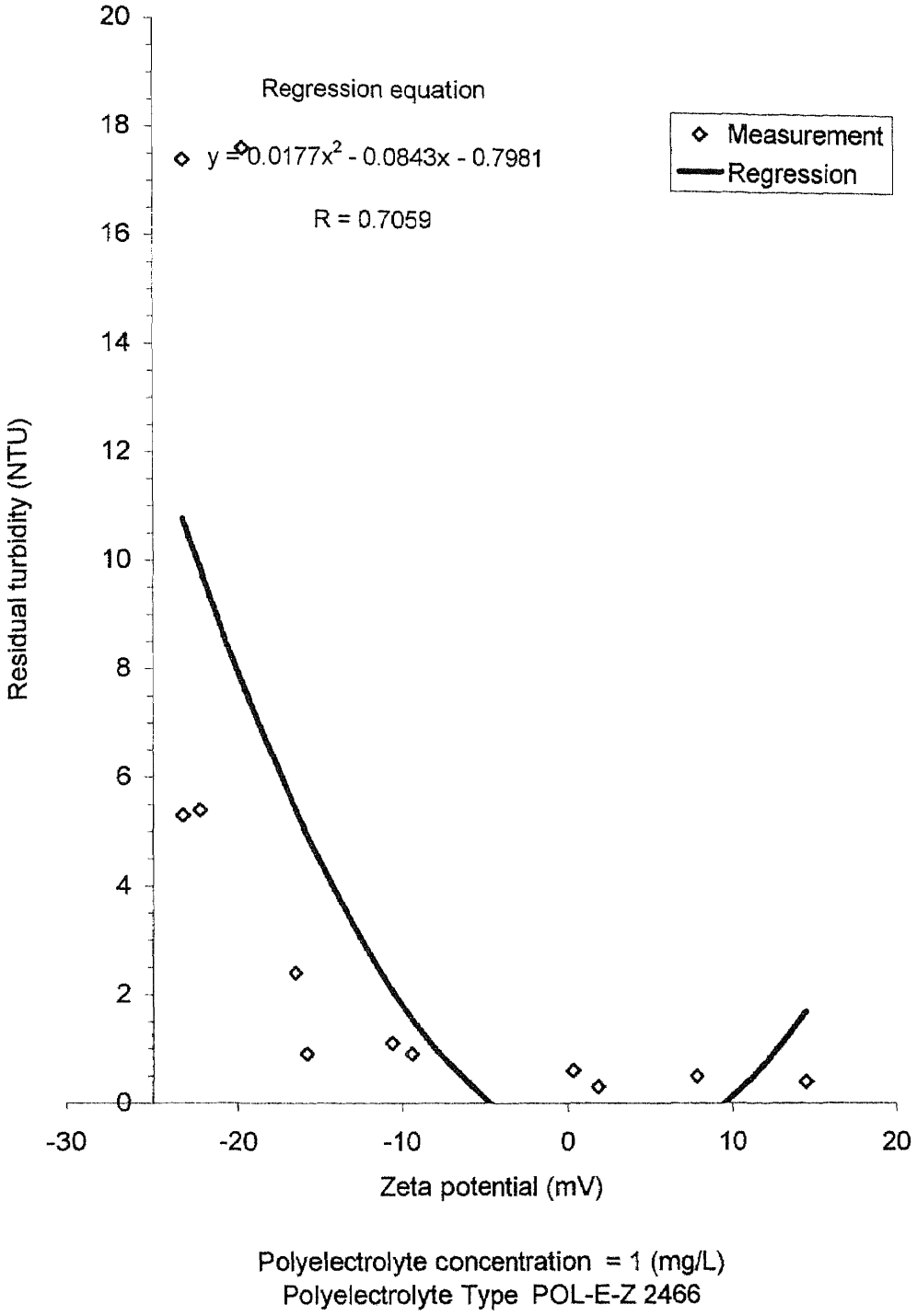

Figure 4-15 Residual Turbidity versus Zeta Potential (Phase II-B)

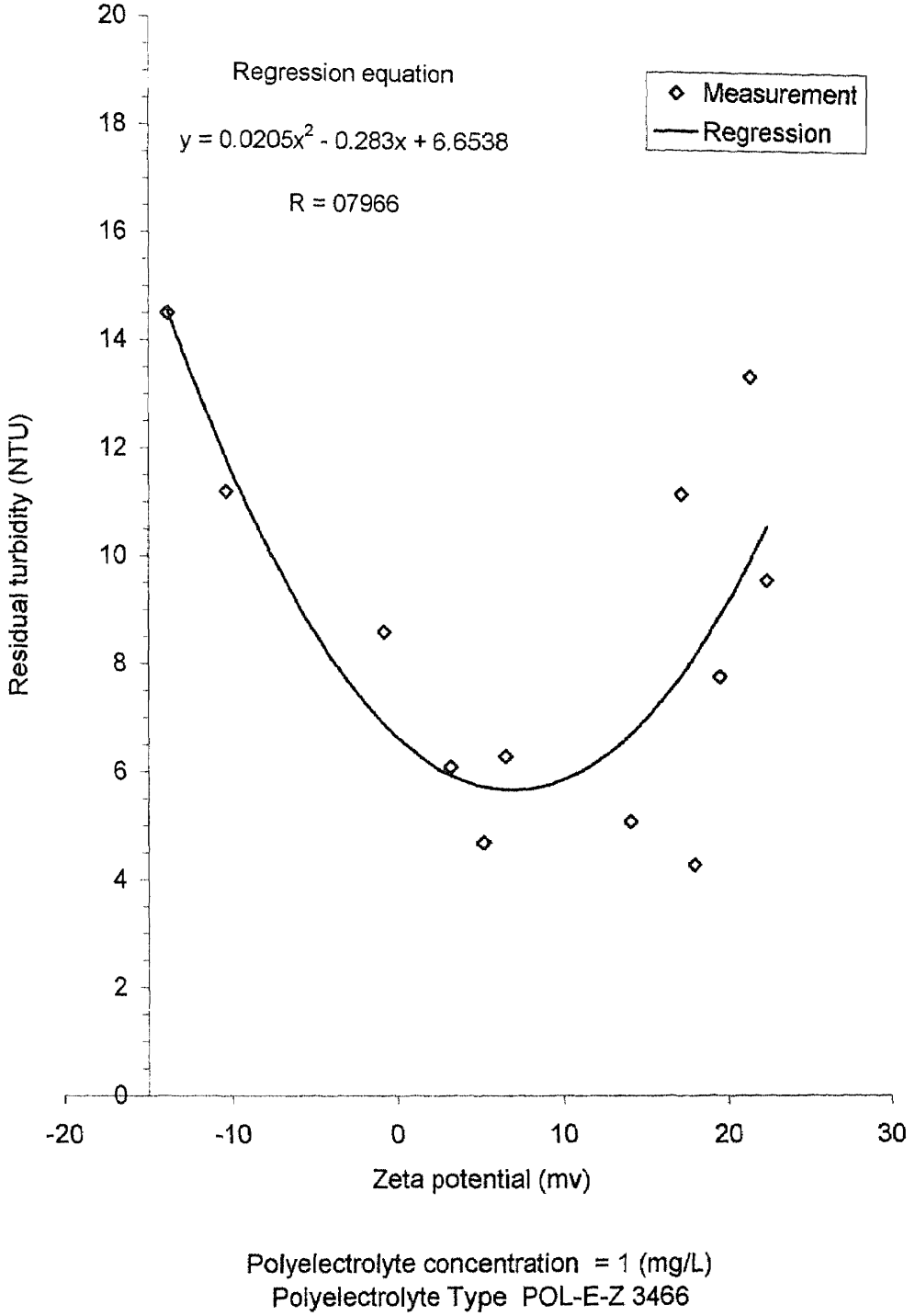

Figure 4-16 Residual Turbidity versus Zeta Potential (Phase II-C)

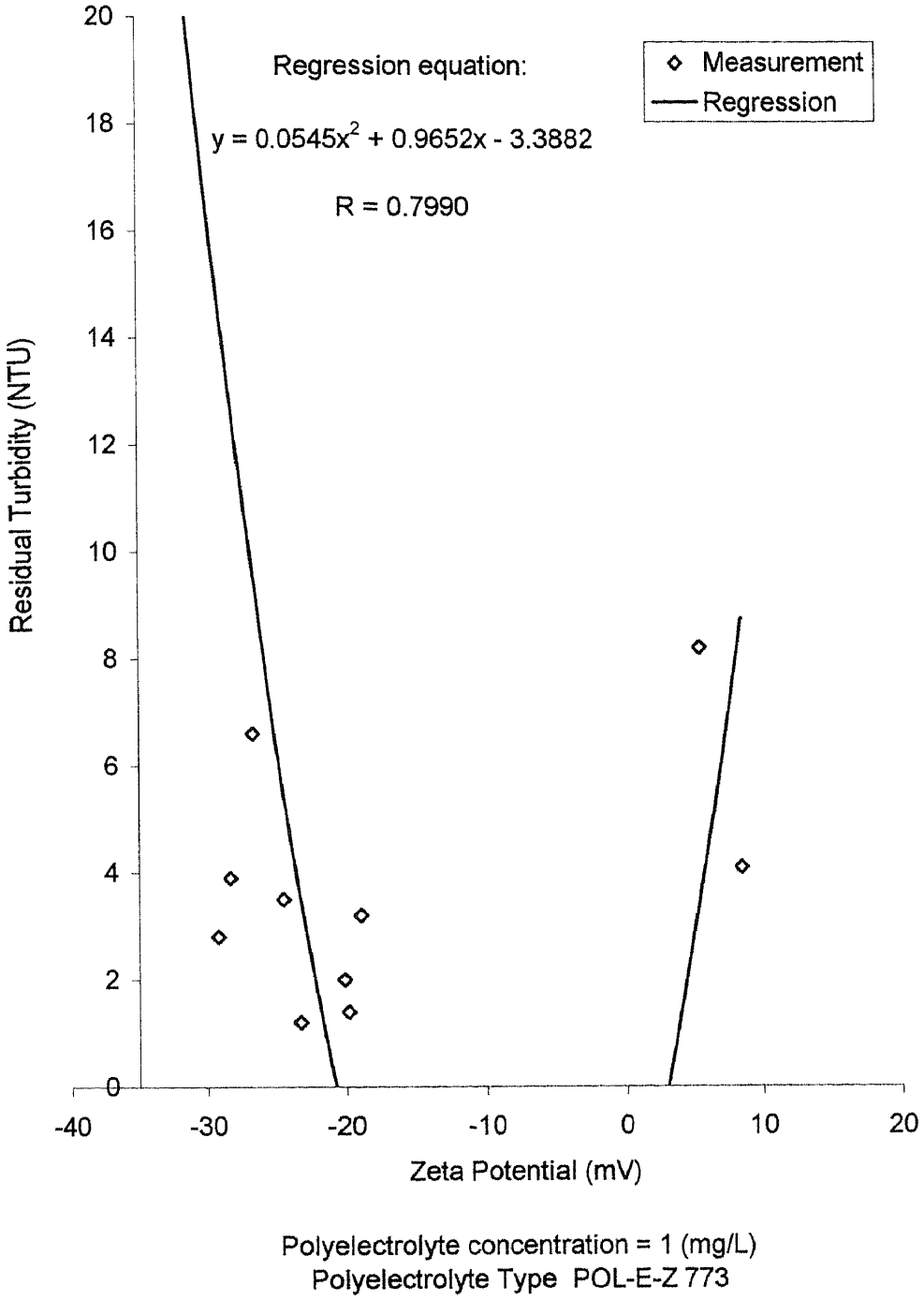

Figure 4-17 Residual Turbidity versus Zeta Potential (Phase II-D)

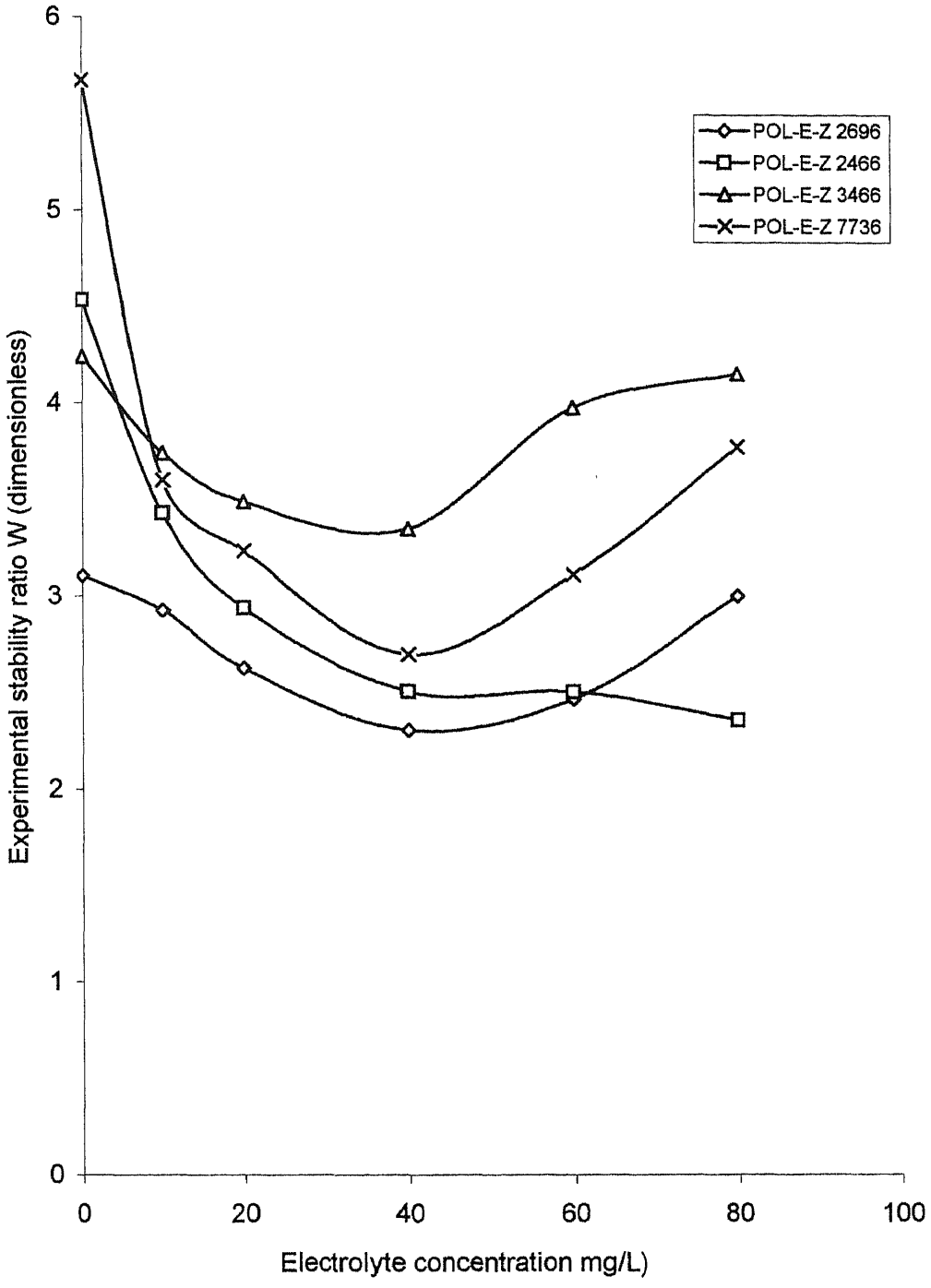

Figure 4-18 Experimental Stability Ratio versus Electrolyte Concentration

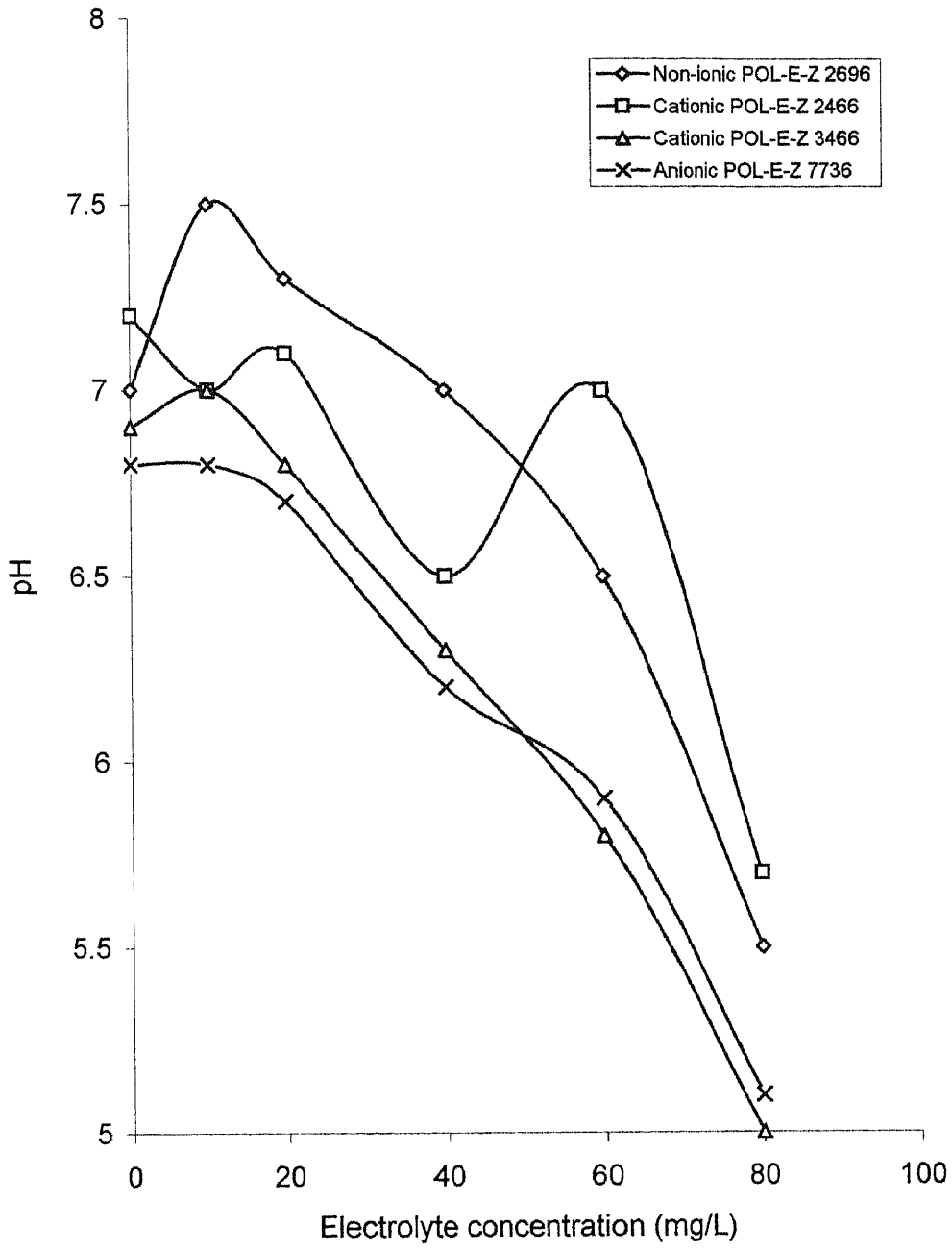

Polyelectrolyte concentration = 1 (mg/L)
Settling time = 3 (min.)

Figure 4-19 pH versus Electrolyte Concentration

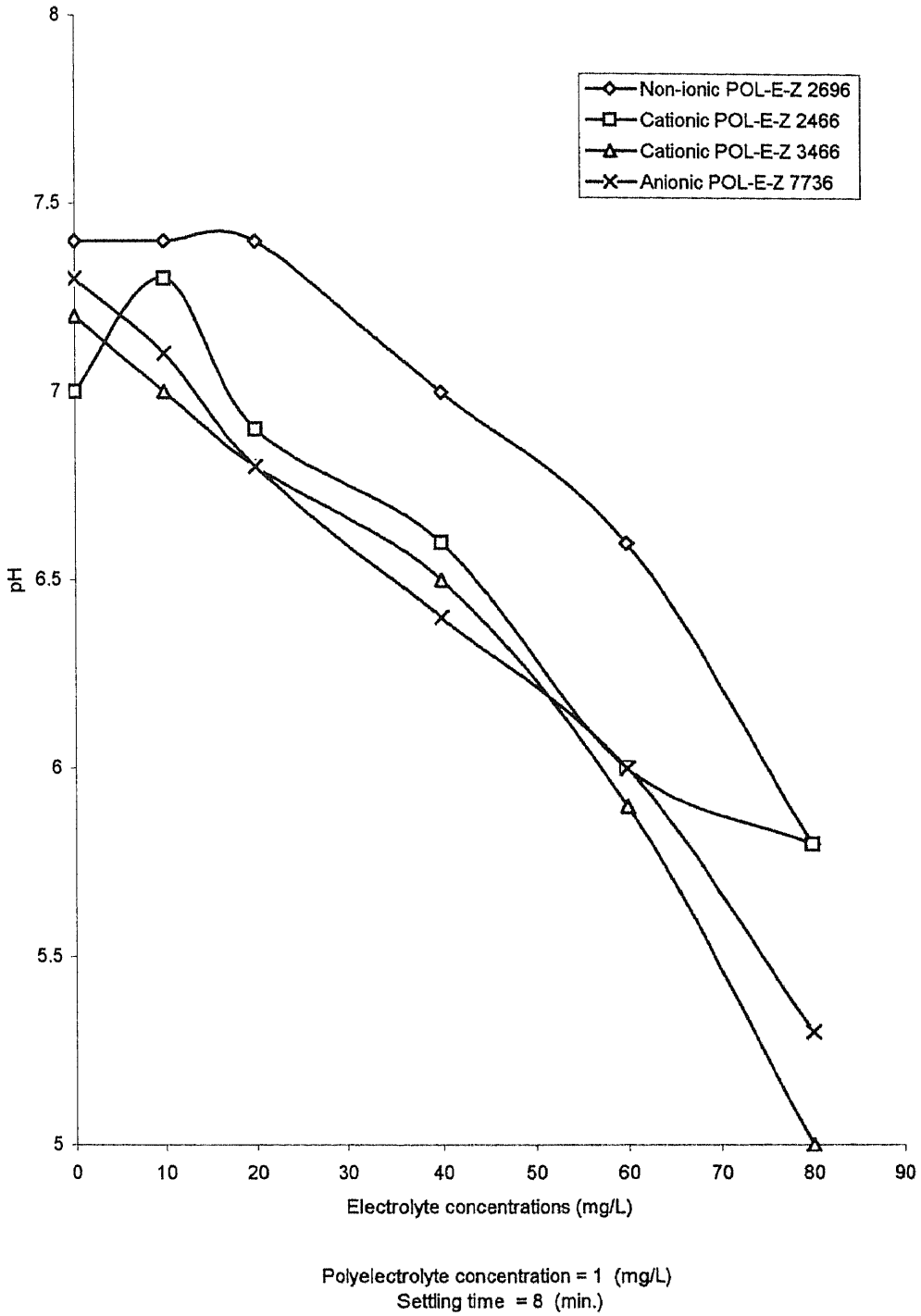

Figure 4-20 pH versus Electrolyte Concentration

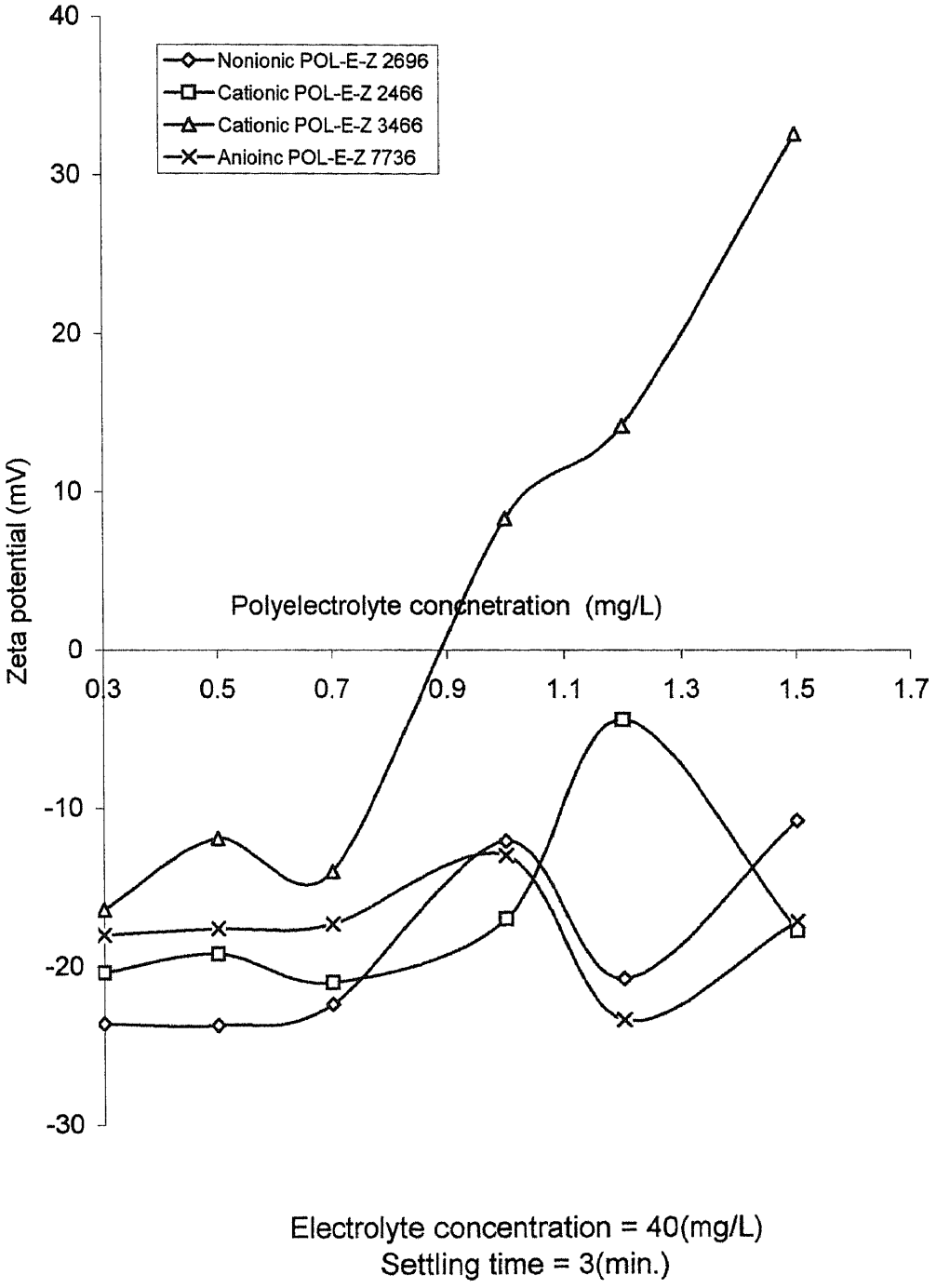

Figure 4-21 Zeta Potential versus Polyelectrolyte Concentration

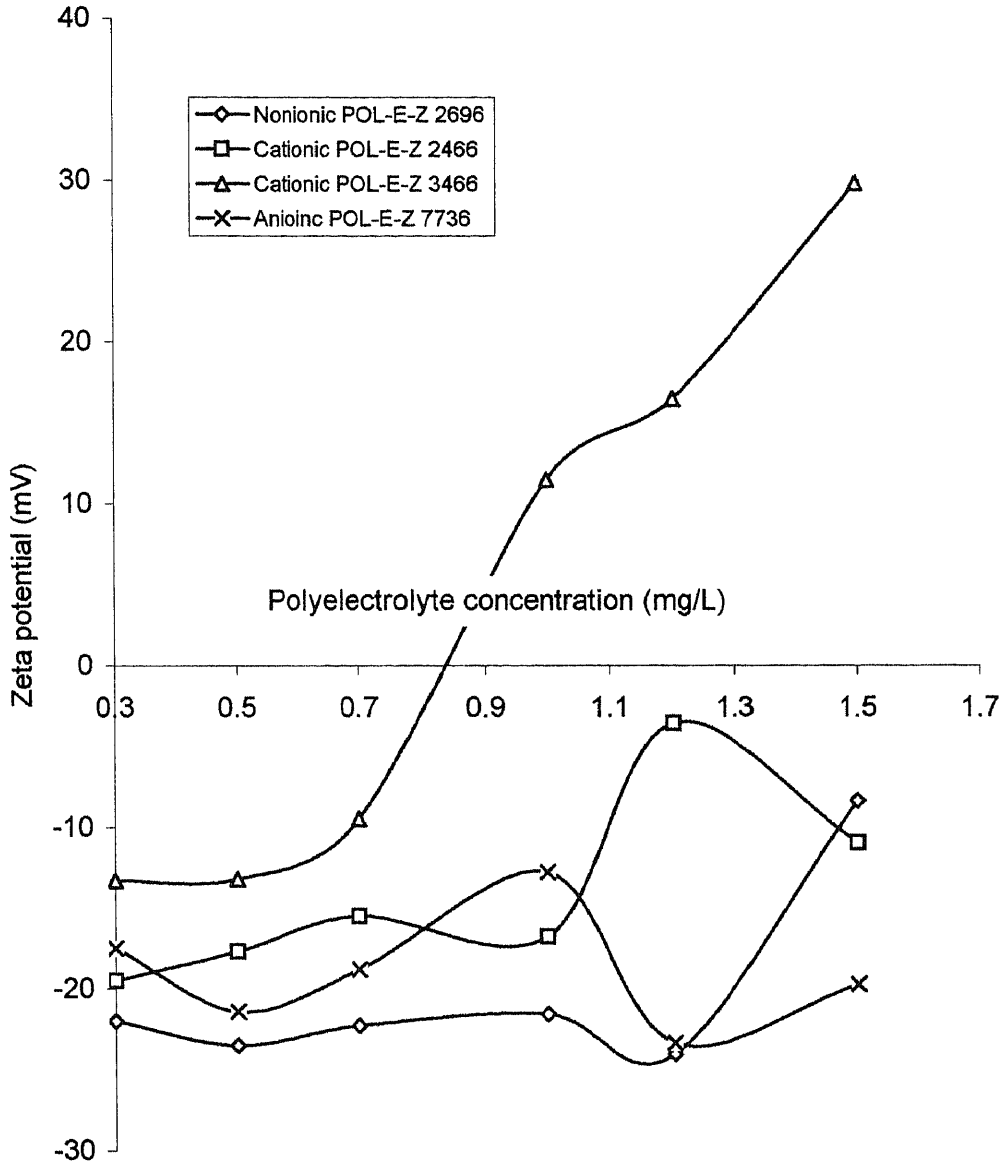

Figure 4-22 Zeta Potential versus Polyelectrolyte Concentration

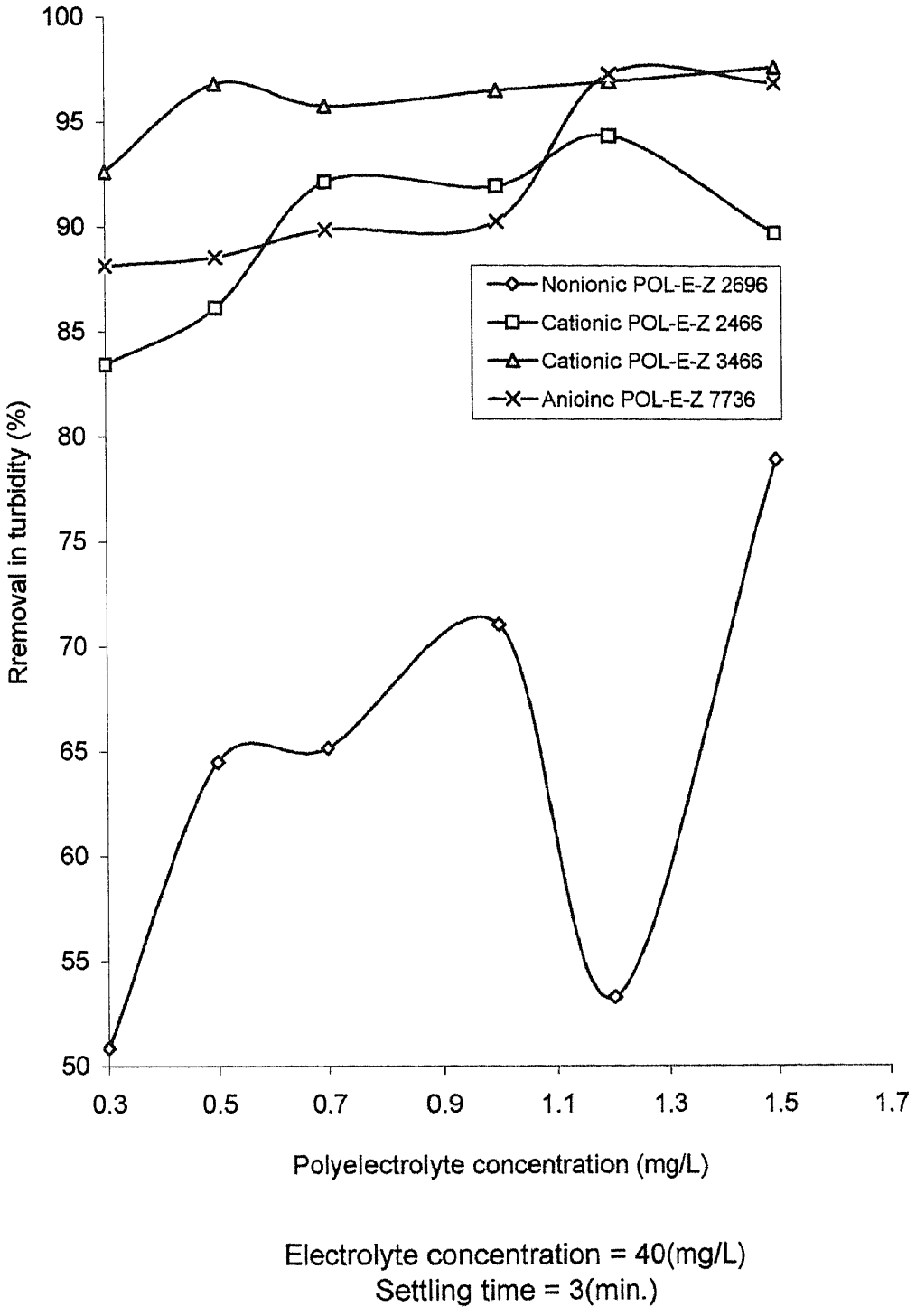

Figure 4-23 Removal in Turbidity versus Polyelectrolytre Concentration

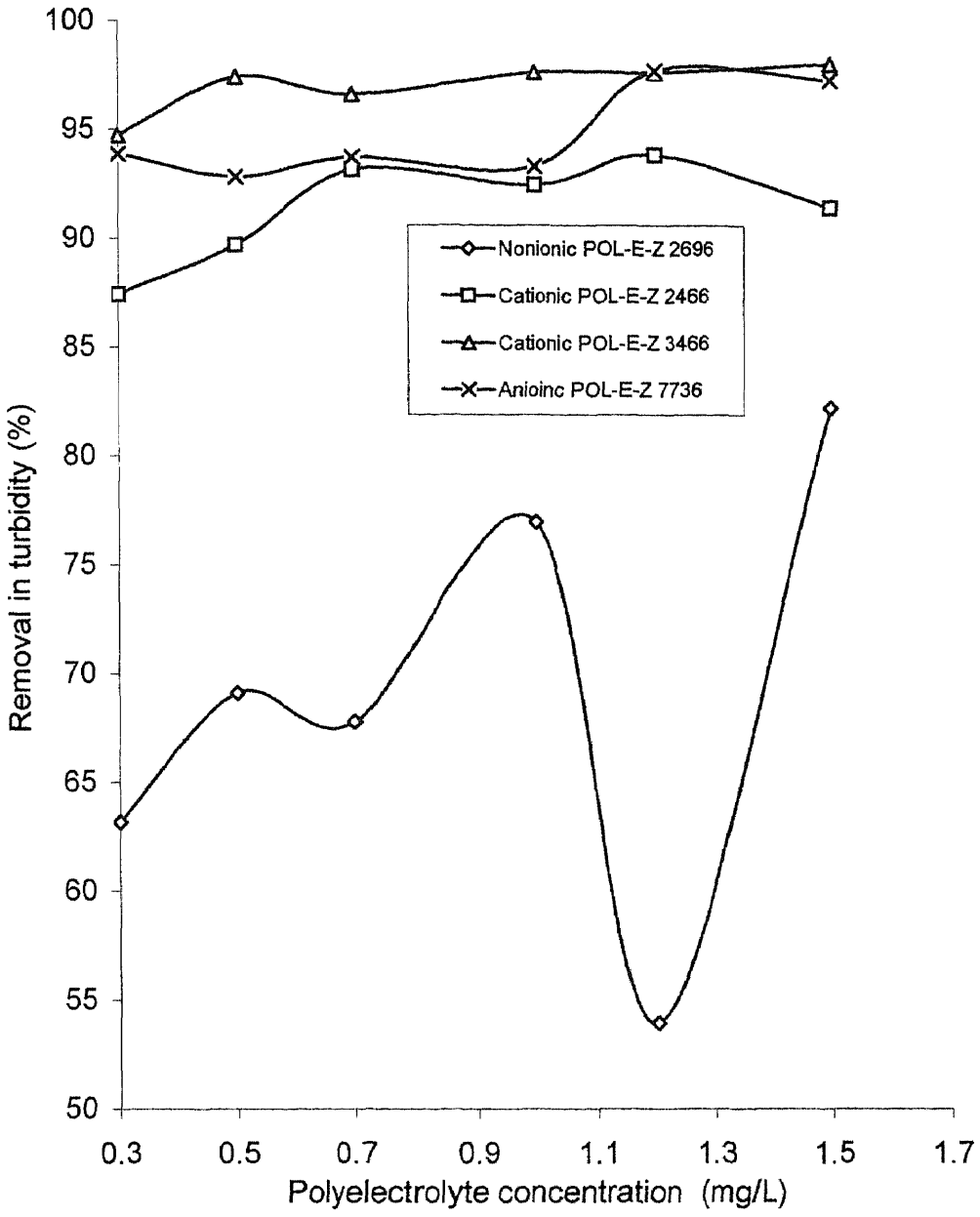

Figure 4-24 Removal in Turbidity versus Polyelectrolyte Concentration

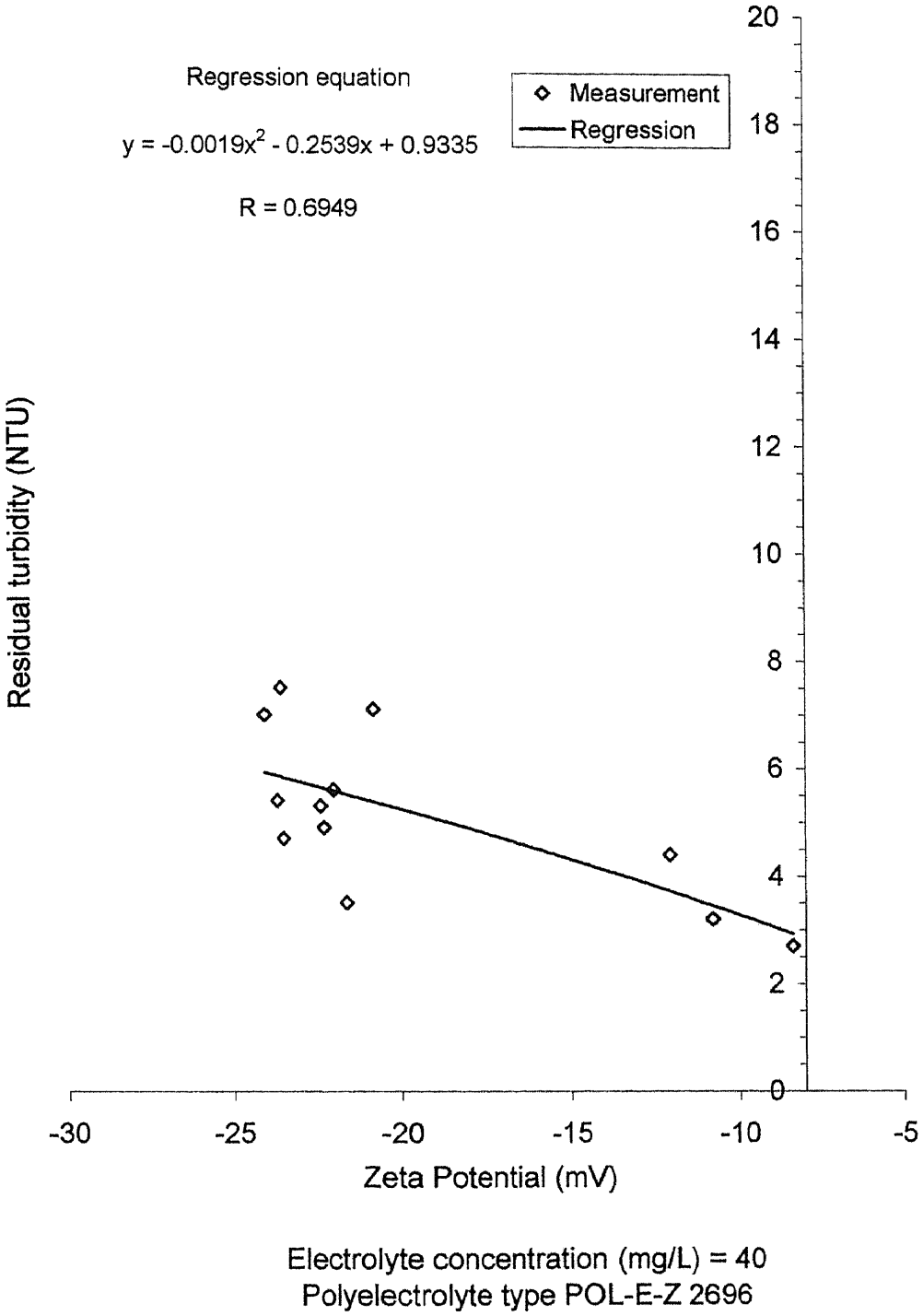

Figure 4-25 Residual Turbidity versus Zeta Potential (Phase III-A)

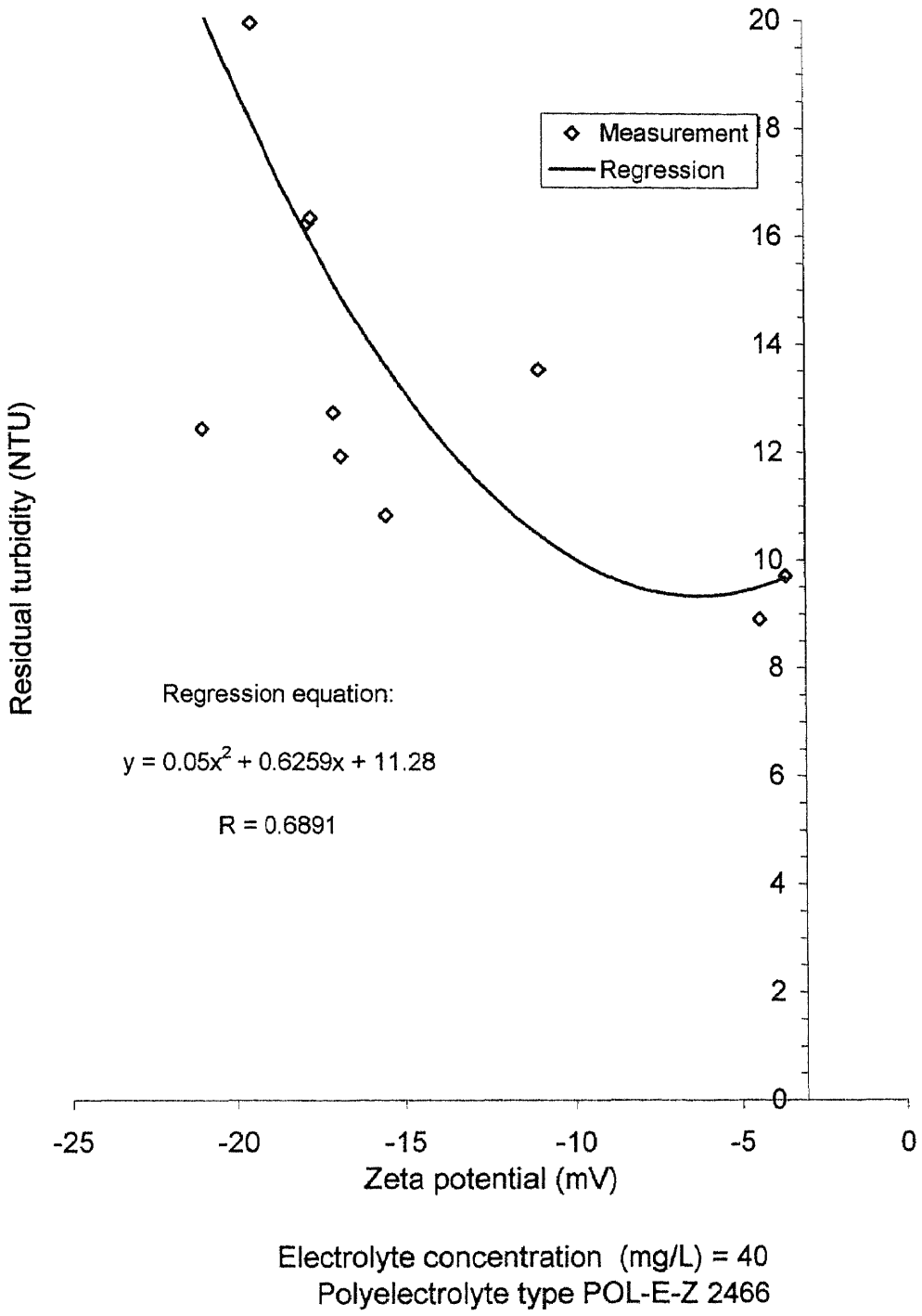

Figure 4-26 Residual Turbidity versus Zeta Potential (Phase III-B)

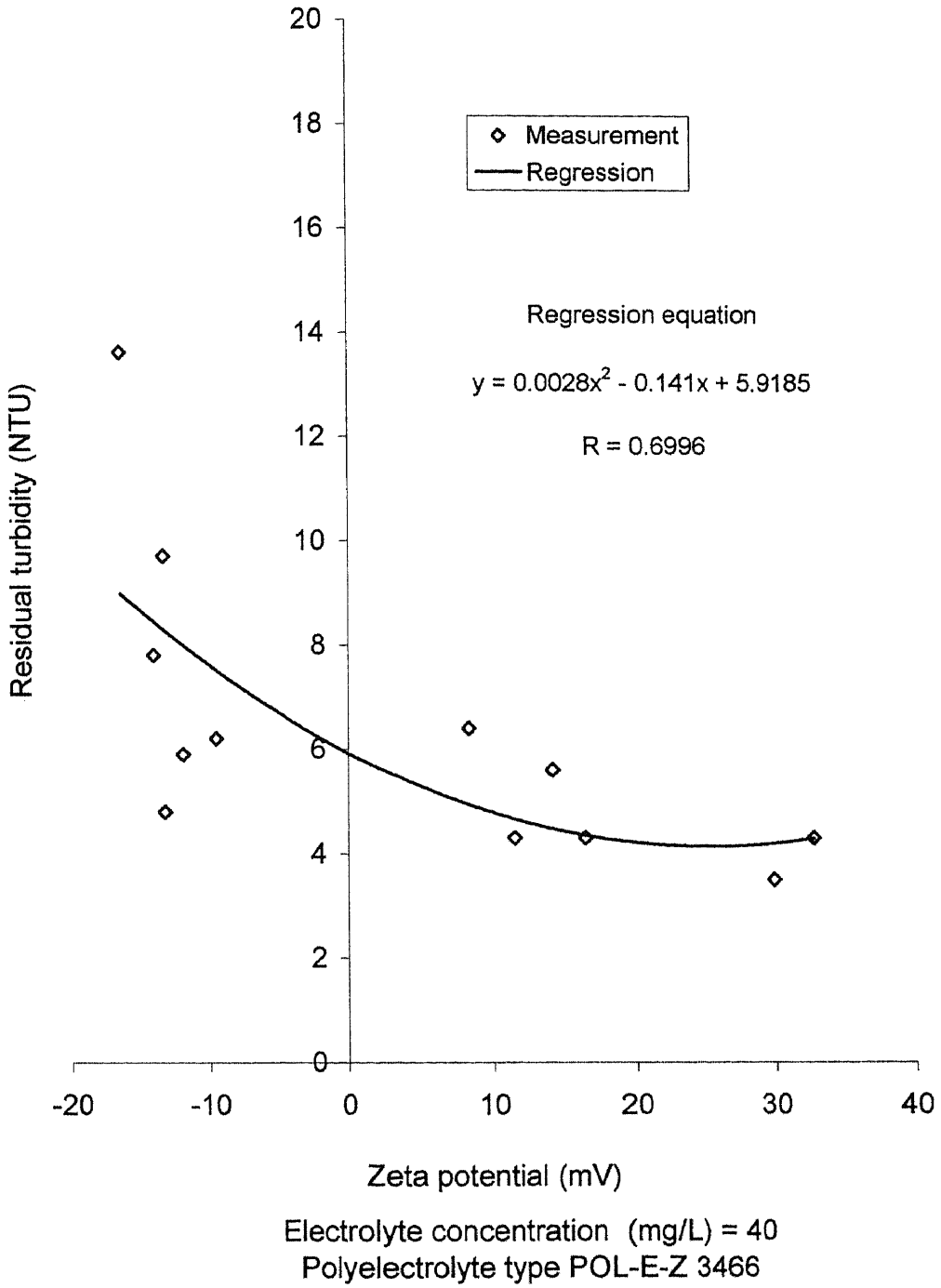

Figure 4-27 Residual Turbidity versus Zeta Potential (Phase III-C)

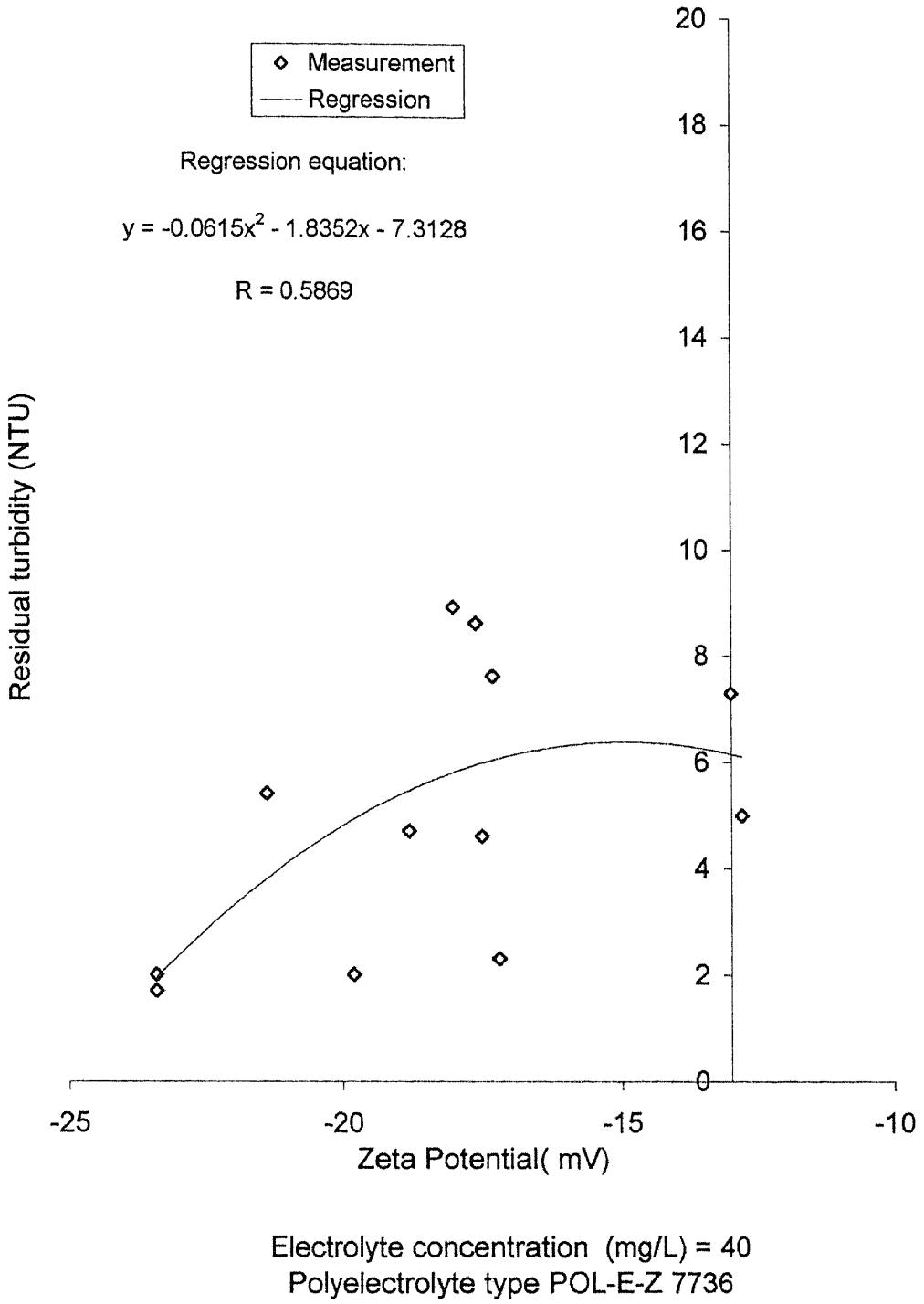

Figure 4-28 Residual Turbidity versus Zeta Potential (Phase III-D)

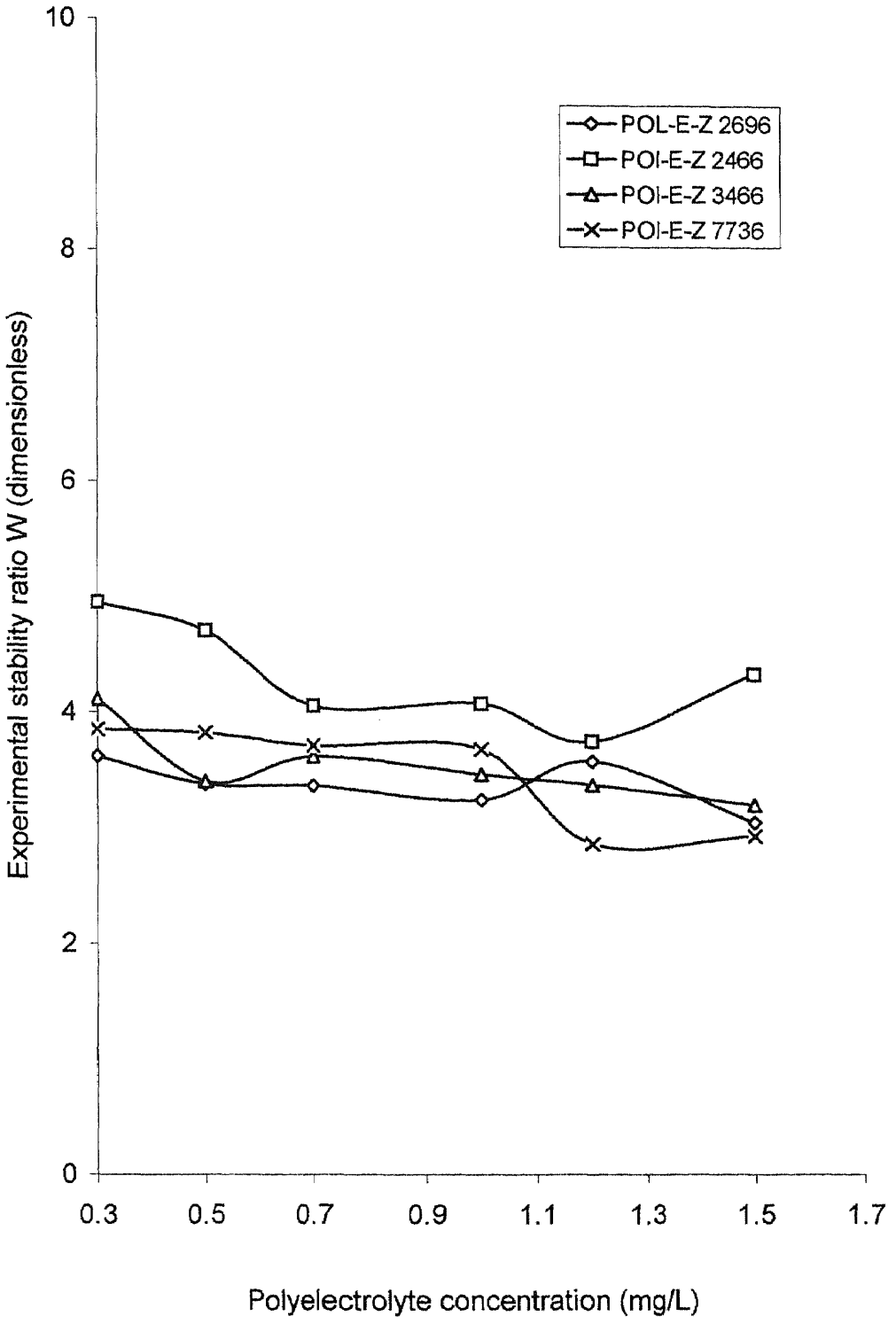

Figure 4-29 Experimental stability Ratio versus Polyelectrolyte Concentration

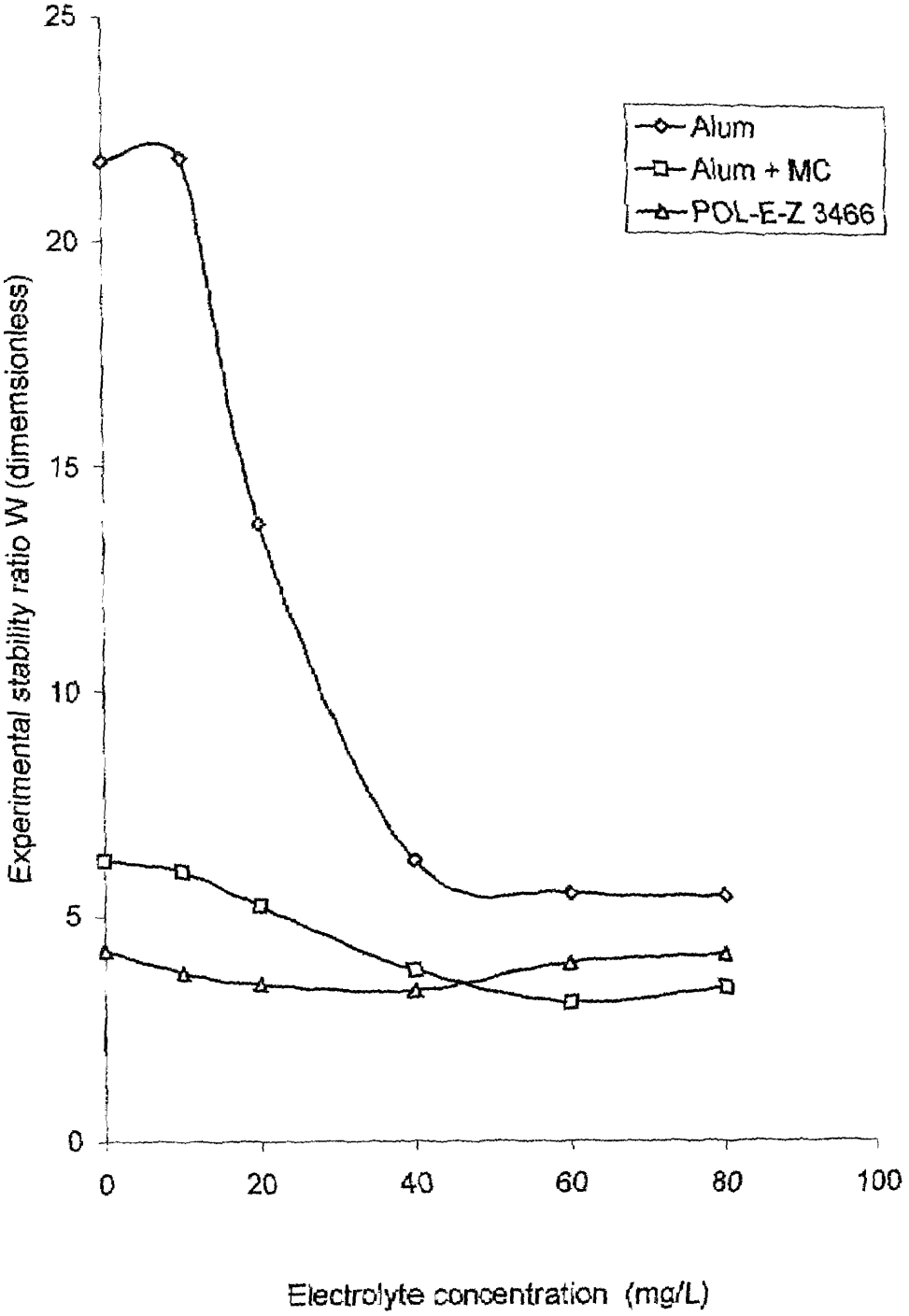

Figure 4-30 Experimental stability Ratio versus Electrolyte Concentration

CHAPTER 6

REFERENCES

1) R. Pitt, R. Field, M. Lalor, and M. Brown, "Urban Stormwater Toxic Pollutants Assessment, Source and Treatability," *Water Environ. Res.*, vol. 67, no. 3, p.260-275, 1995.

2) T.J. Iannuzzi, S. L. Huntley, C. W. Schmidt, B. L. Finely, R. P. Mcnutt, and S. J. Burton, "Combined Sewer Overflows as Sources of Sediment Contamination in the Lower Passaic River, New Jersey. 1. Priority Pollutants and Inorganic Chemicals," *Chemosphere*, vol. 34, no. 20, pp. 213-230, 1997.

3) Y. Tanizaki, T. Shimokwa, and M.Yamazaki, "Physico-Chemical Speciation of Trace Elements in Urban Streams by Size Fractionation," *Water Research*, vol. 26, no. 1, pp. 55-63, 1992.

4) J. B. Ellis, and D. M. Revitt, "Incidence of Heavy Metals in Street Surface Sediments: Solubility and Grain Size Studies," *Water Air and Soil Pollution*, vol.17, no. 1, p.87-95, 1982.

5) M. Vignoles, and L. Herremans, "Metal Pollution of Sediments Contained in Runoff Water in the Toulouse City" *NOVATECH 95, Second International Conference on Innovative Technologies in Urban Storm Drainage*, May 30 – June-1, Lyon, France, organized by Eurydice, and GRAIE, p.611-618, 1995.

6) G. W. Charklis, and M. R. Wiesner, "Particles, Metals and Water Quality in Runoff from Large Urban Watershed," *J. Environ. Eng.*, vol.123, no. 8, pp. 753-759, 1997.

7) R. Sydney, and I. D. Morrison, *Colloid Systems and Interfaces*, A. Halsted Press: A division of John Wiley and Sons, Inc., New York, 1988.

8) W. J. Eilbeck, G. Mattock, *Chemical Processes in Wastewater Treatment*, Halsted Press: A division of John Wiley and Sons, Inc., New York, 1987.

9) C. Cailleaux, E. Pujol, F.de Dianous, and J. C. Druoton, "Study of Weighted Flocculation in View of a New Type of Clarifier" *J Water SRT-Aqua* vol. 41, no. 1, p. 18-27, 1992.

10) J. Gregory, "The Role of Colloid Interactions in Solid-Liquid Separation," *Water Science and Technology*, vol. 27, no.10, p.1-17, 1993.

11) M. Elimelech, J. Gregory, X. Lia, R. Williams, "Surface Interaction Potentials," *Particle Deposition & Aggregation Measurement Modeling and Simulation,* Butterworth Heinemann Publishers, Boston, 1995.

12) W. J. Eilbeck, G. Mattock, *Chemical Processes in Wastewater Treatment,* Halsted Press: A division of John Wiley and Sons, Inc., New York 1987.

13) J. Gregory, "Fundamentals of Flocculation," *Critical Review in Environmental Control,* Vol. 19, issue 3, 1989.

14) R. Hunter, "Applications of the Zeta Potential," *Zeta Potential in Colloid Science,* Academic Press, New York, 1981.

15) M. Elimelech, J. Gregory, X. Lia, R. Williams, "Electrical Properties of Surfaces," *Particle Deposition & Aggregation Measurement Modeling and Simulation,* Butterworth Heinemann Publishers, Boston, 1995.

16) J. Lyklema, "Water at Interfaces: A Colloid Chemical Approach," *J. of Colloids and Interface Sci.,* Vol. 58, pp. 242, 1972.

17) M. Elimelech, J. Gregory, X. Lia, R. Williams, "Surface Interaction Potentials," *Particle Deposition & Aggregation Measurement Modeling and Simulation,* Butterworth Heinemann Publishers, Boston, 1995.

18) W. Adamson, and A. P. Gast, "Electrical Aspects of Physical Chemistry," *Physical Chemistry of Surfaces,* sixth edition, John Wiley and Sons inc., New York, 1997.

19) J. Gregory, "Fundamentals of Flocculation," *Critical Review in Environmental Control,* Vol. 19, issue 3, 1989.

20) J. Gregory, "The Role of Colloid Interactions in Solid-Liquid Separation," *Water Science and Technology,* vol. 27, no.10, p.1-17, 1993.

21) J. Gregory, "Fundamentals of Flocculation," *Critical Review in Environmental Control,* Vol. 19, issue 3, 1989.

22) B. W. Greene, and F. L. Saunders, "In Situ Remediation of Surface Active Agents on Latex Particles III. The Electrolyte Stability of Styrene–Butadiene Latexes," *J. of Colloids and Interface Sci.,* vol. 33, pp. 393, 1970.

23) D. C Grahame, "The Electrical Double Layer and the Theory of Electrocapillarity," *Chemical Review,* V. 41, p.441. 1947.

24) R. M. Pashley, and J. N. Ishraeiachvili, "DLVO and Hydration Forces between Mica Surfaces in Mg^{+2}, Ca^{+2}, Sr^{+2} and Ba^{+2} Chloride Solutions," *J of Colloids and Interface Sci.*, vol. 97, no. 2, p. 446-455, 1984.

25) P. M. Claesson and H. K. Christinson, "Very Large Range Attraction between Uncharged Hydrocarbon and Fluorocarbon Surfaces in Water," *J. of Physical Chemistry*, vol. 92, n.6, p. 1650-1655, 1988.

26) M. R. Jakel, "The Stabilization of Dispersed Mineral Particles by Adsorption of Humic Substances," *Water Research*, vol. 20, n. 12, P.1543-1554, 1986.

27) R. A. Ruehrwein, and A. Ward, "Mechanism of Clay Aggregation by Polyelectrolytes," *Soil Science*, vol. 73, p. 485,1952.

28) A.S. Michaels, "Aggregation of Suspension Polyelectrolytes," *Ind. Eng. Chem.* Vol. 46, p.1485, 1954.

29) J. Gregory, "Rates of Flocculation of Latex Particles by Cationic Polymers," *J. of Colloids and Interface Sci.*, vol. 42, no. 2, p. 448-456, 1973.

30) W. B. Russel, D. A. Saville, and W. R. Schowalter, *Colloidal Dispersions*, Cambridge University Press, New York, 1989.

31) T. W. Healy, and V. K. La Mer, "Energetics of Flocculation and Redispersion by Polymers," *J. of Colloids and Interface Sci.*, vol. 19, p. 323, 1964.

32) R. Hogg, "Collision Efficiency Factors for Polymer Flocculation," *J. of Colloids and Interface Sci.*, vol. 102, no.1, p. 232-236, 1984.

33) B. M. Modugil, B. D. Shah, and H.S. Soto, "Collision Efficiency Factors in Polymer Flocculation of Fine Particles," *J of Colloids and Interface Sci.*, vol. 119, no. 2, p. 466-473, 1987.

34) J. Gregory, "The Role of Colloid Interactions in Solid-Liquid Separation," *Water Science and Technology*, vol. 27, no.10, p.1-17, 1993.

35) C. R. O'Melia, and C. L. Tiller, "Physicochemical Aggregation and Deposition in Aquatic Environments," *Environmental Particles*, Lewis Publishers, New York, 1993.

36) A. Amritharajah, and C. R. O'Melia, "Coagulation Processes: Destabilization, Mixing and Flocculation," *Water Quality and Treatment*, McGraw Hill Publication, New York, 1990.

37) M. Y. Han, and D. F. Lawler, "The Relative Insignificance of G in Flocculation," 1989 Annual Conference Proc., *American Water Works Association*, P. 1327-1332, 1989.

38) I. R. Valioulis, and E. J. List, "Collision Efficiencies of Diffusing Spherical Particles: Hydrodynamic, van der Waals and Electrostatic Forces," Advances Colloids Interface Science, vol 33, p.1, 1984.

39) T. G. M. van de Ven, and S. G. Meson, "The Microrheology of Colloidal Dispersions IV Pairs of Interacting Spheres in Shear Flow," *J. of Colloids and Interface Sci.*, vol. 57, no. 3, p. 505-516, 1976.

40) P. M. Alder, "Heterocoagulation in Shear Flow," *J. of Colloids and Interface Sci.*, vol. 83, no. 1, p. 106-115, 1984.

41) C. R. O'Melia and C. L. Tiller, "Physicochemical Aggregation and Deposition in Aquatic Environments," *Environmental Particles*, Lewis Publishers, New York, 1993.

42) L. Ling, "Effects of Surface Chemistry on Kinetics of Coagulation of Submicron Iron Oxide Particles (α-Fe_2O_3) in Water," Ph. D. dissertation, California Institute of Technology, Pasadena, California, 91125, 1988.

43) C. J. Chin, S. Yiacoumi, and C. Tsouris, " Shear Induced Flocculation of Colloidal Particles in Stirred Tanks," *J. of Colloids and Interface Sci.*, vol. 206, no., p. 532-545, 1998.

44) S. K. Dental, and J. M. Gossett, "Mechanisms of Coagulation with Aluminum Salts," *J. Am. Water Works Assoc.*, vol. 80, no. 4, p.187-198, 1988.

45) R. J. Francois, "Growth Kinetics of Hydroxide Flocs," *J. Am. Water Works Assoc.*, vol. 80, no. 6, p.92-96, 1988.

46) L. Chris, "Coagulation Control and Optimization," *Public Works*, vol. 125, no.12, p.32-33, 1994.

47) S. A. A. Jahn, "Using Moringa Seeds as Coagulants in Developing Countries," *J. Am. Water Works Assoc.*, vol. 80, p.43, 1988.

48) J. Gregory, "Rates of Flocculation of latex Particles by Cationic Polymers," *J. of Colloids and Interface Sci.*, vol. 42, no. 2, p. 448-456, 1973.

49) G. Trivanti, F. Lore, and G. Sonnante, "Influence of the Charge Density of Cationic Polyelectrolytes on Sludge Conditioning," *Water Research*, vol. 19, no. 1, p. 93, 1985.

50) T. Smith-Palmer, et. al. "Flocculation Behavior of Some Cationic Polyelectrolytes," J. *App. Polym. Sci.*, vol. 52, p.1317, 1994.

51) G. M. Lindquist, and R. A. Stratton. "The Role of Polyelectrolyte Charge Density and Molecular Weight on the Adsorption and Flocculation of Colloidal Particles," *J. of Colloids and Interface Sci.*, vol. 55, no. 1, p. 45-59, 1976.

52) J. Gregory, "Rates of Flocculation of Latex Particles by Cationic Polymers," *J. Colloids and Interface Sci.*, vol. 42, no. 2, p. 448-456, 1973.

53) Standard methods For the Examination of Water and Wastewater, 7th Edition, Edited by Lenore S. Clesceri, Arnold E. Greenberg and R. Rhodes Trussel, Prepared and published by American Public Health Association, American Water Works Association and Water Pollution Control Federation, 1989.